Optimal Fault-Tolerant Control for Large-Scale Interconnected Systems with State-Constraints

Journal:	*IEEE Transactions on Systems, Man and Cybernetics: Systems*
Manuscript ID	SMCA-24-04-1441
Manuscript Type:	Regular Paper
Date Submitted by the Author:	29-Apr-2024
Complete List of Authors:	Liu, Qingyi; Nanjing University of Aeronautics and Astronautics, Automation Enggineering Zhang, Ke; Nanjing University of Aeronautics and Astronautics, College of Automation Engineering Jiang, Bin; Nanjing University of Aeronautics and Astronautics, College of Automation Engineering Simani, Silvio; University of Ferrara, Department of Engineering
Key Words:	Fault diagnosis, Fault tolerance, Large-scale systems

Optimal Fault-Tolerant Control for Large-Scale Interconnected Systems with State-Constraints

Qingyi Liu, Ke Zhang, *Senior Member, IEEE*, Bin Jiang, *Fellow, IEEE*, and Silvio Simani, *Senior Member, IEEE*

***Abstract*—Guaranteed system performance under various circumstances remains a challenge in technique and practice. To address this problem, this article investigates the optimal fault-tolerant control strategy for large-scale interconnected systems with intermittent faults. Since the subsystem state is enforced to a limited range, an asymmetric integral barrier Lyapunov function is incorporated into the principle of Bellman optimality to avoid the violation of state-constraints. Also, it can conquer a conservative limitation that the bounds of the transformed error-constraints are known. Subsequently, the critic-actor-identifier framework is constructed in the backstepping step to evaluate the objective function, control behavior and unknown dynamic, respectively. Wherein, the decentralized controller derived from the learning process and the fault-tolerant controller are separated by introducing an intermediate controller. Meanwhile, it is illustrated that the trajectory tracking errors will approach to a small region nearby the origin, and the system states may not beyond the given asymmetric constraint bounds, even in the presence of actuator faults. Finally, results are presented to exhibit the effectiveness and the advantage of the optimal approach through appropriate comparative simulations.**

***Index Terms*—Optimal fault-tolerant control, large-scale interconnected systems, intermittent actuator faults, asymmetric integral barrier Lyapunov function, critic-actor-identifier network.**

I. Introduction

The practical applications such as chemical reactors, public transportation systems, robots, etc., all have a complex connection among multiple subsystems, which can be described by the large-scale interconnected systems (LSIS). However, this connection usually influences the behavior of subsystems and the whole process, hence, many researchers have attempted to design several approaches to stabilize these coupled dynamics well. As a principal technique, the decentralized backstepping control is suited for such a system, because it can devise the control law of each subsystem only using its local knowledge. Hence, the whole system is controlled by several independent controllers that all together combine to form a decentralized controller [1]–[3]. Owing to it, many results on this technique have been investigated for stochastic LSIS [4], time-delay LSIS [5], switched LSIS [6], uncertain LSIS [7], fractional-order LSIS [8], and others.

Nevertheless, some of the physical components (actuators, sensors, and processors) encounter any type of sudden and random faults, which can bring about unsatisfactory performance or even make the system unstable [9], [10]. All these cases improve the fault-tolerant capability to achieve several control objectives and enhance the system robustness efficiently, thus, the fault-tolerant control (FTC) strategies have been developed. Usually, FTC can be divided into an active one and a passive one [11]. The active FTC needs fault information through a fault estimation observer, to reconfigure the nominal controller, which may delay the fault compensation time and bring more computational burden. While the passive FTC mainly counts on the robustness of controller itself to deal with fault effects, i.e., it operates in both normal and faulty conditions. Therefore passive FTC compensates faults faster as compared with active FTC. Recently, many techniques have been coupled with the passive FTC for improving the desirable performance of LSIS with faults, e.g., resilient control [12], prescribed performance control [13], and finite/fixed-time control [14], [15].

However, without considering optimization, the above FTC strategies cannot guarantee a better control performance. The optimal FTC has an extensive application prospect in control fields, aiming at finding a controller during an interval while optimizing the objective function, then the energy consumption is reduced in the case of faults. It is noted that the results on the optimal FTC often require handling the coupled Hamilton-Jacobi-Bellman (HJB) equation, which makes it hard to obtain the analytical solution for such a partial differential equation. The adaptive dynamic programming (ADP) [16], has a certain advantage in dealing with the dimensionality problem of the traditional dynamic programming [17], becoming an emerging approximate optimization method in recent years. The authors in [18], [19] developed the single critic network-based optimal FTC schemes for nonlinear continuous/discrete-time systems, respectively. After that, a typical structure employed in ADP is the critic-actor architecture [20]. The principle is that, there is a critical evaluation for each control action implemented by an actor; therefore, the objective function and the control behavior coupled by HJB equation can be approximated by a critic and an actor subsequently. On this foundation, the optimal FTC approaches have been studied for switched systems [21], affine systems [22], stochastic systems [23], etc. At present, there exist numerous complex scenarios when loss of effectiveness and stuck faults happen, the critic-actor-based learning method

This work was supported in part by the National Key Laboratory Foundation of Helicopter Aeromechanics (2023-HA-LB-067-04), in part by National Natural Science Foundation of China under Grants (62173180, 62020106003), in part by the Natural Science Foundation of Jiangsu Province of China (BK20222012), in part by the Fundamental Research Funds for the Central Universities under Grants (NE2022002, NC2022003).

Q. Liu, K. Zhang, and B. Jiang are with the College of Automation Engineering, Nanjing University of Aeronautics and Astronautics, Nanjing 211106, China (e-mail: qiyiliu1228@163.com, kezhang@nuaa.edu.cn, binjiang@nuaa.edu.cn).

Ke Zhang and Bin Jiang are with the National Key Laboratory of Helicopter Aeromechanics, Nanjing, 210016, China.

S. Simani is with the Department of Engineering, University of Ferrara, Ferrara, Italy (e-mail: silvio.simani@unife.it).

is not yet adaptive for optimal FTC, especially for the high-order LSIS, which is a main motivation of this article.

It is known that most practical applications normally operate under various constraints, e.g., the performance requirements, physical limitations and security considerations. Neglecting to accommodate these constraints may cause some inaccurate performance, system instability, or even unexpected accident. Many efforts have been devoted to solving it, including barrier Lyapunov function (BLF), funnel control [24], [25], model predictive control [26] and others. BLF is a special Lyapunov function, whose value approaches infinity when it nears the boundary of permissible set. It is seen that many types of BLFs in the literature, such as tangent BLF [27], logarithmic BLF [28], [29], and integral BLF (IBLF) based control approaches have been widely used to achieve the output/state-constraints. Among them, the processing of constraints using IBLF have been greatly simplified and relaxed the feasibility conditions, i.e., it has a well calculate capability of not requiring to convert state-constraints into transformed error-constraints, but help to restrict a system state directly. Hence, the conservatism of BLFs-based control can be reduced. Employing the neural networks to estimate the uncertain dynamics, the IBLF has been utilized to solve output/input-constrained problems [30], [31], as well as the state-constrained problems for switched systems [32], block-triangular systems [33], and multi-agent systems [34]. Regarding the practical applications, IBLF has been also applied a flight vehicle with the field-of-view constraints [35], and a recovery carrier with trajectory and posture constraints [36]. Nevertheless, the IBLFs studied in [30]–[36] are only available for constrained problems with symmetric limitations. It remains uncertain whether IBLF can handle an asymmetric constrained problem, which will be recognized as a new idea to extend the optimal FTC design with constraints further.

Inspired by the above-mentioned literature and discussions, this article concentrates on the development of an optimal FTC algorithm for a class of state-constrained LSIS. Meanwhile, the innovations and contributions of this article can be summarized as below:

1) An asymmetric IBLF is incorporated into each back-stepping step to maintain the state-variables in an asymmetric constrained region. This function can enable full state-constraints during the learning process directly, and avoid the complex tracking error-constraints conversion inherent in the conventional BLFs [27]–[29].
2) The principle of Bellman optimality is exploited under a critic-actor-identifier architecture to achieve the optimal FTC. Different from the results in [18], [21] and [22], the proposed strategy is free of exact knowledge of unknown dynamic that is estimated by identifier network.
3) In comparison with existing FTC schemes in [14], [28], which only deal with a finite of actuator faults, the intermittent faults are studied here, and the optimal controller derived by actor network and the fault-tolerant controller are isolated by creating an intermediate controller.

This article is organized as follows: Section II provides the system descriptions and some preliminaries. The main work on optimal FTC algorithm is presented in Section III. Section IV and Section V give the stability analysis and simulation results, respectively. Finally, the conclusions are drawn in Section VI.

II. Problem Formulation and Preliminaries

Consider a class of LSIS that is composed of N subsystems connected by their outputs, and the dynamic model of the ith subsystem has the following form:

$$\begin{cases} \dot{\mathbf{x}}_{i,1} = \mathbf{g}_{i,1}(\mathbf{x}_{i,1})\mathbf{x}_{i,2} + \mathbf{f}_{i,1}(\mathbf{x}_{i,1}) + \Delta_{i,1}(\bar{\mathbf{y}}) \\ \dot{\mathbf{x}}_{i,\hbar} = \mathbf{g}_{i,\hbar}(\bar{\mathbf{x}}_{i,\hbar})\mathbf{x}_{i,\hbar+1} + \mathbf{f}_{i,\hbar}(\bar{\mathbf{x}}_{i,\hbar}) + \Delta_{i,\hbar}(\bar{\mathbf{y}}) \\ \dot{\mathbf{x}}_{i,\mathrm{n}_i} = \sum_{\mathrm{k}=1}^{\mathrm{m}_i} \mathbf{g}_{i,\mathrm{n}_i}^{\mathrm{k}}(\bar{\mathbf{x}}_{i,\mathrm{n}_i})\mathbf{u}_{i,\mathrm{k}}^{\mathrm{F}} + \mathbf{f}_{i,\mathrm{n}_i}(\bar{\mathbf{x}}_{i,\mathrm{n}_i}) + \Delta_{i,\mathrm{n}_i}(\bar{\mathbf{y}}) \\ \mathbf{y}_i = \mathbf{x}_{i,1},\ i = 1,2,\ldots,\mathrm{N},\ \hbar = 2,\ldots,\mathrm{n}_i - 1 \end{cases} \tag{1}$$

where $\mathbf{x}_{i,\iota}$, $\iota = 1,2,\ldots,\mathrm{n}_i$ is the measurable subsystem state variable with $\bar{\mathbf{x}}_{i,\iota} = [\mathbf{x}_{i,1}, \mathbf{x}_{i,2}, \ldots, \mathbf{x}_{i,\iota}]^{\mathrm{T}} \in \mathcal{R}^{\iota}$. $\mathbf{y}_i \in \mathcal{R}$ denotes the control output vector. $\mathbf{f}_{i,\iota}(\bar{\mathbf{x}}_{i,\iota})$ and $\mathbf{g}_{i,\iota}(\bar{\mathbf{x}}_{i,\iota})$ depict the unknown functions, and $\Delta_{i,\iota}(\bar{\mathbf{y}})$ is the interconnection among N subsystems with $\bar{\mathbf{y}} = [\mathbf{y}_1, \mathbf{y}_2, \ldots, \mathbf{y}_{\mathrm{N}}]^{\mathrm{T}} \in \mathcal{R}^{\mathrm{N}}$.

For simplicity, the functions $\mathbf{f}_{i,\iota}(\bar{\mathbf{x}}_{i,\iota})$, $\mathbf{g}_{i,\iota}(\bar{\mathbf{x}}_{i,\iota})$ and $\Delta_{i,\iota}(\bar{\mathbf{y}})$ are abbreviated by $\mathbf{f}_{i,\iota}$, $\mathbf{g}_{i,\iota}$ and $\Delta_{i,\iota}$, respectively.

Similar to [8], [13], the intermittent actuator faults contain both the loss of effectiveness and the stuck faults, which are modeled as below:

$$\mathbf{u}_{i,\mathrm{k}}^{\mathrm{F}} = \psi_{i,\mathrm{k}}^{\mathrm{h}}\mathbf{u}_{i,\mathrm{k}} + \zeta_{i,\mathrm{k}}^{\mathrm{h}},\ \mathrm{t} \in [\mathrm{t}^{\mathrm{h}}, \mathrm{t}^{\mathrm{h}+1}),\ \mathrm{h} = 1,2,\ldots \tag{2}$$

where h denotes the number of faults, $\psi_{i,\mathrm{k}}^{\mathrm{h}} \in (0,1]$ is the coefficient of the loss of effectiveness faults, and $\zeta_{i,\mathrm{k}}^{\mathrm{h}}$ depicts an unknown time-varying function in the hth faulty mode. It is assumed that there exists an unknown positive constant $\bar{\zeta}_{i,\mathrm{k}}^{\mathrm{h}}$ such that $|\zeta_{i,\mathrm{k}}^{\mathrm{h}}| \le \bar{\zeta}_{i,\mathrm{k}}^{\mathrm{h}}$. Up to $\mathrm{m}_i - 1$ controllers lie in faults, and the others continue to operate.

Remark 2.1. The actuator of the ith subsystem mainly can experiment with the following four cases: i) $\psi_{i,\mathrm{k}}^{\mathrm{h}} \in (0,1)$ and $\zeta_{i,\mathrm{k}}^{\mathrm{h}} \neq 0$ indicate that the ith subsystem has the loss of control effectiveness and stuck faults at the same time; ii) $\psi_{i,\mathrm{k}}^{\mathrm{h}} \in (0,1)$ and $\zeta_{i,\mathrm{k}}^{\mathrm{h}} = 0$ imply that it can only output a fraction of the control input; iii) $\psi_{i,\mathrm{k}}^{\mathrm{h}} = 1$ and $\zeta_{i,\mathrm{k}}^{\mathrm{h}} \neq 0$ signify stuck faults only; iv) $\psi_{i,\mathrm{k}}^{\mathrm{h}} = 1$ and $\zeta_{i,\mathrm{k}}^{\mathrm{h}} = 0$ means the fault-free case.

Remark 2.2. The fault number h in [14], [28] is limited to finite under a single occurrence time. In contrast to this, the more general case is considered as Eq.(2), which indicates that the actuator can be intermittently revert to normal operation, or alternate intermittently between different fault modes. It is applicable not only to the actuator faults with uniform interval periods but to those with non-uniform interval periods.

In this article, the main control objective is to devise an optimal FTC scheme, so that the subsystem output $\mathbf{y}_i$ can follow the reference signal $\mathbf{y}_{i,\mathrm{d}}$, and the constraint requirements are not violated (i.e., the state-variable $\mathbf{x}_{i,\iota}$, $\iota = 1,2,\ldots,\mathrm{n}_i$ satisfies the inequality $-\mathrm{k}_{i,\iota}^{\mathrm{l}} < \mathbf{x}_{i,\iota} < \mathrm{k}_{i,\iota}^{\mathrm{u}}$ with the positive constants $\mathrm{k}_{i,\iota}^{\mathrm{l}}$, $\mathrm{k}_{i,\iota}^{\mathrm{u}}$).

To further achieve the purpose, a learning-based algorithm with the asymmetric IBLF is employed to tackle the optimal FTC problem for LSIS. Common assumptions and lemmas are also needed to introduce as below.

Assumption 2.1 [37]. There exist positive constants $\bar{\mathrm{g}}_{i,\iota}$ and $\underline{\mathrm{g}}_{i,\iota}$ satisfy $\underline{\mathrm{g}}_{i,\iota} \leq |\mathbf{g}_{i,\iota}| \leq \bar{\mathrm{g}}_{i,\iota}$ for the unknown functions $\mathbf{g}_{i,\iota}$. However, the sign function of $\mathbf{g}^{\mathrm{k}}_{i,\mathrm{n}_i}$ is known, i.e., $\mathrm{sign}(\mathbf{g}^{\mathrm{k}}_{i,\mathrm{n}_i})$ is known for $\mathrm{k} = 1, 2, \ldots, \mathrm{m}_i$.

Assumption 2.2 [6]–[8]. The interconnected items among the subsystems consist of all the subsystem outputs (i.e., $\bar{\mathbf{y}}$), which are formulated as $\Delta_{i,\iota}$ satisfy the inequality $|\Delta_{i,\iota}| \leq \sum_{\mathrm{s}=1}^{\mathrm{p}_{i,\iota}} \sum_{l=1}^{\mathrm{N}} \mathrm{q}^{\mathrm{s}}_{i,\iota,l} |\mathbf{y}_l|^{\mathrm{s}}$ for a known constant $\mathrm{q}^{\mathrm{s}}_{i,\iota,l}$ and a known integer $\mathrm{p} = \max_{1\leq\iota\leq\mathrm{N}}\{\mathrm{p}_{i,\iota}\}$.

Assumption 2.3 [8], [37]. It is assumed that there exists the upper bound $\bar{\mathbf{y}}_{i,\iota}$, such that the desired reference signal $\mathbf{y}_{i,\mathrm{d}}$ and its time-derivative fulfill the conditions $-\mathrm{k}^{\mathrm{l}}_{i,\iota} \leq \mathbf{y}_{i,\mathrm{d}} \leq \mathrm{k}^{\mathrm{u}}_{i,\iota}$ and $\mathbf{y}^{(\iota)}_{i,\mathrm{d}} < \bar{\mathbf{y}}_{i,\iota}$ for $\iota = 1, 2, \ldots, \mathrm{n}_i$.

Remark 2.3. As a kind of typical LSIS, the form of Eq.(1) can be found in several practical applications [14], [38], [39]. It should be underlined that Assumptions 2.1-2.3 are the standard and necessary requirements in the optimal FTC design during the subsequent section.

Lemma 2.1 (Neural Network Approximation [7], [8]). For an unknown continuous function $\mathbf{h}(\mathbf{x})$, there exists a neural network $\mathrm{W}^{*\mathrm{T}}_{\mathbf{h}}\mathrm{S}_{\mathbf{h}}(\mathbf{x})$ making the following relation holds:

$$\mathbf{h}(\mathbf{x}) = \mathrm{W}^{*\mathrm{T}}_{\mathbf{h}}\mathrm{S}_{\mathbf{h}}(\mathbf{x}) + \epsilon_{\mathbf{h}}, \ |\epsilon_{\mathbf{h}}| \leq \bar{\epsilon}_{\mathbf{h}} \tag{3}$$

where $\mathrm{W}^*_{\mathbf{h}}$ and $\mathrm{S}_{\mathbf{h}}(\mathbf{x})$ depicts the ideal weight vector and the basis function vector, and $\epsilon_{\mathbf{h}}$ denotes the approximation error.

Lemma 2.2 (Young's inequality [4]). For any vectors $\mathrm{x}, \mathrm{y} \in \mathcal{R}^{\mathrm{n}}$, the following inequality holds:

$$\mathrm{xy} \leq \frac{\eta^{\mathrm{a}}}{\mathrm{a}}|\mathrm{x}|^{\mathrm{a}} + \frac{1}{\mathrm{b}\eta^{\mathrm{b}}}|\mathrm{x}|^{\mathrm{b}} \tag{4}$$

where $\eta > 0$, $\mathrm{a} > 1$, $\mathrm{b} > 1$ and $(\mathrm{a}-1)(\mathrm{b}-1) = 1$.

III. Optimal FTC Scheme Design

In this section, the optimal virtual and actual control input are exhibited, to follow the desired reference trajectory $\mathbf{y}_i$ of LSIS in Eq.(1) with asymmetric state-constraints by using the asymmetric IBLF.

Owing to the high-dimensional characteristic of the overall system, the design procedure has a hierarchical structure. As is shown in Fig.1, the backstepping control technique is used to derive the optimal virtual control inputs $\hat{\mathbf{a}}^*_{i,\hbar-1}$ and $\hat{\mathbf{a}}^*_{i,\mathrm{n}_i-1}$ in each phase sequentially, and the optimal FTC input $\mathbf{u}^*_{i,\mathrm{k}}$ is derived by constructing an intermediate controller $\mathbf{v}^*_i$. The proposed algorithm consists the following steps.

Before presenting the design procedure of the optimal fault-tolerant controller, the transformation errors are defined as:

$$\begin{cases} \mathbf{z}_{i,1} = \mathbf{x}_{i,1} - \mathbf{y}_{i,\mathrm{d}} \\ \mathbf{z}_{i,\hbar} = \mathbf{x}_{i,\hbar} - \hat{\mathbf{a}}^*_{i,\hbar-1} \\ \mathbf{z}_{i,\mathrm{n}_i} = \mathbf{x}_{i,\mathrm{n}_i} - \hat{\mathbf{a}}^*_{i,\mathrm{n}_i-1} \end{cases} \tag{5}$$

where $\hat{\mathbf{a}}^*_{i,\hbar-1}$, $\hbar = 2, \ldots, \mathrm{n}_i - 1$ is the estimation of the virtual optimized control input $\mathbf{a}^*_{i,\hbar-1}$, and $\mathbf{x}_{i,\hbar}$ is viewed as $\mathbf{a}^*_{i,\hbar-1}$.

Step i,1. As for the first backstepping step, the associated objective function is selected as:

$$\begin{aligned} \mathrm{J}^*_{i,1}(\mathbf{z}_{i,1}) &= \min_{\mathbf{a}_{i,1}\in\Psi_{i,1}} \int_{\mathrm{t}}^{\infty} (\mathrm{M}_{i,1}(\tau) + \mathbf{a}^2_{i,1}(\tau))\mathrm{d}\tau \\ &= \int_{\mathrm{t}}^{\infty} (\mathrm{M}_{i,1}(\tau) + \mathbf{a}^{*2}_{i,1}(\tau))\mathrm{d}\tau \end{aligned} \tag{6}$$

where $\mathrm{M}_{i,1}(\tau) = \int_0^{\mathbf{z}_{i,1}(\tau)} \frac{(\mathrm{k}^{\mathrm{l}}_{i,1}+\mathrm{k}^{\mathrm{u}}_{i,1})^2\sigma_{i,1}}{\bar{\mathrm{k}}^{\mathrm{l}}_{i,1}\bar{\mathrm{k}}^{\mathrm{u}}_{i,1}}\mathrm{d}\sigma_{i,1}$ with $\bar{\mathrm{k}}^{\mathrm{l}}_{i,1} = \mathrm{k}^{\mathrm{l}}_{i,1} + \sigma_{i,1} + \mathbf{y}_{i,\mathrm{d}}$ and $\bar{\mathrm{k}}^{\mathrm{u}}_{i,1} = \mathrm{k}^{\mathrm{u}}_{i,1} - \sigma_{i,1} - \mathbf{y}_{i,\mathrm{d}}$. The compact set containing origin is denoted as $\Psi_{i,1} = \{\mathbf{x}_{i,1} : -\mathrm{k}^{\mathrm{l}}_{i,1} < \mathbf{x}_{i,1} < \mathrm{k}^{\mathrm{u}}_{i,1}\}$ with $\mathrm{k}^{\mathrm{l}}_{i,1}$ and $\mathrm{k}^{\mathrm{u}}_{i,1}$ being the positive constants.

Remark 3.1. The proposed asymmetric IBLF extends the application of symmetric IBLF when asymmetric state limitation boundaries are considered, that is to say, the symmetric IBLF $\bar{\mathrm{M}}_{i,1}(\iota) = \int_0^{\mathbf{z}_{i,1}(\iota)} \frac{\mathrm{k}^2_{i,1}\sigma_{i,1}}{\mathrm{k}^2_{i,1}-(\sigma_{i,1}-\mathbf{y}_{i,\mathrm{d}})^2}\mathrm{d}\sigma_{i,1}$ in [30]–[36] is a special case of $\mathrm{M}_{i,1}(\iota)$. That is to say, if $\mathrm{k}^{\mathrm{l}}_{i,1} = \mathrm{k}^{\mathrm{u}}_{i,1} = \mathrm{k}_{i,1}$, it has $\mathrm{M}_{i,1}(\iota) = 4\bar{\mathrm{M}}_{i,1}(\iota)$ accordingly.

The HJB equation of $\mathbf{z}_{i,1}$-subsystem that is correlative with the Eq.(6) can be generated as below:

$$\begin{aligned} \mathrm{H}_{i,1}(\mathbf{z}_{i,1}, \mathbf{a}^*_{i,1}, \mathrm{J}^*_{\mathbf{z}_{i,1}}) = \mathrm{J}^*_{\mathbf{z}_{i,1}}(\mathbf{g}_{i,1}\mathbf{a}^*_{i,1} + \mathbf{f}_{i,1} + \Delta_{i,1} \\ - \dot{\mathbf{y}}_{i,\mathrm{d}}) + \mathrm{M}_{i,1} + \mathbf{a}^{*2}_{i,1} \end{aligned} \tag{7}$$

where $\mathrm{J}^*_{\mathbf{z}_{i,1}} = \frac{\partial \mathrm{J}^*_{i,1}(\mathbf{z}_{i,1})}{\partial \mathbf{z}_{i,1}}$. By resolving $\frac{\partial \mathrm{H}_{i,1}(\mathbf{z}_{i,1}, \mathbf{a}^*_{i,1}, \mathrm{J}^*_{\mathbf{z}_{i,1}})}{\partial \mathbf{a}^*_{i,1}} = 0$, the optimal virtual control input $\mathbf{a}^*_{i,1}$ can be obtained as:

$$\mathbf{a}^*_{i,1} = -\frac{\mathbf{g}_{i,1}}{2}\mathrm{J}^*_{\mathbf{z}_{i,1}} \triangleq -\frac{1}{2}\bar{\mathrm{J}}^*_{\mathbf{z}_{i,1}} \tag{8}$$

where $\bar{\mathrm{J}}^*_{\mathbf{z}_{i,1}} = \mathbf{g}_{i,1}\mathrm{J}^*_{\mathbf{z}_{i,1}}$.

By decomposing the term $\bar{\mathrm{J}}^*_{\mathbf{z}_{i,1}}$ into the following form:

$$\bar{\mathrm{J}}^*_{\mathbf{z}_{i,1}} \triangleq 2\mathrm{K}_{i,1}\mathbf{z}_{i,1} + \mathrm{J}^\circ_{i,1}(\zeta_{i,1}) + \mathbf{h}_{i,1}(\zeta_{i,1}) + 2\underline{\mathbf{g}}^{-1}_{i,1}\mathrm{w}_{i,1}\phi_{i,1} \tag{9}$$

where $\mathrm{K}_{i,1} > 0$, $\phi_{i,1} = \frac{(\mathrm{k}^{\mathrm{l}}_{i,1}+\mathrm{k}^{\mathrm{u}}_{i,1})^2\mathbf{z}_{i,1}}{(\mathrm{k}^{\mathrm{l}}_{i,1}+\mathbf{x}_{i,1})(\mathrm{k}^{\mathrm{u}}_{i,1}-\mathbf{x}_{i,1})}$ and $\mathrm{J}^\circ_{i,1}(\zeta_{i,1}) = -2\mathrm{K}_{i,1}\mathbf{z}_{i,1} - \mathbf{h}_{i,1}(\zeta_{i,1}) - 2\underline{\mathbf{g}}^{-1}_{i,1}\mathrm{w}_{i,1}\phi_{i,1} + \bar{\mathrm{J}}^*_{\mathbf{z}_{i,1}}$, $\mathbf{h}_{i,1}(\zeta_{i,1}) = 2\mathbf{f}_{i,1} - 2\mathbf{z}_{i,1}\dot{\mathbf{y}}_{i,\mathrm{d}}\eta_{i,1}/\phi_{i,1} + \sum_{\mathrm{s}=1}^{\mathrm{p}} 2^{2\mathrm{s}+1}\mathbf{q}_{\mathrm{l},1,i}|\mathbf{z}_{i,1}|^{2\mathrm{s}}/\phi_{i,1}$ with the input vector $\zeta_{i,1} = [\mathbf{x}_{i,1}, \mathbf{z}_{i,1}, \mathbf{y}_{i,\mathrm{d}}, \dot{\mathbf{y}}_{i,\mathrm{d}}]^{\mathrm{T}}$. (The detailed forms of $\mathbf{q}_{\mathrm{l},1,i}$ and $\eta_{i,1}$ refer to the subsequent section).

In what follows, $\mathrm{J}^\circ_{i,1}(\zeta_{i,1})$ and $\mathbf{h}_{i,1}(\zeta_{i,1})$ are abbreviated by $\mathrm{J}^\circ_{i,1}$ and $\mathbf{h}_{i,1}$, respectively.

Since these functions are both unknown but continuous, two independent neural networks would be utilized to approximate these uncertain terms as:

$$\mathrm{J}^\circ_{i,1} = \mathrm{W}^{*\mathrm{T}}_{\mathrm{J}_{i,1}}\mathrm{S}_{\mathrm{J}_{i,1}} + \epsilon_{\mathrm{J}_{i,1}}, \ |\epsilon_{\mathrm{J}_{i,1}}| \leq \bar{\epsilon}_{\mathrm{J}_{i,1}} \tag{10a}$$

$$\mathbf{h}_{i,1} = \mathrm{W}^{*\mathrm{T}}_{\mathbf{h}_{i,1}}\mathrm{S}_{\mathbf{h}_{i,1}} + \epsilon_{\mathbf{h}_{i,1}}, \ |\epsilon_{\mathbf{h}_{i,1}}| \leq \bar{\epsilon}_{\mathbf{h}_{i,1}} \tag{10b}$$

where $\mathrm{W}^{*\mathrm{T}}_{\mathrm{J}_{i,1}}$ and $\mathrm{W}^{*\mathrm{T}}_{\mathbf{h}_{i,1}}$ are the ideal weight vectors, $\mathrm{S}_{\mathrm{J}_{i,1}}$ and $\mathrm{S}_{\mathbf{h}_{i,1}}$ indicate the basis function vectors, while $\epsilon_{\mathrm{J}_{i,1}}$ and $\epsilon_{\mathbf{h}_{i,1}}$ stand for the approximation errors, respectively.

With this design, substituting the Eqs.(10a) and (10b) into the Eqs.(8) and (9), it derives that:

$$\begin{aligned} \bar{\mathrm{J}}^*_{\mathbf{z}_{i,1}} &= 2\mathrm{K}_{i,1}\mathbf{z}_{i,1} + \mathrm{W}^{*\mathrm{T}}_{\mathrm{J}_{i,1}}\mathrm{S}_{\mathrm{J}_{i,1}} + \epsilon_{\mathrm{J}_{i,1}} \\ &\quad + \mathrm{W}^{*\mathrm{T}}_{\mathbf{h}_{i,1}}\mathrm{S}_{\mathbf{h}_{i,1}} + \epsilon_{\mathbf{h}_{i,1}} + 2\underline{\mathbf{g}}^{-1}_{i,1}\mathrm{w}_{i,1}\phi_{i,1} \end{aligned} \tag{11a}$$

$$\begin{aligned} \mathbf{a}^*_{i,1} &= -\mathrm{K}_{i,1}\mathbf{z}_{i,1} - \frac{1}{2}\mathrm{W}^{*\mathrm{T}}_{\mathrm{J}_{i,1}}\mathrm{S}_{\mathrm{J}_{i,1}} - \frac{1}{2}\epsilon_{\mathrm{J}_{i,1}} \\ &\quad - \frac{1}{2}\mathrm{W}^{*\mathrm{T}}_{\mathbf{h}_{i,1}}\mathrm{S}_{\mathbf{h}_{i,1}} - \frac{1}{2}\epsilon_{\mathbf{h}_{i,1}} - \underline{\mathbf{g}}^{-1}_{i,1}\mathrm{w}_{i,1}\phi_{i,1} \end{aligned} \tag{11b}$$

Note that $\bar{\mathrm{J}}^*_{\mathbf{z}_{i,1}}$ and $\mathbf{a}^*_{i,1}$ are still unavailable due to the fact that $\mathrm{W}^*_{\mathrm{J}_{i,1}}$ and $\mathrm{W}^*_{\mathbf{h}_{i,1}}$ are unknown only for analysis purpose. Hence, the following critic-actor-identifier learning technique

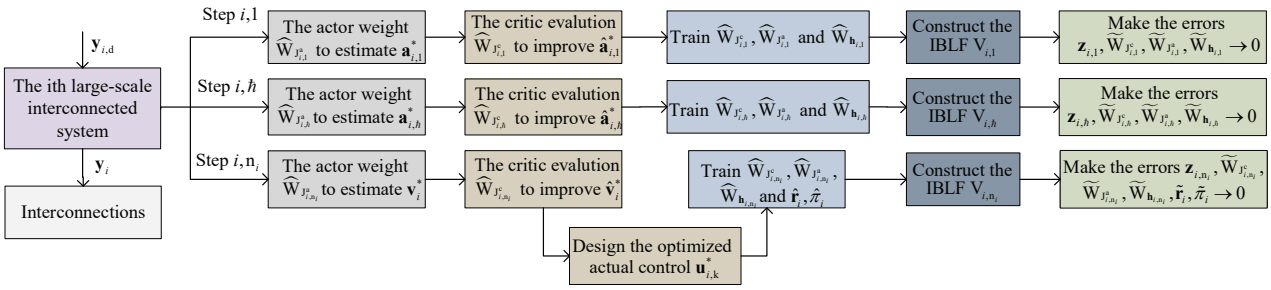

Fig. 1. The block diagram of the proposed learning-based optimal FTC design.

is implemented to separately evaluate the cost performance index, the control behavior and the unknown dynamic function:

$$\hat{\dot{\mathrm{J}}}^*_{\mathbf{z}_{i,1}} = 2\mathrm{K}_{i,1}\mathbf{z}_{i,1} + \hat{\mathrm{W}}^{\mathrm{T}}_{\mathrm{J}^{\mathrm{c}}_{i,1}}\mathrm{S}_{\mathrm{J}_{i,1}} + \hat{\mathrm{W}}^{\mathrm{T}}_{\mathbf{h}_{i,1}}\mathrm{S}_{\mathbf{h}_{i,1}} + 2\underline{\mathrm{g}}^{-1}_{i,1}\mathrm{w}_{i,1}\phi_{i,1} \tag{12a}$$

$$\hat{\mathbf{a}}^*_{i,1} = -\mathrm{K}_{i,1}\mathbf{z}_{i,1} - \frac{1}{2}\hat{\mathrm{W}}^{\mathrm{T}}_{\mathrm{J}^{\mathrm{a}}_{i,1}}\mathrm{S}_{\mathrm{J}_{i,1}} - \frac{1}{2}\hat{\mathrm{W}}^{\mathrm{T}}_{\mathbf{h}_{i,1}}\mathrm{S}_{\mathbf{h}_{i,1}} - \underline{\mathrm{g}}^{-1}_{i,1}\mathrm{w}_{i,1}\phi_{i,1} \tag{12b}$$

$$\hat{\mathbf{h}}_{i,1} = \hat{\mathrm{W}}^{\mathrm{T}}_{\mathbf{h}_{i,1}}\mathrm{S}_{\mathbf{h}_{i,1}} \tag{12c}$$

where $\hat{\mathrm{W}}_{\mathrm{J}^{\mathrm{c}}_{i,1}}$, $\hat{\mathrm{W}}_{\mathrm{J}^{\mathrm{a}}_{i,1}}$ and $\hat{\mathrm{W}}_{\mathbf{h}_{i,1}}$ separately denote the estimated critic, actor and identifier neural weight vectors.

The training laws of the above-mentioned neural weight vectors are given as:

$$\dot{\hat{\mathrm{W}}}_{\mathrm{J}^{\mathrm{c}}_{i,1}} = -\lambda^{\mathrm{c}}_{i,1}\bar{\mathrm{S}}_{\mathrm{J}_{i,1}}\hat{\mathrm{W}}_{\mathrm{J}^{\mathrm{c}}_{i,1}} \tag{13a}$$

$$\dot{\hat{\mathrm{W}}}_{\mathrm{J}^{\mathrm{a}}_{i,1}} = -\lambda^{\mathrm{a}}_{i,1}\bar{\mathrm{S}}_{\mathrm{J}_{i,1}}\hat{\mathrm{W}}_{\mathrm{J}^{\mathrm{a}}_{i,1}} + \bar{\lambda}_{i,1}\bar{\mathrm{S}}_{\mathrm{J}_{i,1}}\hat{\mathrm{W}}_{\mathrm{J}^{\mathrm{c}}_{i,1}} \tag{13b}$$

$$\dot{\hat{\mathrm{W}}}_{\mathbf{h}_{i,1}} = \Upsilon_{i,1}(\frac{1}{2}\phi_{i,1}\mathrm{S}_{\mathbf{h}_{i,1}} - \lambda^{\mathrm{d}}_{i,1}\hat{\mathrm{W}}_{\mathbf{h}_{i,1}}) \tag{13c}$$

where $\bar{\mathrm{S}}_{\mathrm{J}_{i,1}} = \mathrm{S}_{\mathrm{J}_{i,1}}\mathrm{S}^{\mathrm{T}}_{\mathrm{J}_{i,1}}$. $\Upsilon_{i,1}$ stands for a positive-definite matrix, $\lambda^{\mathrm{c}}_{i,1}$, $\lambda^{\mathrm{a}}_{i,1}$ and $\lambda^{\mathrm{d}}_{i,1}$ are positive constants to be designed later with $\bar{\lambda}_{i,1} = \lambda^{\mathrm{a}}_{i,1} - \lambda^{\mathrm{c}}_{i,1}$.

Remark 3.2. The optimal virtual control input $\hat{\mathbf{a}}^*_{i,1}$ is decomposed into a model-based part $-\mathrm{K}_{i,1}\mathbf{z}_{i,1} - \underline{\mathrm{g}}^{-1}_{i,1}\mathrm{w}_{i,1}\phi_{i,1}$ and a learning part $-\frac{1}{2}\hat{\mathrm{W}}^{\mathrm{T}}_{\mathrm{J}^{\mathrm{a}}_{i,1}}\mathrm{S}_{\mathrm{J}_{i,1}} - \frac{1}{2}\hat{\mathrm{W}}^{\mathrm{T}}_{\mathbf{h}_{i,1}}\mathrm{S}_{\mathbf{h}_{i,1}}$, by means of the asymmetric IBLF and the neural networks. For the learning part, the identifier training law is selected in conformity to the stability analysis, while the critic and actor training laws are chosen by the gradient-descent method as in [23], [40].

Remark 3.3. The existing results in [41], [42] need the persistent excitation (PE) condition to stabilize the system. In contrast, we illustrate that the Bellman residual error tends to zero regardless of the PE condition. This can also be verified by defining a function $\mathrm{E}_i = \mathrm{Tr}\{(\hat{\mathrm{W}}_{\mathrm{J}^{\mathrm{a}}_{i,1}} - \hat{\mathrm{W}}_{\mathrm{J}^{\mathrm{c}}_{i,1}})^{\mathrm{T}}(\hat{\mathrm{W}}_{\mathrm{J}^{\mathrm{a}}_{i,1}} - \hat{\mathrm{W}}_{\mathrm{J}^{\mathrm{c}}_{i,1}})\}$. It can be verified that $\mathrm{E}_i = 0$ and $\frac{\partial \mathrm{H}_{i,1}(\mathbf{z}_{i,1},\mathbf{a}_{i,1},\mathrm{J}_{\mathbf{z}_{i,1}})}{\partial \hat{\mathrm{W}}_{\mathrm{J}^{\mathrm{a}}_{i,1}}} = 0$ are equivalent. Since $\frac{\partial \mathrm{E}_i}{\partial \hat{\mathrm{W}}_{\mathrm{J}^{\mathrm{a}}_{i,1}}} = -\frac{\partial \mathrm{E}_i}{\partial \hat{\mathrm{W}}_{\mathrm{J}^{\mathrm{c}}_{i,1}}} = 2(\hat{\mathrm{W}}_{\mathrm{J}^{\mathrm{a}}_{i,1}} - \hat{\mathrm{W}}_{\mathrm{J}^{\mathrm{c}}_{i,1}})$, the time-derivative of E_i can be calculated as:

$$\begin{aligned}\dot{\mathrm{E}}_i &= \mathrm{Tr}\{\frac{\partial \mathrm{E}_i}{\partial \hat{\mathrm{W}}_{\mathrm{J}^{\mathrm{a}}_{i,1}}}\dot{\hat{\mathrm{W}}}_{\mathrm{J}^{\mathrm{a}}_{i,1}} + \frac{\partial \mathrm{E}_i}{\partial \hat{\mathrm{W}}_{\mathrm{J}^{\mathrm{c}}_{i,1}}}\dot{\hat{\mathrm{W}}}_{\mathrm{J}^{\mathrm{c}}_{i,1}}\} \\ &= -\frac{\lambda^{\mathrm{a}}_{i,1}}{2}\mathrm{Tr}\{\frac{\partial \mathrm{E}_i}{\partial \hat{\mathrm{W}}^{\mathrm{T}}_{\mathrm{J}^{\mathrm{a}}_{i,1}}}\bar{\mathrm{S}}_{\mathrm{J}_{i,1}}\frac{\partial \mathrm{E}_i}{\partial \hat{\mathrm{W}}_{\mathrm{J}^{\mathrm{a}}_{i,1}}}\} \le 0\end{aligned} \tag{14}$$

which implies that the learning laws of Eqs.(13a) and (13b) can ensure the satisfaction of (14), and the Bellman residual error can approach to zero independently of the PE condition.

Remark 3.4. The main advantages for the designed critic and actor training laws are: 1) it simplifies the design procedure in comparison to the existing optimal methods in [41], [42]; 2) it can reduce the computational complexity due to the unknown functions $\mathbf{f}_{i,1}(\bar{\mathbf{x}}_{i,1})$ and $\Delta_{i,1}(\bar{\mathbf{y}})$; 3) it enables to remove the PE condition commonly required in the optimal control.

Step $i,\hbar$. Similarly, the optimal function interrelated with the subsystem dynamic has the form as:

$$\begin{aligned}\mathrm{J}^*_{i,\hbar}(\mathbf{z}_{i,\hbar}) &= \min_{\mathbf{a}_{i,\hbar}\in\Psi_{i,\hbar}}\int_{\mathrm{t}}^{\infty}(\mathrm{M}_{i,\hbar}(\tau) + \mathbf{a}^2_{i,\hbar}(\tau))\mathrm{d}\tau \\ &= \int_{\mathrm{t}}^{\infty}(\mathrm{M}_{i,\hbar}(\tau) + \mathbf{a}^{*2}_{i,\hbar}(\tau))\mathrm{d}\tau\end{aligned} \tag{15}$$

where $\mathrm{M}_{i,\hbar}(\tau) = \int_0^{\mathbf{z}_{i,\hbar}(\tau)}\frac{(\mathrm{k}^{\mathrm{l}}_{i,\hbar}+\mathrm{k}^{\mathrm{u}}_{i,\hbar})^2\sigma_{i,\hbar}}{\mathrm{k}^{\mathrm{l}}_{i,\hbar}\mathrm{k}^{\mathrm{u}}_{i,\hbar}}\mathrm{d}\sigma_{i,\hbar}$, $\Psi_{i,\hbar}(\Omega_{\mathbf{x}}) = \{\mathbf{x}_{i,\hbar} : -\mathrm{k}^{\mathrm{l}}_{i,\hbar} \le \mathbf{x}_{i,\hbar} \le \mathrm{k}^{\mathrm{u}}_{i,\hbar}\}$ with $\bar{\mathrm{k}}^{\mathrm{l}}_{i,\hbar} = \mathrm{k}^{\mathrm{l}}_{i,\hbar} + \sigma_{i,\hbar} + \hat{\mathbf{a}}^*_{i,\hbar_i-1}$, $\bar{\mathrm{k}}^{\mathrm{u}}_{i,\hbar} = \mathrm{k}^{\mathrm{u}}_{i,\hbar} - \sigma_{i,\hbar} - \hat{\mathbf{a}}^*_{i,\hbar_i-1}$ and $\mathrm{k}^{\mathrm{l}}_{i,\hbar}$, $\mathrm{k}^{\mathrm{u}}_{i,\hbar} > 0$.

Then, the HJB equation is yielded as:

$$\begin{aligned}\mathrm{H}_{i,\hbar}(\mathbf{z}_{i,\hbar}, \mathbf{a}^*_{i,\hbar}, \mathrm{J}^*_{\mathbf{z}_{i,\hbar}}) = \mathrm{J}^*_{\mathbf{z}_{i,\hbar}}(\mathbf{g}_{i,\hbar}\mathbf{a}^*_{i,\hbar} + \mathbf{f}_{i,\hbar} + \Delta_{i,\hbar} \\ - \dot{\hat{\mathbf{a}}}^*_{i,\hbar-1}) + \mathrm{M}_{i,\hbar} + \mathbf{a}^{*2}_{i,\hbar}\end{aligned} \tag{16}$$

where $\mathrm{J}^*_{\mathbf{z}_{i,\hbar}} = \frac{\partial \mathrm{J}^*_{i,\hbar}(\mathbf{z}_{i,\hbar})}{\partial \mathbf{z}_{i,\hbar}}$.

Similar to the aforementioned step, settle with the condition $\frac{\partial \mathrm{H}_{i,\hbar}(\mathbf{z}_{i,\hbar},\mathbf{a}^*_{i,\hbar},\mathrm{J}^*_{\mathbf{z}_{i,\hbar}})}{\partial \mathbf{a}^*_{i,\hbar}} = 0$ to achieve the optimal virtual control input $\mathbf{a}^*_{i,\hbar}$ that yields to:

$$\mathbf{a}^*_{i,\hbar} = -\frac{\mathbf{g}_{i,\hbar}}{2}\mathrm{J}^*_{\mathbf{z}_{i,\hbar}} \triangleq -\frac{1}{2}\bar{\mathrm{J}}^*_{i,\hbar}(\mathbf{z}_{i,\hbar}) \tag{17}$$

and the term $\bar{\mathrm{J}}^*_{i,\hbar}(\mathbf{z}_{i,\hbar})$ is disintegrated as:

$$\begin{aligned}\bar{\mathrm{J}}^*_{i,\hbar}(\mathbf{z}_{i,\hbar}) \triangleq 2\mathrm{K}_{i,\hbar}\mathbf{z}_{i,\hbar} + \mathrm{J}^{\circ}_{i,\hbar}(\zeta_{i,\hbar}) + \mathbf{h}_{i,\hbar}(\zeta_{i,\hbar}) \\ + 2\underline{\mathrm{g}}^{-1}_{i,\hbar}(\mathrm{w}_{i,\hbar}\phi_{i,\hbar} + \bar{\mathbf{g}}_{i,\hbar-1}\mathbf{z}_{i,\hbar}\phi_{i,\hbar-1}/\phi_{i,\hbar})\end{aligned} \tag{18}$$

where $\mathrm{K}_{i,\hbar}$ is a positive constant, $\phi_{i,\hbar} = \frac{(\mathrm{k}^{\mathrm{l}}_{i,\hbar}+\mathrm{k}^{\mathrm{u}}_{i,\hbar})^2\mathbf{z}_{i,\hbar}}{(\mathrm{k}^{\mathrm{l}}_{i,\hbar}+\mathbf{x}_{i,\hbar})(\mathrm{k}^{\mathrm{u}}_{i,\hbar}-\mathbf{x}_{i,\hbar})}$. $\mathrm{J}^{\circ}_{i,\hbar}(\zeta_{i,\hbar}) = \bar{\mathrm{J}}^*_{i,\hbar}(\mathbf{z}_{i,\hbar}) - 2\mathrm{K}_{i,\hbar}\mathbf{z}_{i,\hbar} - \mathbf{h}_{i,\hbar}(\zeta_{i,\hbar}) - 2\underline{\mathrm{g}}^{-1}_{i,\hbar}(\mathrm{w}_{i,\hbar}\phi_{i,\hbar} + \bar{\mathbf{g}}_{i,\hbar-1}\phi_{i,\hbar-1}/\phi_{i,\hbar})$, $\mathbf{h}_{i,\hbar}(\zeta_{i,\hbar}) = 2\mathbf{f}_{i,\hbar} - 2\mathbf{z}_{i,\hbar}\dot{\hat{\mathbf{a}}}^*_{i,\hbar-1}\eta_{i,\hbar}/\phi_{i,\hbar} + \sum_{\mathrm{s}=1}^{\mathrm{p}} 2^{2\mathrm{s}+1}\mathbf{q}_{\mathrm{l},\hbar,i}|\mathbf{z}_{i,1}|^{2\mathrm{s}}/\phi_{i,\hbar}$ with $\zeta_{i,\hbar} = [\mathbf{x}_{i,\hbar}, \mathbf{z}_{i,1}, \mathbf{z}_{i,\hbar}, \hat{\mathbf{a}}^*_{i,\hbar-1}, \dot{\hat{\mathbf{a}}}^*_{i,\hbar-1}]^{\mathrm{T}}$.

By substituting the above Eqs.(17) and (18), we have the following critic-actor-identifier architecture:

$$\hat{\dot{\mathrm{J}}}^{*}_{i,\hbar} = 2\mathrm{K}_{i,\hbar}\mathbf{z}_{i,\hbar} + \hat{\mathrm{W}}^{\mathrm{T}}_{\mathrm{J}^{\mathrm{c}}_{i,\hbar}}\mathrm{S}_{\mathrm{J}_{i,\hbar}} + \hat{\mathrm{W}}^{\mathrm{T}}_{\mathbf{h}_{i,\hbar}}\mathrm{S}_{\mathbf{h}_{i,\hbar}} + 2\underline{\mathbf{g}}^{-1}_{i,\hbar}(\mathrm{w}_{i,\hbar}\phi_{i,\hbar} + \overline{\mathbf{g}}_{i,\hbar-1}\mathbf{z}_{i,\hbar}\phi_{i,\hbar-1}/\phi_{i,\hbar}) \tag{19a}$$

$$\hat{\mathbf{a}}^{*}_{i,\hbar} = -\mathrm{K}_{i,\hbar}\mathbf{z}_{i,\hbar} - \frac{1}{2}\hat{\mathrm{W}}^{\mathrm{T}}_{\mathrm{J}^{\mathrm{c}}_{i,\hbar}}\mathrm{S}_{\mathrm{J}_{i,\hbar}} - \frac{1}{2}\hat{\mathrm{W}}^{\mathrm{T}}_{\mathbf{h}_{i,\hbar}}\mathrm{S}_{\mathbf{h}_{i,\hbar}} - \underline{\mathbf{g}}^{-1}_{i,\hbar}(\mathrm{w}_{i,\hbar}\phi_{i,\hbar} + \overline{\mathbf{g}}_{i,\hbar-1}\mathbf{z}_{i,\hbar}\phi_{i,\hbar-1}/\phi_{i,\hbar}) \tag{19b}$$

$$\hat{\mathbf{h}}_{i,\hbar} = \hat{\mathrm{W}}^{\mathrm{T}}_{\mathbf{h}_{i,\hbar}}\mathrm{S}_{\mathbf{h}_{i,\hbar}} \tag{19c}$$

where $\hat{\mathrm{W}}_{\mathrm{J}^{\mathrm{c}}_{i,\hbar}}$, $\hat{\mathrm{W}}_{\mathrm{J}^{\mathrm{a}}_{i,\hbar}}$ and $\hat{\mathrm{W}}_{\mathbf{h}_{i,\hbar}}$ represent the networks weight vectors, respectively.

The training laws of the critic, actor and identifier networks weights are constructed as:

$$\dot{\hat{\mathrm{W}}}_{\mathrm{J}^{\mathrm{c}}_{i,\hbar}} = -\lambda^{\mathrm{c}}_{i,\hbar}\bar{\mathrm{S}}_{\mathrm{J}_{i,\hbar}}\hat{\mathrm{W}}_{\mathrm{J}^{\mathrm{c}}_{i,\hbar}} \tag{20a}$$

$$\dot{\hat{\mathrm{W}}}_{\mathrm{J}^{\mathrm{a}}_{i,\hbar}} = -\lambda^{\mathrm{a}}_{i,\hbar}\bar{\mathrm{S}}_{\mathrm{J}_{i,\hbar}}\hat{\mathrm{W}}_{\mathrm{J}^{\mathrm{a}}_{i,\hbar}} + \bar{\lambda}_{i,\hbar}\bar{\mathrm{S}}_{\mathrm{J}_{i,\hbar}}\hat{\mathrm{W}}_{\mathrm{J}^{\mathrm{c}}_{i,\hbar}} \tag{20b}$$

$$\dot{\hat{\mathrm{W}}}_{\mathbf{h}_{i,\hbar}} = \Upsilon_{i,\hbar}\big(\frac{1}{2}\phi_{\mathbf{h}_{i,\hbar}}\mathrm{S}_{\mathbf{h}_{i,\hbar}} - \lambda^{\mathrm{d}}_{i,\hbar}\hat{\mathrm{W}}_{\mathbf{h}_{i,\hbar}}\big) \tag{20c}$$

where $\bar{\mathrm{S}}_{\mathrm{J}_{i,\hbar}} = \mathrm{S}_{\mathrm{J}_{i,\hbar}}\mathrm{S}^{\mathrm{T}}_{\mathrm{J}_{i,\hbar}}$. $\lambda^{\mathrm{c}}_{i,\hbar}$, $\lambda^{\mathrm{a}}_{i,\hbar}$ and $\lambda^{\mathrm{d}}_{i,\hbar}$ denote designed parameters with $\bar{\lambda}_{i,\hbar} = \lambda^{\mathrm{a}}_{i,\hbar} - \lambda^{\mathrm{c}}_{i,\hbar}$, and $\Upsilon_{i,\hbar}$ is a positive-definite matrix with appropriate dimension.

Step i, n_i. According to Eq.(5), the following tracking error dynamics can be acquired in the presence of the actuator fault:

$$\dot{\mathbf{z}}_{i,\mathrm{n}_i} = \sum\nolimits_{\mathrm{k}=1}^{\mathrm{m}_i}\mathbf{g}^{\mathrm{k}}_{i,\mathrm{n}_i}(\psi^{\mathrm{h}}_{i,\mathrm{k}}\mathbf{u}_{i,\mathrm{k}} + \zeta^{\mathrm{h}}_{i,\mathrm{k}}) - \mathbf{v}_i + \mathbf{v}_i + \mathbf{f}_{i,\mathrm{n}_i} + \Delta_{i,\mathrm{n}_i} - \dot{\hat{\mathbf{a}}}^{*}_{i,\mathrm{n}_i-1} \tag{21}$$

where $\mathbf{v}_i$ is an intermediate controller to be designed.

Now, we denote $\mathbf{s}_i = \inf_{\mathrm{t}\geq 0}\{\sum_{\mathrm{k}=1}^{\mathrm{m}_i}|\mathbf{g}^{\mathrm{k}}_{i,\mathrm{n}_i}|\psi^{\mathrm{h}}_{i,\mathrm{k}}\}$, $\mathbf{r}_i = 1/\mathbf{s}_i$ and $\pi_i = \sup_{\mathrm{t}\geq 0}\{\sum_{\mathrm{k}=1}^{\mathrm{m}_i}\mathbf{g}^{\mathrm{k}}_{i,\mathrm{n}_i}\zeta^{\mathrm{h}}_{i,\mathrm{k}}\}$, which will be estimated by the designed updating laws.

Subsequently, the form of the optimal performance index function is obtained as:

$$\mathrm{J}^{*}_{i,\mathrm{n}_i}(\mathbf{z}_{i,\mathrm{n}_i}) = \min_{\mathbf{a}_{i,\mathrm{n}_i}\in\Psi_{i,\mathrm{n}_i}}\int_{\mathrm{t}}^{\infty}(\mathrm{M}_{i,\mathrm{n}_i}(\tau) + \mathbf{v}^2_i(\tau))\mathrm{d}\tau = \int_{\mathrm{t}}^{\infty}(\mathrm{M}_{i,\mathrm{n}_i}(\tau) + \mathbf{v}^{*2}_i(\tau))\mathrm{d}\tau \tag{22}$$

with $\mathrm{M}_{i,\mathrm{n}_i}(\tau) = \int_0^{\mathbf{z}_{i,\mathrm{n}_i}(\tau)}\frac{(\mathrm{k}^{\mathrm{l}}_{i,\mathrm{n}_i}+\mathrm{k}^{\mathrm{u}}_{i,\mathrm{n}_i})^2\sigma_{i,\mathrm{n}_i}}{\mathrm{k}^{\mathrm{l}}_{i,\mathrm{n}_i}\mathrm{k}^{\mathrm{u}}_{i,\mathrm{n}_i}}\mathrm{d}\sigma_{i,\mathrm{n}_i}$ with $\bar{\mathrm{k}}^{\mathrm{l}}_{i,\mathrm{n}_i} = \mathrm{k}^{\mathrm{l}}_{i,\mathrm{n}_i} + \sigma_{i,\mathrm{n}_i} + \hat{\mathbf{a}}^{*}_{i,\mathrm{n}_i-1}$, $\bar{\mathrm{k}}^{\mathrm{u}}_{i,\mathrm{n}_i} = \mathrm{k}^{\mathrm{u}}_{i,\mathrm{n}_i} - \sigma_{i,\mathrm{n}_i} - \hat{\mathbf{a}}^{*}_{i,\mathrm{n}_i-1}$, and $\mathrm{k}^{\mathrm{l}}_{i,\mathrm{n}_i}$, $\mathrm{k}^{\mathrm{u}}_{i,\mathrm{n}_i}$ are known positive constants.

Thus, the HJB equation becomes:

$$\mathrm{H}_{i,\mathrm{n}_i}(\mathbf{z}_{i,\mathrm{n}_i}, \mathbf{v}^{*}_i, \mathrm{J}^{*}_{\mathbf{z}_{i,\mathrm{n}_i}}) = \mathrm{J}^{*}_{\mathbf{z}_{i,\mathrm{n}_i}}\big(\mathbf{f}_{i,\mathrm{n}_i} + \Delta_{i,\mathrm{n}_i} - \mathbf{v}^{*}_i + \sum\nolimits_{\mathrm{k}=1}^{\mathrm{m}_i}\mathbf{g}^{\mathrm{k}}_{i,\mathrm{n}_i}(\psi^{\mathrm{h}}_{i,\mathrm{k}}\mathbf{u}_{i,\mathrm{k}} + \zeta^{\mathrm{h}}_{i,\mathrm{k}}) + \mathbf{v}_i - \dot{\hat{\mathbf{a}}}^{*}_{i,\mathrm{n}_i-1}\big) + \mathrm{M}_{i,\mathrm{n}_i} + \mathbf{v}^{*2}_i \tag{23}$$

where $\mathrm{J}^{*}_{\mathbf{z}_{i,\mathrm{n}_i}} = \frac{\mathrm{J}^{*}_{i,\mathrm{n}_i}(\mathbf{z}_{i,\mathrm{n}_i})}{\partial\mathbf{z}_{i,\mathrm{n}_i}}$. By solving $\frac{\mathrm{H}_{i,\mathrm{n}_i}(\mathbf{z}_{i,\mathrm{n}_i},\mathbf{v}^{*}_i,\mathrm{J}^{*}_{\mathbf{z}_{i,\mathrm{n}_i}})}{\partial\mathbf{v}^{*}_i} = 0$, it derives that $\mathbf{v}^{*}_i = \frac{1}{2}\mathrm{J}^{*}_{\mathbf{z}_{i,\mathrm{n}_i}}$.

To achieve the optimal FTC, the term $\mathrm{J}^{*}_{\mathbf{z}_{i,\mathrm{n}_i}}$ will be decoupled into:

$$\mathrm{J}^{*}_{\mathbf{z}_{i,\mathrm{n}_i}} \triangleq 2\mathrm{K}_{i,\mathrm{n}_i}\mathbf{z}_{i,\mathrm{n}_i} + \mathrm{J}^{\circ}_{i,\mathrm{n}_i}(\zeta_{i,\mathrm{n}_i}) + \mathbf{h}_{i,\mathrm{n}_i}(\zeta_{i,\mathrm{n}_i}) + 2\mathrm{w}_{i,\mathrm{n}_i}\phi_{i,\mathrm{n}_i} + 2\pi_i\tanh(\phi_{i,\mathrm{n}_i}/\varepsilon_i) + 2\overline{\mathbf{g}}_{i,\mathrm{n}_i-1}\mathbf{z}_{i,\mathrm{n}_i}\phi_{i,\mathrm{n}_i-1}/\phi_{i,\mathrm{n}_i} \tag{24}$$

where $\mathrm{K}_{i,\mathrm{n}_i} > 0$, $\phi_{i,\mathrm{n}_i} = \frac{(\mathrm{k}^{\mathrm{l}}_{i,\mathrm{n}_i}+\mathrm{k}^{\mathrm{u}}_{i,\mathrm{n}_i})^2\mathbf{z}_{i,\mathrm{n}_i}}{(\mathrm{k}^{\mathrm{l}}_{i,\mathrm{n}_i}+\mathbf{x}_{i,\mathrm{n}_i})(\mathrm{k}^{\mathrm{u}}_{i,\mathrm{n}_i}-\mathbf{x}_{i,\mathrm{n}_i})}$. $\mathrm{J}^{\circ}_{i,\mathrm{n}_i}(\zeta_{i,\mathrm{n}_i}) = \mathrm{J}^{*}_{\mathbf{z}_{i,\mathrm{n}_i}} - 2\mathrm{K}_{i,\mathrm{n}_i}\mathbf{z}_{i,\mathrm{n}_i} - \mathbf{h}_{i,\mathrm{n}_i}(\zeta_{i,\mathrm{n}_i}) - 2\pi_i\tanh(\phi_{i,\mathrm{n}_i}/\varepsilon_i) - 2\overline{\mathbf{g}}_{i,\mathrm{n}_i-1}\mathbf{z}_{i,\mathrm{n}_i}\phi_{i,\mathrm{n}_i-1}/\phi_{i,\mathrm{n}_i} - 2\mathrm{w}_{i,\mathrm{n}_i}\phi_{i,\mathrm{n}_i}$, $\mathbf{h}_{i,\mathrm{n}_i}(\zeta_{i,\mathrm{n}_i}) = 2\mathbf{f}_{i,\mathrm{n}_i} - 2\mathbf{z}_{i,\mathrm{n}_i}\dot{\hat{\mathbf{a}}}^{*}_{i,\mathrm{n}_i-1}\eta_{i,\mathrm{n}_i}/\phi_{i,\mathrm{n}_i} + \sum_{\mathrm{s}=1}^{\mathrm{p}}2^{2\mathrm{s}+1}\mathbf{q}_{\mathrm{l},\mathrm{n}_i,i}|\mathbf{z}_{i,1}|^{2\mathrm{s}}/\phi_{i,\mathrm{n}_i}$ with $\zeta_{i,\mathrm{n}_i} = [\mathbf{x}_{i,\mathrm{n}_i}, \mathbf{z}_{i,1}, \mathbf{z}_{i,\mathrm{n}_i}, \hat{\mathbf{a}}^{*}_{i,\mathrm{n}_i-1}, \dot{\hat{\mathbf{a}}}^{*}_{i,\mathrm{n}_i-1}]^{\mathrm{T}}$.

Similar to the previous steps, the learning method is carried out in the following to obtain the required control. The critic, actor and identifier neural networks and their's updating laws are separately designed as below:

$$\hat{\mathrm{J}}^{*}_{\mathbf{z}_{i,\mathrm{n}_i}} = 2\mathrm{K}_{i,\mathrm{n}_i}\mathbf{z}_{i,\mathrm{n}_i} + \hat{\mathrm{W}}^{\mathrm{T}}_{\mathrm{J}^{\mathrm{c}}_{i,\mathrm{n}_i}}\mathrm{S}_{\mathrm{J}_{i,\mathrm{n}_i}} + \hat{\mathrm{W}}^{\mathrm{T}}_{\mathbf{h}_{i,\mathrm{n}_i}}\mathrm{S}_{\mathbf{h}_{i,\mathrm{n}_i}} + 2\mathrm{w}_{i,\mathrm{n}_i}\phi_{i,\mathrm{n}_i} + 2\hat{\pi}_i\tanh(\phi_{i,\mathrm{n}_i}/\varepsilon_i) + 2\overline{\mathbf{g}}_{i,\mathrm{n}_i-1}\mathbf{z}_{i,\mathrm{n}_i}\phi_{i,\mathrm{n}_i-1}/\phi_{i,\mathrm{n}_i} \tag{25a}$$

$$\hat{\mathbf{v}}^{*}_i = \mathrm{K}_{i,\mathrm{n}_i}\mathbf{z}_{i,\mathrm{n}_i} + \frac{1}{2}\hat{\mathrm{W}}^{\mathrm{T}}_{\mathrm{J}^{\mathrm{c}}_{i,\mathrm{n}_i}}\mathrm{S}_{\mathrm{J}_{i,\mathrm{n}_i}} + \frac{1}{2}\hat{\mathrm{W}}^{\mathrm{T}}_{\mathbf{h}_{i,\mathrm{n}_i}}\mathrm{S}_{\mathbf{h}_{i,\mathrm{n}_i}} + \mathrm{w}_{i,\mathrm{n}_i}\phi_{i,\mathrm{n}_i} + \hat{\pi}_i\tanh(\phi_{i,\mathrm{n}_i}/\varepsilon_i) + \overline{\mathbf{g}}_{i,\mathrm{n}_i-1}\mathbf{z}_{i,\mathrm{n}_i}\phi_{i,\mathrm{n}_i-1}/\phi_{i,\mathrm{n}_i} \tag{25b}$$

$$\hat{\mathbf{h}}_{i,\mathrm{n}_i} = \hat{\mathrm{W}}^{\mathrm{T}}_{\mathbf{h}_{i,\mathrm{n}_i}}\mathrm{S}_{\mathbf{h}_{i,\mathrm{n}_i}} \tag{25c}$$

and

$$\dot{\hat{\mathrm{W}}}_{\mathrm{J}^{\mathrm{c}}_{i,\mathrm{n}_i}} = -\lambda^{\mathrm{c}}_{i,\mathrm{n}_i}\bar{\mathrm{S}}_{\mathrm{J}_{i,\mathrm{n}_i}}\hat{\mathrm{W}}_{\mathrm{J}^{\mathrm{c}}_{i,\mathrm{n}_i}} \tag{26a}$$

$$\dot{\hat{\mathrm{W}}}_{\mathrm{J}^{\mathrm{a}}_{i,\mathrm{n}_i}} = -\lambda^{\mathrm{a}}_{i,\mathrm{n}_i}\bar{\mathrm{S}}_{\mathrm{J}_{i,\mathrm{n}_i}}\hat{\mathrm{W}}_{\mathrm{J}^{\mathrm{a}}_{i,\mathrm{n}_i}} + \bar{\lambda}_{i,\mathrm{n}_i}\bar{\mathrm{S}}_{\mathrm{J}_{i,\mathrm{n}_i}}\hat{\mathrm{W}}_{\mathrm{J}^{\mathrm{c}}_{i,\mathrm{n}_i}} \tag{26b}$$

$$\dot{\hat{\mathrm{W}}}_{\mathbf{h}_{i,\mathrm{n}_i}} = \Upsilon_{i,\mathrm{n}_i}\big(\frac{1}{2}\phi_{i,\mathrm{n}_i}\mathrm{S}_{\mathbf{h}_{i,\mathrm{n}_i}} - \lambda^{\mathrm{d}}_{i,\mathrm{n}_i}\hat{\mathrm{W}}_{\mathbf{h}_{i,\mathrm{n}_i}}\big) \tag{26c}$$

where $\bar{\mathrm{S}}_{\mathrm{J}_{i,\mathrm{n}_i}} = \mathrm{S}_{\mathrm{J}_{i,\mathrm{n}_i}}\mathrm{S}^{\mathrm{T}}_{\mathrm{J}_{i,\mathrm{n}_i}}$. $\hat{\mathrm{W}}_{\mathrm{J}^{\mathrm{c}}_{i,\mathrm{n}_i}}$, $\hat{\mathrm{W}}_{\mathrm{J}^{\mathrm{a}}_{i,\mathrm{n}_i}}$ and $\hat{\mathrm{W}}_{\mathbf{h}_{i,\mathrm{n}_i}}$ indicate the neural network weights, $\lambda^{\mathrm{c}}_{i,\mathrm{n}_i}$, $\lambda^{\mathrm{a}}_{i,\mathrm{n}_i}$ and $\lambda^{\mathrm{d}}_{i,\mathrm{n}_i}$ are the designed constants with $\bar{\lambda}_{i,\mathrm{n}_i} = \lambda^{\mathrm{a}}_{i,\mathrm{n}_i} - \lambda^{\mathrm{c}}_{i,\mathrm{n}_i}$, and $\Upsilon_{i,\mathrm{n}_i}$ is a positive-definite matrix.

Furthermore, the optimized actual control input is:

$$\mathbf{u}^{*}_{i,\mathrm{k}} = -\mathrm{sign}(\mathbf{g}^{\mathrm{k}}_{i,\mathrm{n}_i})\frac{\hat{\mathbf{v}}^{*2}_i\hat{\mathbf{r}}^{2}_i\phi_{i,\mathrm{n}_i}}{\sqrt{\epsilon^{2}_{i,1} + \hat{\mathbf{v}}^{*2}_i\hat{\mathbf{r}}^{2}_i\phi^{2}_{i,\mathrm{n}_i}}} \tag{27}$$

where $\epsilon_{i,1} > 0$. Also, the updating laws of the two unknown parameters $\mathbf{r}_i$, π_i are given as:

$$\dot{\hat{\mathbf{r}}}_i = \bar{\Upsilon}_{i,1}(\phi_{i,\mathrm{n}_i}\hat{\mathbf{v}}^{*}_i - \epsilon_{i,2}\hat{\mathbf{r}}_i) \tag{28a}$$

$$\dot{\hat{\pi}}_i = \bar{\Upsilon}_{i,2}(\phi_{i,\mathrm{n}_i}\tanh(\phi_{i,\mathrm{n}_i}/\varepsilon_i) - \epsilon_{i,3}\hat{\pi}_i) \tag{28b}$$

where $\epsilon_{i,2} > 0$, $\epsilon_{i,3} > 0$, and $\bar{\Upsilon}_{i,1}$, $\bar{\Upsilon}_{i,2}$ denote the positive-definite matrices.

Remark 3.5. The proposed design algorithm includes the following procedures: 1) the formulated system controlled by optimizing the virtual input in each $\mathrm{n}_i - 1$ dimension and the actual input in the n_i dimension with asymmetric constraints; 2) the critic-actor-identifier framework is used to approximate the control policy, the value index and the nonlinear function, respectively; 3) with the defined condition for the principle of Bellman optimality, the actor/critic/identifier training laws are designed in accordance with the stability analysis; 4) by iterative updating the neural networks, the HJB equation and the optimality are finally satisfied.

IV. Stability Analysis

At this stage, the optimal FTC approach is realized for system (1) with state-constraints, that the boundedness of the signal is guaranteed in the sense of asymmetric IBLF, and the system output can track the desired signal well.

Theorem 4.1. Consider the LSIS with intermittent actuator faults (1). With the critic-actor-identifier framework (13), (20) and (26), the virtual control inputs (12b), (19b) and the actual control input (27) can be optimized to satisfy the principle of Bellman optimality in each step.

Proof: In accordance with the aforementioned control design, the stability analysis is also divided into three steps.

Step $i.1$. Construct the integral-type Lyapunov functional candidate for the $\mathbf{z}_{i,1}$-subsystem as below:

$$\begin{aligned}\mathrm{V}_{i,1} = &\int_0^{\mathbf{z}_{i,1}} \frac{(\mathrm{k}^{\mathrm{l}}_{i,1}+\mathrm{k}^{\mathrm{u}}_{i,1})^2\sigma_{i,1}}{\bar{\mathrm{k}}^{\mathrm{l}}_{i,1}\bar{\mathrm{k}}^{\mathrm{u}}_{i,1}}\mathrm{d}\sigma_{i,1} + \frac{1}{2}\tilde{\mathrm{W}}^{\mathrm{T}}_{\mathrm{J}^{\mathrm{c}}_{i,1}}\tilde{\mathrm{W}}_{\mathrm{J}^{\mathrm{c}}_{i,1}} \\ &+ \frac{1}{2}\tilde{\mathrm{W}}^{\mathrm{T}}_{\mathrm{J}^{\mathrm{a}}_{i,1}}\tilde{\mathrm{W}}_{\mathrm{J}^{\mathrm{a}}_{i,1}} + \frac{1}{2}\tilde{\mathrm{W}}^{\mathrm{T}}_{\mathbf{h}_{i,1}}\Upsilon^{-1}_{i,1}\tilde{\mathrm{W}}_{\mathbf{h}_{i,1}}\end{aligned} \tag{29}$$

where $\tilde{\mathrm{W}}_{\mathrm{J}^{\mathrm{c}}_{i,1}} = \hat{\mathrm{W}}_{\mathrm{J}^{\mathrm{c}}_{i,1}} - \mathrm{W}^*_{\mathrm{J}_{i,1}}$, $\tilde{\mathrm{W}}_{\mathrm{J}^{\mathrm{a}}_{i,1}} = \hat{\mathrm{W}}_{\mathrm{J}^{\mathrm{a}}_{i,1}} - \mathrm{W}^*_{\mathrm{J}_{i,1}}$ and $\tilde{\mathrm{W}}_{\mathbf{h}_{i,1}} = \hat{\mathrm{W}}_{\mathbf{h}_{i,1}} - \mathrm{W}^*_{\mathbf{h}_{i,1}}$ depict the networks weights errors.

According to the condition $\mathbf{z}_{i,2} = \mathbf{x}_{i,2} - \hat{\mathbf{a}}^*_{i,1}$, the derivative of $\mathrm{V}_{i,1}$ along with time is:

$$\begin{aligned}\dot{\mathrm{V}}_{i,1} = &\phi_{i,1}(\mathbf{g}_{i,1}(\mathbf{z}_{i,2}+\hat{\mathbf{a}}^*_{i,1}) + \mathbf{f}_{i,1} + \Delta_{i,1} - \dot{\mathbf{y}}_{i,\mathrm{d}}) \\ &+ \dot{\mathbf{y}}_{i,\mathrm{d}}(\phi_{i,1} - \mathbf{z}_{i,1}\eta_{i,1}) + \tilde{\mathrm{W}}^{\mathrm{T}}_{\mathrm{J}^{\mathrm{c}}_{i,1}}\dot{\hat{\mathrm{W}}}_{\mathrm{J}^{\mathrm{c}}_{i,1}} \\ &+ \tilde{\mathrm{W}}^{\mathrm{T}}_{\mathrm{J}^{\mathrm{a}}_{i,1}}\dot{\hat{\mathrm{W}}}_{\mathrm{J}^{\mathrm{a}}_{i,1}} + \tilde{\mathrm{W}}^{\mathrm{T}}_{\mathbf{h}_{i,1}}\Upsilon^{-1}_{i,1}\dot{\hat{\mathrm{W}}}_{\mathbf{h}_{i,1}}\end{aligned} \tag{30}$$

where $\eta_{i,1} = \frac{\mathrm{k}^{\mathrm{l}}_{i,1}+\mathrm{k}^{\mathrm{u}}_{i,1}}{\mathbf{z}_{i,1}}\ln\frac{(\mathrm{k}^{\mathrm{l}}_{i,1}+\mathrm{x}_{i,1})(\mathrm{k}^{\mathrm{u}}_{i,1}-\mathrm{y}_{i,\mathrm{d}})}{(\mathrm{k}^{\mathrm{u}}_{i,1}-\mathrm{x}_{i,1})(\mathrm{k}^{\mathrm{l}}_{i,1}+\mathrm{y}_{i,\mathrm{d}})}$.

From the Assumption 2.2 and the Lemma 2.2, one has:

$$\phi_{i,1}\Delta_{i,1} \le \frac{1}{4}\phi^2_{i,1} + \sum\nolimits_{\mathrm{s}=1}^{\mathrm{p}} 2^{2\mathrm{s}}\mathbf{q}_{\mathrm{l},1,i}(|\mathbf{z}_{i,1}|^{2\mathrm{s}} + |\mathbf{y}_{i,\mathrm{d}}|^{2\mathrm{s}}) \tag{31}$$

where $\mathbf{q}_{\mathrm{l},1,i} = \mathrm{Np}\sum_{\mathrm{l}=1}^{\mathrm{N}}\mathrm{q}^{2\mathrm{s}}_{i,1,\mathrm{l}}$.

Substituting $\hat{\mathbf{a}}^*_{i,1}$ in Eq.(12b) into $\dot{\mathrm{V}}_{i,1}$, it becomes:

$$\begin{aligned}\dot{\mathrm{V}}_{i,1} \le &-\underline{\mathbf{g}}_{i,1}\mathrm{K}_{i,1}\phi_{i,1}\mathbf{z}_{i,1} + \overline{\mathbf{g}}_{i,1}\phi_{i,1}\mathbf{z}_{i,2} + \varpi_{i,1} \\ &- (\mathrm{w}_{i,1} - \frac{1}{2} - \frac{\overline{\mathbf{g}}_{i,1}}{4})\phi^2_{i,1} - (\lambda^{\mathrm{c}}_{i,1} - \frac{\lambda^{\mathrm{a}}_{i,1}}{2})(\hat{\mathrm{W}}^{\mathrm{T}}_{\mathrm{J}^{\mathrm{c}}_{i,1}}\mathrm{S}_{\mathrm{J}_{i,1}})^2 \\ &- (\frac{\lambda^{\mathrm{a}}_{i,1}}{2} - \frac{\overline{\mathbf{g}}_{i,1}}{4})(\hat{\mathrm{W}}^{\mathrm{T}}_{\mathrm{J}^{\mathrm{a}}_{i,1}}\mathrm{S}_{\mathrm{J}_{i,1}})^2 - \frac{\lambda^{\mathrm{c}}_{i,1}\lambda^{\min}_{\bar{\mathrm{S}}_{i,1}}}{2}\tilde{\mathrm{W}}^{\mathrm{T}}_{\mathrm{J}^{\mathrm{c}}_{i,1}}\tilde{\mathrm{W}}_{\mathrm{J}^{\mathrm{c}}_{i,1}} \\ &- \frac{\lambda^{\mathrm{c}}_{i,1}\lambda^{\min}_{\bar{\mathrm{S}}_{i,1}}}{2}\tilde{\mathrm{W}}^{\mathrm{T}}_{\mathrm{J}^{\mathrm{a}}_{i,1}}\tilde{\mathrm{W}}_{\mathrm{J}^{\mathrm{a}}_{i,1}} - \frac{\lambda^{\mathrm{d}}_{i,1}}{2\lambda^{\max}_{\Upsilon_{i,1}}}\tilde{\mathrm{W}}^{\mathrm{T}}_{\mathbf{h}_{i,1}}\Upsilon^{-1}_{i,1}\tilde{\mathrm{W}}_{\mathbf{h}_{i,1}}\end{aligned} \tag{32}$$

where $\varpi_{i,1} = \frac{1}{4}\bar{\epsilon}^2_{\mathbf{h}_{i,1}} + \sum_{\mathrm{s}=1}^{\mathrm{p}} 2^{2\mathrm{s}}\mathbf{q}_{\mathrm{l},1,i}|\mathbf{y}_{i,\mathrm{d}}|^{2\mathrm{s}} + (\lambda^{\mathrm{a}}_{i,1} + \lambda^{\mathrm{c}}_{i,1})\lambda^{\max}_{\mathrm{S}}\mathrm{W}^{*\mathrm{T}}_{\mathrm{J}_{i,1}}\mathrm{W}^*_{\mathrm{J}_{i,1}}/2 + \lambda^{\mathrm{d}}_{i,1}\mathrm{W}^{*\mathrm{T}}_{\mathbf{h}_{i,1}}\mathrm{W}^*_{\mathbf{h}_{i,1}}/2$. $\lambda^{\min}_{\bar{\mathrm{S}}_{i,1}}$ and $\lambda^{\max}_{\Upsilon_{i,1}}$ depict the minimal and maximal eigenvalues of $\bar{\mathrm{S}}_{\mathrm{J}_{i,1}}$ and $\Upsilon^{-1}_{i,1}$.

Note that there is $\int_0^{\mathbf{z}_{i,1}} \frac{(\mathrm{k}^{\mathrm{l}}_{i,1}+\mathrm{k}^{\mathrm{u}}_{i,1})^2\sigma_{i,1}}{\bar{\mathrm{k}}^{\mathrm{l}}_{i,1}\bar{\mathrm{k}}^{\mathrm{u}}_{i,1}}\mathrm{d}\sigma_{i,1} \le \phi_{i,1}\mathbf{z}_{i,1}$ holds in [43], it implies that if we select the constants $\lambda^{\mathrm{a}}_{i,1}$ and $\mathrm{w}_{i,1}$ satisfy the following conditions:

$$\lambda^{\mathrm{a}}_{i,1} \ge \frac{\overline{\mathbf{g}}_{i,1}}{2},\ \mathrm{w}_{i,1} \ge \frac{1}{2} + \frac{\overline{\mathbf{g}}_{i,1}}{4} \tag{33}$$

then $\dot{\mathrm{V}}_{i,1}$ can be rewritten as:

$$\dot{\mathrm{V}}_{i,1} \le -\bar{\mathrm{K}}_{i,1}\mathrm{V}_{i,1} + \varpi_{i,1} + \overline{\mathbf{g}}_{i,1}\phi_{i,1}\mathbf{z}_{i,2} \tag{34}$$

with $\bar{\mathrm{K}}_{i,1} = \min\{\underline{\mathbf{g}}_{i,1}\mathrm{K}_{i,1}, \lambda^{\mathrm{c}}_{i,1}\lambda^{\min}_{\mathrm{S}}/2, \lambda^{\mathrm{d}}_{i,1}/2\lambda^{\max}_{\Upsilon_{i,1}}\}$.

Step $i.\hbar$. Similarly, the Lyapunov functional has the form:

$$\begin{aligned}\mathrm{V}_{i,\hbar} = &\sum_{\kappa=1}^{\hbar-1}\mathrm{V}_{i,\kappa} + \int_0^{\mathbf{z}_{i,\hbar}} \frac{(\mathrm{k}^{\mathrm{l}}_{i,\hbar}+\mathrm{k}^{\mathrm{u}}_{i,\hbar})^2\sigma_{i,\hbar}}{\bar{\mathrm{k}}^{\mathrm{l}}_{i,\hbar}\bar{\mathrm{k}}^{\mathrm{u}}_{i,\hbar}}\mathrm{d}\sigma_{i,\hbar} \\ &+ \frac{1}{2}\tilde{\mathrm{W}}^{\mathrm{T}}_{\mathrm{J}^{\mathrm{c}}_{i,\hbar}}\tilde{\mathrm{W}}_{\mathrm{J}^{\mathrm{c}}_{i,\hbar}} + \frac{1}{2}\tilde{\mathrm{W}}^{\mathrm{T}}_{\mathrm{J}^{\mathrm{a}}_{i,\hbar}}\tilde{\mathrm{W}}_{\mathrm{J}^{\mathrm{a}}_{i,\hbar}} + \frac{1}{2}\tilde{\mathrm{W}}^{\mathrm{T}}_{\mathbf{h}_{i,\hbar}}\Upsilon^{-1}_{i,\hbar}\tilde{\mathrm{W}}_{\mathbf{h}_{i,\hbar}}\end{aligned} \tag{35}$$

where $\tilde{\mathrm{W}}_{\mathrm{J}^{\mathrm{c}}_{i,\hbar}} = \hat{\mathrm{W}}_{\mathrm{J}^{\mathrm{c}}_{i,\hbar}} - \mathrm{W}^*_{\mathrm{J}_{i,\hbar}}$, $\tilde{\mathrm{W}}_{\mathrm{J}^{\mathrm{a}}_{i,\hbar}} = \hat{\mathrm{W}}_{\mathrm{J}^{\mathrm{a}}_{i,\hbar}} - \mathrm{W}^*_{\mathrm{J}_{i,\hbar}}$ and $\tilde{\mathrm{W}}_{\mathbf{h}_{i,\hbar}} = \hat{\mathrm{W}}_{\mathbf{h}_{i,\hbar}} - \mathrm{W}^*_{\mathbf{h}_{i,\hbar}}$ represent networks weights errors.

After several simple calculations, $\dot{\mathrm{V}}_{i,\hbar}$ can turn into:

$$\begin{aligned}\dot{\mathrm{V}}_{i,\hbar} \le &\sum_{\kappa=1}^{\hbar-1}\dot{\mathrm{V}}_{i,\kappa} - \underline{\mathbf{g}}_{i,\hbar}\mathrm{K}_{i,\hbar}\phi_{i,\hbar}\mathbf{z}_{i,\hbar} + \overline{\mathbf{g}}_{i,\hbar}\phi_{i,\hbar}\mathbf{z}_{i,\hbar+1} \\ &- \frac{\lambda^{\mathrm{c}}_{i,\hbar}\lambda^{\min}_{\bar{\mathrm{S}}_{i,\hbar}}}{2}\tilde{\mathrm{W}}^{\mathrm{T}}_{\mathrm{J}^{\mathrm{c}}_{i,\hbar}}\tilde{\mathrm{W}}_{\mathrm{J}^{\mathrm{c}}_{i,\hbar}} - \frac{\lambda^{\mathrm{d}}_{i,\hbar}}{2\lambda^{\max}_{\Upsilon_{i,\hbar}}}\tilde{\mathrm{W}}^{\mathrm{T}}_{\mathbf{h}_{i,\hbar}}\Upsilon^{-1}_{i,\hbar}\tilde{\mathrm{W}}_{\mathbf{h}_{i,\hbar}} \\ &- \frac{\lambda^{\mathrm{c}}_{i,\hbar}\lambda^{\min}_{\bar{\mathrm{S}}_{i,\hbar}}}{2}\tilde{\mathrm{W}}^{\mathrm{T}}_{\mathrm{J}^{\mathrm{a}}_{i,\hbar}}\tilde{\mathrm{W}}_{\mathrm{J}^{\mathrm{a}}_{i,\hbar}} - (\mathrm{w}_{i,\hbar} - \frac{1}{2} - \frac{\overline{\mathbf{g}}_{i,\hbar}}{4})\phi^2_{i,\hbar} \\ &- \overline{\mathbf{g}}_{i,\hbar-1}\phi_{i,\hbar-1}\mathbf{z}_{i,\hbar} - (\lambda^{\mathrm{c}}_{i,\hbar} - \frac{\lambda^{\mathrm{a}}_{i,\hbar}}{2})(\hat{\mathrm{W}}^{\mathrm{T}}_{\mathrm{J}^{\mathrm{c}}_{i,\hbar}}\mathrm{S}_{\mathrm{J}_{i,\hbar}})^2 \\ &- (\frac{\lambda^{\mathrm{a}}_{i,\hbar}}{2} - \frac{\overline{\mathbf{g}}_{i,\hbar}}{4})(\hat{\mathrm{W}}^{\mathrm{T}}_{\mathrm{J}^{\mathrm{a}}_{i,\hbar}}\mathrm{S}_{\mathrm{J}_{i,\hbar}})^2 + \varpi_{i,\hbar}\end{aligned} \tag{36}$$

where $\varpi_{i,\hbar} = \frac{1}{4}\bar{\epsilon}^2_{\mathbf{h}_{i,\hbar}} + \sum_{\mathrm{s}=1}^{\mathrm{p}} 2^{2\mathrm{s}}\mathbf{q}_{\mathrm{l},\hbar,i}|\mathbf{y}_{i,\mathrm{d}}|^{2\mathrm{s}} + (\lambda^{\mathrm{a}}_{i,\hbar} + \lambda^{\mathrm{c}}_{i,\hbar})\lambda^{\max}_{\mathrm{S}}\mathrm{W}^{*\mathrm{T}}_{\mathrm{J}_{i,\hbar}}\mathrm{W}^*_{\mathrm{J}_{i,\hbar}}/2 + \lambda^{\mathrm{d}}_{i,\hbar}\mathrm{W}^{*\mathrm{T}}_{\mathbf{h}_{i,\hbar}}\mathrm{W}^*_{\mathbf{h}_{i,\hbar}}/2$ and $\mathbf{q}_{\mathrm{l},\hbar,i} = \mathrm{Np}\sum_{\mathrm{l}=1}^{\mathrm{N}}\mathrm{q}^{2\mathrm{s}}_{i,\hbar,\mathrm{l}}$. $\lambda^{\min}_{\bar{\mathrm{S}}_{i,\hbar}}$ and $\lambda^{\max}_{\Upsilon_{i,\hbar}}$ are the minimal and maximal eigenvalues of $\bar{\mathrm{S}}_{i,\hbar}$ and $\Upsilon^{-1}_{i,\hbar}$.

From $\int_0^{\mathbf{z}_{i,\hbar}} \frac{(\mathrm{k}^{\mathrm{l}}_{i,\hbar}+\mathrm{k}^{\mathrm{u}}_{i,\hbar})^2\sigma_{i,\hbar}}{\bar{\mathrm{k}}^{\mathrm{l}}_{i,\hbar}\bar{\mathrm{k}}^{\mathrm{u}}_{i,\hbar}}\mathrm{d}\sigma_{i,\hbar} \le \phi_{i,\hbar}\mathbf{z}_{i,\hbar}$, and we make the constants $\lambda^{\mathrm{a}}_{i,\hbar}$ and $\mathrm{w}_{i,\hbar}$ satisfy

$$\lambda^{\mathrm{a}}_{i,\hbar} \ge \overline{\mathbf{g}}_{i,\hbar}/2,\ \mathrm{w}_{i,\hbar} \ge 1/2 + \overline{\mathbf{g}}_{i,\hbar}/4 \tag{37}$$

then we have the following inequality:

$$\dot{\mathrm{V}}_{i,\hbar} \le -\bar{\mathrm{K}}_{i,\hbar}\mathrm{V}_{i,\hbar} + \sum_{\kappa=1}^{\hbar-1}\varpi_{i,\kappa} + \varpi_{i,\hbar} + \overline{\mathbf{g}}_{i,\hbar}\phi_{i,\hbar}\mathbf{z}_{i,\hbar+1} \tag{38}$$

where $\bar{\mathrm{K}}_{i,\hbar} = \min\{\bar{\mathrm{K}}_{i,1}, \ldots, \bar{\mathrm{K}}_{i,\hbar-1}, \underline{\mathbf{g}}_{i,\hbar}\mathrm{K}_{i,\hbar}, \lambda^{\mathrm{c}}_{i,\hbar}\lambda^{\min}_{\mathrm{S}}/2, \lambda^{\mathrm{d}}_{i,\hbar}/2\lambda^{\max}_{\Upsilon_{i,\hbar}}\}$.

Step i, n_i. Select the Lyapunov function candidate as:

$$\begin{aligned}\mathrm{V}_{i,\mathrm{n}_i} = &\sum_{\bar{\kappa}=1}^{\mathrm{n}_i-1}\mathrm{V}_{i,\bar{\kappa}} + \int_0^{\mathbf{z}_{i,\mathrm{n}_i}} \frac{(\mathrm{k}^{\mathrm{l}}_{i,\mathrm{n}_i}+\mathrm{k}^{\mathrm{u}}_{i,\mathrm{n}_i})^2\sigma_{i,\mathrm{n}_i}}{\bar{\mathrm{k}}^{\mathrm{l}}_{i,\mathrm{n}_i}\bar{\mathrm{k}}^{\mathrm{u}}_{i,\mathrm{n}_i}}\mathrm{d}\sigma_{i,\mathrm{n}_i} \\ &+ \frac{1}{2}\tilde{\mathbf{r}}^{\mathrm{T}}_i\mathbf{s}_i\bar{\Upsilon}^{-1}_{i,1}\tilde{\mathbf{r}}_i + \frac{1}{2}\tilde{\pi}^{\mathrm{T}}_i\bar{\Upsilon}^{-1}_{i,2}\tilde{\pi}_i + \frac{1}{2}\tilde{\mathrm{W}}^{\mathrm{T}}_{\mathrm{J}^{\mathrm{c}}_{i,\mathrm{n}_i}}\tilde{\mathrm{W}}_{\mathrm{J}^{\mathrm{c}}_{i,\mathrm{n}_i}} \\ &+ \frac{1}{2}\tilde{\mathrm{W}}^{\mathrm{T}}_{\mathrm{J}^{\mathrm{a}}_{i,\mathrm{n}_i}}\tilde{\mathrm{W}}_{\mathrm{J}^{\mathrm{a}}_{i,\mathrm{n}_i}} + \frac{1}{2}\tilde{\mathrm{W}}^{\mathrm{T}}_{\mathbf{h}_{i,\mathrm{n}_i}}\Upsilon^{-1}_{i,\mathrm{n}_i}\tilde{\mathrm{W}}_{\mathbf{h}_{i,\mathrm{n}_i}}\end{aligned} \tag{39}$$

where $\tilde{\mathbf{r}}_i = \hat{\mathbf{r}}_i - \mathbf{r}_i$ and $\tilde{\pi}_i = \hat{\pi}_i - \pi_i$ denote the approximation errors of $\mathbf{r}_i$ and π_i. In addition, $\tilde{\mathrm{W}}_{\mathrm{J}^{\mathrm{c}}_{i,\mathrm{n}_i}} = \hat{\mathrm{W}}_{\mathrm{J}^{\mathrm{c}}_{i,\mathrm{n}_i}} - \mathrm{W}_{\mathrm{J}^*_{i,\mathrm{n}_i}}$, $\tilde{\mathrm{W}}_{\mathrm{J}^{\mathrm{a}}_{i,\mathrm{n}_i}} = \hat{\mathrm{W}}_{\mathrm{J}^{\mathrm{a}}_{i,\mathrm{n}_i}} - \mathrm{W}_{\mathrm{J}^*_{i,\mathrm{n}_i}}$ and $\tilde{\mathrm{W}}_{\mathbf{h}_{i,\mathrm{n}_i}} = \hat{\mathrm{W}}_{\mathbf{h}_{i,\mathrm{n}_i}} - \mathrm{W}_{\mathbf{h}^*_{i,\mathrm{n}_i}}$ are the networks weights errors.

As shown in references [8], [13], the following inequalities are verified in the derivative of $\mathrm{V}_{i,\mathrm{n}_i}$ along with time:

$$\phi_{i,\mathrm{n}_i}\sum_{\mathrm{k}=1}^{\mathrm{m}_i}\mathbf{g}^{\mathrm{k}}_{i,\mathrm{n}_i}\psi^{\mathrm{h}}_{i,\mathrm{k}}\mathbf{u}^*_{i,\mathrm{k}} \le \mathbf{s}_i\epsilon_{i,1} - \mathbf{s}_i\hat{\mathbf{r}}_i\phi_{i,\mathrm{n}_i}\hat{\mathbf{v}}^*_i \tag{40a}$$

$$|\phi_{i,\mathrm{n}_i}| - \phi_{i,\mathrm{n}_i}\tanh(\phi_{i,\mathrm{n}_i}/\varepsilon_i) \le 0.2785\varepsilon_i \tag{40b}$$

Substituting the Eqs.(28a) and (28b) into the inequality (39), there is:

$$\begin{aligned}\dot{\mathrm{V}}_{i,\mathrm{n}_i} \leq & \sum_{\bar{\kappa}=1}^{\mathrm{n}_i-1} \dot{\mathrm{V}}_{i,\bar{\kappa}} - \mathrm{K}_{i,\mathrm{n}_i}\phi_{i,\mathrm{n}_i} - \frac{\lambda_{i,\mathrm{n}_i}^{\mathrm{c}}\lambda_{\bar{\mathrm{S}}_{i,\mathrm{n}_i}}^{\min}}{2}\tilde{\mathrm{W}}_{\mathrm{J}_{i,\mathrm{n}_i}^{\mathrm{c}}}^{\mathrm{T}}\tilde{\mathrm{W}}_{\mathrm{J}_{i,\mathrm{n}_i}^{\mathrm{c}}} \\ & - \frac{\lambda_{i,\mathrm{n}_i}^{\mathrm{c}}\lambda_{\bar{\mathrm{S}}_{i,\mathrm{n}_i}}^{\min}}{2}\tilde{\mathrm{W}}_{\mathrm{J}_{i,\mathrm{n}_i}^{\mathrm{a}}}^{\mathrm{T}}\tilde{\mathrm{W}}_{\mathrm{J}_{i,\mathrm{n}_i}^{\mathrm{a}}} - \frac{\lambda_{i,\mathrm{n}_i}^{\mathrm{d}}}{2\lambda_{\Upsilon_{i,\mathrm{n}_i}}^{\max}}\tilde{\mathrm{W}}_{\mathbf{h}_{i,\mathrm{n}_i}}^{\mathrm{T}}\Upsilon_{i,\mathrm{n}_i}^{-1}\tilde{\mathrm{W}}_{\mathbf{h}_{i,\mathrm{n}_i}} \\ & - (\lambda_{i,\mathrm{n}_i}^{\mathrm{c}} - \frac{\lambda_{i,\mathrm{n}_i}^{\mathrm{a}}}{2})(\hat{\mathrm{W}}_{\mathrm{J}_{i,\mathrm{n}_i}^{\mathrm{c}}}^{\mathrm{T}}\mathrm{S}_{\mathrm{J}_{i,n_i}})^2 - \frac{\epsilon_{i,2}\mathbf{s}_i}{2\lambda_{\bar{\Upsilon}_{i,1}}^{\max}}\tilde{\mathbf{r}}_i^{\mathrm{T}}\bar{\Upsilon}_{i,1}^{-1}\tilde{\mathbf{r}}_i \\ & - (\frac{\lambda_{i,\mathrm{n}_i}^{\mathrm{a}}}{2} - \frac{\overline{\mathbf{g}}_{i,\mathrm{n}_i}}{4})(\hat{\mathrm{W}}_{\mathrm{J}_{i,\mathrm{n}_i}^{\mathrm{a}}}^{\mathrm{T}}\mathrm{S}_{\mathrm{J}_{i,n_i}})^2 - \frac{\epsilon_{i,3}}{2\lambda_{\bar{\Upsilon}_{i,2}}^{\max}}\tilde{\pi}_i^{\mathrm{T}}\bar{\Upsilon}_{i,2}^{-1}\tilde{\pi}_i \\ & - (\mathrm{w}_{i,\mathrm{n}_i} - \frac{1}{2} - \frac{\overline{\mathbf{g}}_{i,\mathrm{n}_i}}{4})\phi_{i,\mathrm{n}_i}^2 + \varpi_{i,\mathrm{n}_i} \end{aligned} \tag{41}$$

where $\lambda_{\bar{\mathrm{S}}_{i,\mathrm{n}_i}}^{\min}$ is the minimal eigenvalue of $\bar{\mathrm{S}}_{i,\mathrm{n}_i}$, and $\lambda_{\bar{\Upsilon}_{i,1}}^{\max}$, $\lambda_{\bar{\Upsilon}_{i,2}}^{\max}$ and $\lambda_{\Upsilon_{i,\mathrm{n}_i}}^{\max}$ present the maximal eigenvalues of $\bar{\Upsilon}_{i,1}^{-1}$, $\bar{\Upsilon}_{i,2}^{-1}$ and $\Upsilon_{i,\mathrm{n}_i}^{-1}$. $\varpi_{i,\mathrm{n}_i} = \frac{1}{4}\bar{\epsilon}_{\mathbf{h}_{i,\mathrm{n}_i}}^2 + \sum_{\mathrm{s}=1}^{\mathrm{p}} 2^{2\mathrm{s}}\mathbf{q}_{\mathrm{l},\mathrm{n}_i,i}|\mathbf{y}_{i,\mathrm{d}}|^{2\mathrm{s}} + 0.2785\varepsilon_i\pi_i + \mathbf{s}_i\epsilon_{i,1} + \epsilon_{i,2}\mathbf{s}_i\mathbf{r}_i^{\mathrm{T}}\mathbf{r}_i/2 + \epsilon_{i,3}\pi_i^{\mathrm{T}}\pi_i/2 + (\lambda_{i,\mathrm{n}_i}^{\mathrm{a}} + \lambda_{i,\mathrm{n}_i}^{\mathrm{c}})\lambda_{\mathrm{S}}^{\max}\mathrm{W}_{\mathrm{J}_{i,\mathrm{n}_i}}^{*\mathrm{T}}\mathrm{W}_{\mathrm{J}_{i,\mathrm{n}_i}}^{*}/2 + \lambda_{i,\mathrm{n}_i}^{\mathrm{d}}\mathrm{W}_{\mathbf{h}_{i,n_i}}^{*\mathrm{T}}\mathrm{W}_{\mathbf{h}_{i,1}}^{*}/2$, which can be bounded by a positive constant.

Moreover, if we select the constants satisfy the conditions:

$$\lambda_{i,\mathrm{n}_i}^{\mathrm{a}} \geq \overline{\mathbf{g}}_{i,\mathrm{n}_i}/2,\ \mathrm{w}_{i,\mathrm{n}_i} \geq 1/2 + \overline{\mathbf{g}}_{i,\mathrm{n}_i}/4 \tag{42}$$

and $\dot{\mathrm{V}}_{i,\mathrm{n}_i}$ can be derived as:

$$\dot{\mathrm{V}}_{i,\mathrm{n}_i} \leq -\bar{\mathrm{K}}_{i,\mathrm{n}_i}\mathrm{V}_{i,n_i} + \sum_{\kappa=1}^{\mathrm{n}_i-1}\varpi_{i,\kappa} + \varpi_{i,\mathrm{n}_i} \tag{43}$$

where $\bar{\mathrm{K}}_{i,\mathrm{n}_i} = \min\{\bar{\mathrm{K}}_{i,1},\ldots,\bar{\mathrm{K}}_{i,\mathrm{n}_i-1},\mathrm{K}_{i,\mathrm{n}_i},\frac{\epsilon_{i,2}\mathbf{s}_i}{2\lambda_{\bar{\Upsilon}_{i,1}}^{\max}},\frac{\epsilon_{i,3}}{2\lambda_{\bar{\Upsilon}_{i,2}}^{\max}},\frac{\lambda_{i,\hbar}^{\mathrm{d}}}{2\lambda_{\Upsilon_{i,\mathrm{n}_i}}^{\max}},\frac{\lambda_{i,\mathrm{n}_i}^{\mathrm{c}}\lambda_{\mathrm{S}}^{\min}}{2}\}$.

Therefore, it can be easily concluded that the transformation errors $\mathbf{z}_{i,\iota}$, the estimated parameter errors $\hat{\mathrm{W}}_{\mathrm{J}_{i,\iota}^{\mathrm{c}}}$, $\hat{\mathrm{W}}_{\mathrm{J}_{i,\iota}^{\mathrm{a}}}$, $\hat{\mathrm{W}}_{\mathbf{h}_{i,\iota}}$ with $\iota = 1,2,\ldots,\mathrm{n}_i$, and $\hat{\mathbf{r}}_i$, $\hat{\pi}_i$ of the ith subsystem are uniformly ultimately bounded, which completes the proof. ■

Remark 4.1. It is noteworthy that the stability of the whole system was not analyzed in the above discussions, that is, the transformation and approximation errors of each subsystem remain in the corresponding compact sets under the optimal FTC algorithm. This implies that the proposed algorithm can also stabilize the LSIS with N subsystems.

Remark 4.2. In [27]–[29], it needs to compute the constraint bounds on the error variables $\mathrm{z}_{i,\iota}$. Therefore, it is essential to know the bounds of the virtual controllers. From the Eqs.(29), (35) and (39), it can be concluded that the constraint bounds are directly utilized in the control design. In this paper, this conservatism can be solved.

Remark 4.3. From (43), it is known that larger $\bar{\mathrm{K}}_{i,\iota}$ and smaller $\varpi_{i,\iota}$ can achieve an exceptional system performance, i.e., one can increase the value of $\mathrm{K}_{i,\iota}$ and decrease the values of $\epsilon_{i,1}$, $\bar{\Upsilon}_{i,1}$, $\bar{\Upsilon}_{i,2}$, $\bar{\epsilon}_{\mathbf{h}_{i,\iota}}$, $\Upsilon_{i,\iota}$, $\iota = 1,2,\ldots,\mathrm{n}_i$. Nevertheless, over-adjusting these values may lead to an excessive control input magnitude. Hence, the tuning procedure may require a tradeoff between the achievement of the system performance and the input characteristic.

V. Simulation Results

Further, the practical LSIS are implemented to demonstrate the effectiveness of the learning-based optimized fault-tolerant controller.

Example 4.1 [38]. In this work, an electrical power system composed of two-machine subsystems is investigated as below

$$\dot{\mathbf{x}}_{i,1} = \mathbf{x}_{i,2},\ i = 1,2 \tag{44a}$$

$$\begin{aligned}\dot{\mathbf{x}}_{i,2} = & -\frac{\mathrm{D}_i}{\mathrm{M}_i}\mathbf{x}_{i,2} + \frac{1}{\mathrm{M}_i}\sum_{\mathrm{k}=1}^{2}\mathbf{u}_{i,\mathrm{k}}^{\mathrm{F}} + \sum_{j=1}^{2}\frac{\mathrm{E}_i\mathrm{E}_j\mathrm{Y}_{i,j}}{\mathrm{M}_i} \\ & \times(\cos(\delta_{i,j}^0 - \theta_{i,j}) - \cos(\mathbf{x}_{i,1} - \mathbf{x}_{j,1} + \delta_{i,j}^0 - \theta_{i,j}))\end{aligned} \tag{44b}$$

where $\mathbf{x}_{i,1}$ and $\mathbf{x}_{i,2}$ denote the absolute rotor angle and the angular velocity of the ith machine. M_i, D_i and E_i separately represent the inertia coefficient, the damping coefficient and the internal voltage. Also, $\mathrm{Y}_{i,j}$, $\delta_{i,j}^0$ and $\theta_{i,j}$ are the constants depending on the topology, the physical properties of the network and the loads (admittance matrix) between the ith and jth machine. The values of these parameters are $\mathrm{M}_1 = 1.03$, $\mathrm{M}_2 = 1.25$, $\mathrm{D}_1 = 0.8$, $\mathrm{D}_2 = 1.2$, $\mathrm{E}_1 = 1.017$, $\mathrm{E}_2 = 1.005$, $\mathrm{Y}_{i,j} = 1.98$, $\delta_{1,2}^0 = 1.2$, $\delta_{2,1}^0 = -1.2$, $\theta_{1,2} = 1.5$ and $\theta_{2,1} = -1.5$, respectively.

Due to the prolonged high-speed rotation in the electrical power system and the harsh, remote environment, the motors are susceptible to an infinite number of actuator faults. Hence, the intermittent actuator faults are more common in this type of system. The intermittent actuator faults are assumed as $\mathbf{u}_{1,\mathrm{k}}^{\mathrm{F}} = 0.2\mathbf{u}_{1,\mathrm{k}} + 1$ and $\mathbf{u}_{2,\mathrm{k}}^{\mathrm{F}} = 0.3\mathbf{u}_{2,\mathrm{k}} + 1.5$ when $\mathrm{t} \in [\mathrm{hT}^*, (\mathrm{h}+1)\mathrm{T}^*)$, for $\mathrm{h} = 1,3,5,\ldots$, and $\mathrm{T}^* = 4$s.

The critic, actor and identifier neural networks for Eqs.(13), (20) and (26) are to have 60 neurons, and the centers of the receptive fields are in -5 to 5. The critic and actor updating laws are with the parameters $\lambda_{i,\iota}^{\mathrm{c}} = 20$, $\lambda_{i,\iota}^{\mathrm{a}} = 10$, $\iota = 1,2$, and the initial values of the network weights are set as $\hat{\mathrm{W}}_{\mathrm{J}_{i,1}^{\mathrm{c}}}(0) = \hat{\mathrm{W}}_{\mathrm{J}_{i,1}^{\mathrm{a}}}(0) = 0.5\mathrm{I}_{60*1}$ and $\hat{\mathrm{W}}_{\mathrm{J}_{i,2}^{\mathrm{c}}}(0) = \hat{\mathrm{W}}_{\mathrm{J}_{i,2}^{\mathrm{a}}}(0) = 0.4\mathrm{I}_{60*1}$. The identifier updating law is with the design parameters $\lambda_{i,\iota}^{\mathrm{d}} = 0.1$ and $\Upsilon_{i,\iota} = \mathrm{I}_{60*60}$ with I being the identity matrix, and the initial values of the network weight is $\hat{\mathrm{W}}_{\mathbf{h}_{i,1}}(0) = 0.5\mathrm{I}_{60*1}$, $\hat{\mathrm{W}}_{\mathbf{h}_{i,2}}(0) = 0.4\mathrm{I}_{60*1}$. The optimized fault-tolerant controller is with the designed parameters $\mathrm{w}_{i,\iota} = 1$ and $\mathrm{K}_{i,\iota} = 15$.

Under the zero initial conditions, the simulation results are exhibited in Fig.2-7, the trajectory of the output-variable $\mathbf{y}_i$ and the tracking reference signal $\mathbf{y}_{i,\mathrm{d}}$ are depicted in Fig.2. As illustrated before, both output-variables are under control during the whole learning period and approach the reference signals stay within the predefined constraint boundary in the presence of faults. Fig.3 displays the boundedness of critic, actor and identifier neural network weights of two backstepping steps, i.e., the boundedness of $\|\hat{\mathrm{W}}_{\mathrm{J}_{i,\iota}^{\mathrm{c}}}\|$, $\|\hat{\mathrm{W}}_{\mathrm{J}_{i,\iota}^{\mathrm{a}}}\|$ and $\|\hat{\mathrm{W}}_{\mathbf{h}_{i,\iota}}\|$. Fig.4 shows the boundedness of actuator control input $\mathbf{u}_{i,\mathrm{k}}$ and actuator control output $\mathbf{u}_{i,\mathrm{k}}^{\mathrm{F}}$. It can be determined that the designed FTC method can achieve the desired objectives. To further verify the effectiveness of the proposed FTC scheme, we utilize Eq.(25b) without using (27) and (28) to control system (1). In the simulation, the initial conditions of variables

and parameters are selected similar to the above case. From Fig.5, it is clear that the subsystems are unstable.

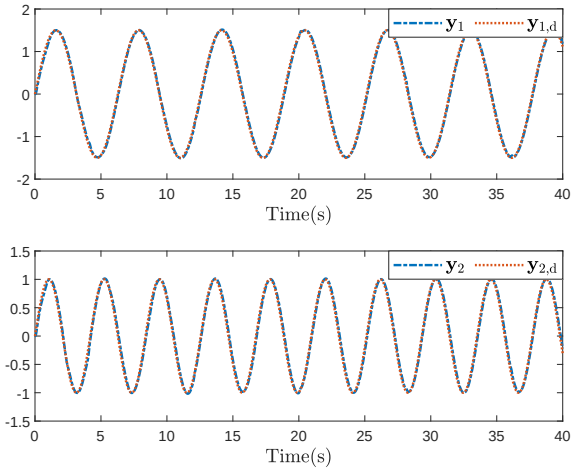

Fig. 2. Tracking trajectories of $\mathbf{y}_i$ and $\mathbf{y}_{i,\mathrm{d}}$.

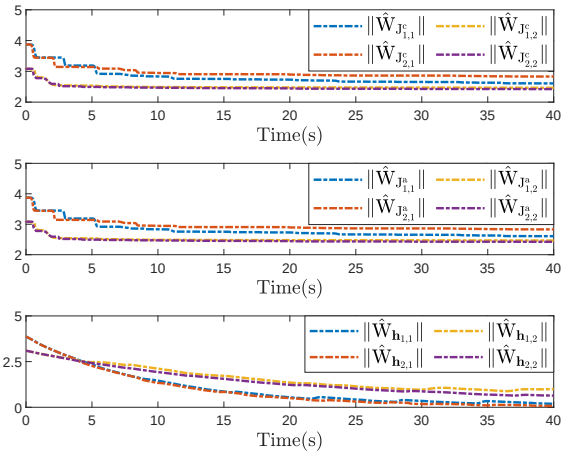

Fig. 3. The critic, actor and identifier neural network weight norms for Steps 1 and 2.

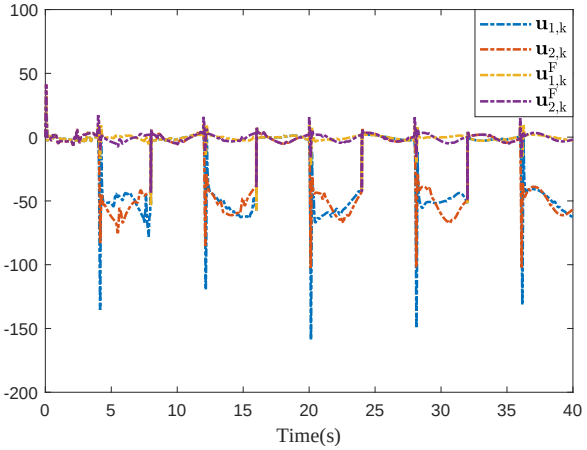

Fig. 4. Trajectories of control input $\mathbf{u}_{i,\mathrm{k}}$ and control output $\mathbf{u}^{\mathrm{F}}_{i,\mathrm{k}}$.

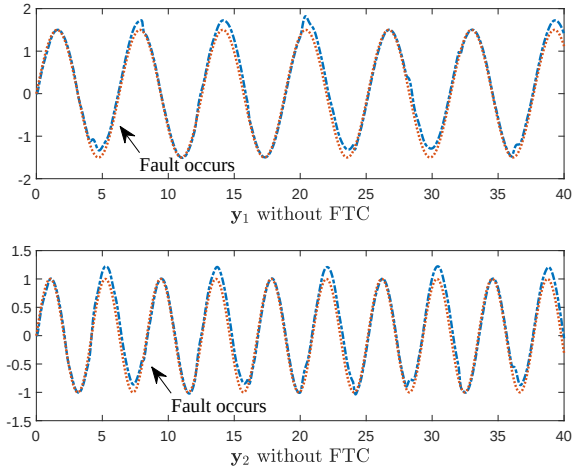

Fig. 5. Tracking trajectory result of $\mathbf{y}_i$ without FTC.

Finally, here, the control performance of the asymmetric IBLF (the blue line), the tangent BLF in [27] ($\mathbf{y}_i^{\mathrm{T}}$ and $\mathbf{z}_{i,1}^{\mathrm{T}}$, the red line) and the logarithmic BLF in [29] ($\mathbf{y}_i^{\mathrm{L}}$ and $\mathbf{z}_{i,1}^{\mathrm{L}}$, the yellow line) are displayed in Fig.6, i.e., (a1)-(a2) are tracking trajectories, and (b1)-(b2) are tracking errors. These three types BLFs have seen similar performance in the tracking control, however, the output-variable with the proposed IBLF is closer to the actual trajectories than the others due to its smaller tracking error. Through the selected mean square error performance criteria $\mathrm{MSE} = (1/\mathrm{T})\sum_{\mathrm{t}=0}^{\mathrm{T}}(\mathbf{y}_i(\mathrm{t}) - \mathbf{y}_{i,\mathrm{d}}(\mathrm{t}))^2$, it is possible to verify the well tracking performance and less conservative features of the proposed algorithm. Additionally, Fig.7 shows the comparative results of the tracking performance between the proposed algorithm and the algorithm with no optimization ($\mathbf{z}_{i,1}^{\mathrm{N}}$, the red line), also, the MSE results of the proposed algorithm illustrate its efficiency than the one with no optimization.

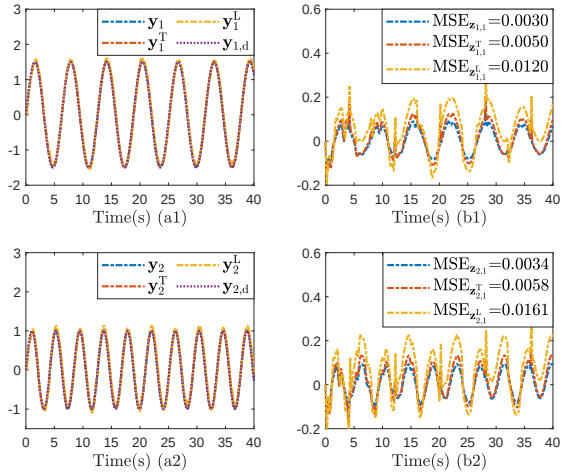

Fig. 6. The comparative tracking trajectories and the tracking errors of the asymmetric IBLF (the blue line), the tangent BLF in [27] ($\mathbf{y}_i^{\mathrm{T}}$ and $\mathbf{z}_{i,1}^{\mathrm{T}}$, the red line) and the logarithmic BLF in [29] ($\mathbf{y}_i^{\mathrm{L}}$ and $\mathbf{z}_{i,1}^{\mathrm{L}}$, the yellow line).

Example 4.2 [39]. Consider the thigh and knee motions of a

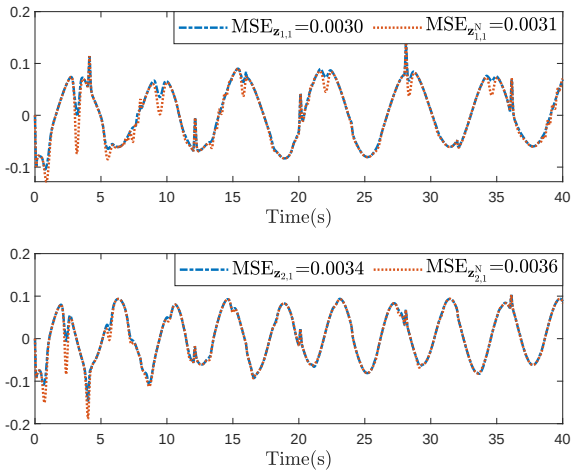

Fig. 7. The comparative tracking errors of the proposed algorithm and the algorithm with no optimization ($\mathbf{z}^{\mathrm{N}}_{i,1}$, the red line).

walking robot composed by three interconnected subsystems:

$$\ddot{\xi}_1 = 0.1(1-5.25\xi_{1\mathrm{e}}^2)\dot{\xi}_1 - \xi_{1\mathrm{e}} + \sum_{\mathrm{k}=1}^{2}\mathbf{u}^{\mathrm{F}}_{1,\mathrm{k}} \tag{45a}$$

$$\ddot{\xi}_2 = 0.01(1-6070\xi_{2\mathrm{e}}^2)\dot{\xi}_2 - 4\xi_{2\mathrm{e}} + 0.057\xi_1\dot{\xi}_1 + \sum_{\mathrm{k}=1}^{2}\mathbf{u}^{\mathrm{F}}_{2,\mathrm{k}} + 0.1(\dot{\xi}_2 - \dot{\xi}_3) \tag{45b}$$

$$\ddot{\xi}_3 = 0.01(1-192\xi_{3\mathrm{e}}^2)\dot{\xi}_3 - 4\xi_{3\mathrm{e}} + 0.057\xi_1\dot{\xi}_1 + \sum_{\mathrm{k}=1}^{2}\mathbf{u}^{\mathrm{F}}_{3,\mathrm{k}} + 0.1(\dot{\xi}_3 - \dot{\xi}_2) \tag{45c}$$

where ξ_1 is the relative angle between two thighs, ξ_2 and ξ_3 depict the right and left knee angles, respectively. $\xi_{i\mathrm{e}} = \xi_i - \xi_{i,\mathrm{d}}$ with $\xi_{i,\mathrm{d}}$ being the reference trajectory for $i = 1, 2, 3$. The control objective is to devise the optimal fault-tolerant controller $\mathbf{u}^*_{i,\mathrm{k}}$ such that the system output $\mathbf{y}_i$ can track the signals $\xi_{1,\mathrm{d}} = 0.1\sin(\mathrm{t}) + 0.3\sin(2\mathrm{t})$, $\xi_{2,\mathrm{d}} = 0.2\sin(\mathrm{t}) + 0.35\sin(1.5\mathrm{t})$ and $\xi_{3,\mathrm{d}} = 0.15\sin(2\mathrm{t}) + 0.25\sin(2.5\mathrm{t})$.

For this simulation, the faulty actuator model is selected as $\mathbf{u}^{\mathrm{F}}_{1,\mathrm{k}} = 0.2\mathbf{u}_{1,\mathrm{k}} + 1.3$, $\mathbf{u}^{\mathrm{F}}_{2,\mathrm{k}} = 0.3\mathbf{u}_{2,\mathrm{k}} + 1.25$ and $\mathbf{u}^{\mathrm{F}}_{3,\mathrm{k}} = 0.25\mathbf{u}_{2,\mathrm{k}} + 1.2$ when $\mathrm{t} \in [\mathrm{hT}^*, (\mathrm{h}+1)\mathrm{T}^*)$, for $\mathrm{h} = 1, 3, 5, \ldots$, and $\mathrm{T}^* = 5$s, which implies that the actuator works normally every 5s, and then encounters partial loss of effectiveness and stuck faults every 5s for the next 5s. In addition, the design parameters of the optimal FTC are chosen as $\mathrm{k}^{\mathrm{l}}_{i,\iota} = -4$, $\mathrm{k}^{\mathrm{u}}_{i,\iota} = 5$, $\mathrm{K}_{i,\iota} = 20$, $\mathrm{w}_{i,\iota} = 1$, $\lambda^{\mathrm{c}}_{i,\iota} = 10$, $\lambda^{\mathrm{a}}_{i,\iota} = 15$, $\lambda^{\mathrm{d}}_{i,\iota} = 0.1$, $\varepsilon_i = 0.1$, $\epsilon_{i,\iota} = 1$, $\bar{\Upsilon}_{i,1} = 0.1$, $\bar{\Upsilon}_{i,2} = 0.1$, $\Upsilon_{i,\iota} = \mathrm{I}_{10*10}$ with I being the identity matrix and $\iota = 1, 2, 3$.

Under the initial weight conditions of $\hat{\mathrm{W}}_{\mathrm{J}^{\mathrm{c}}_{i,\iota}}(0) = \mathrm{I}_{10*1}$, $\hat{\mathrm{W}}_{\mathrm{J}^{\mathrm{a}}_{i,\iota}}(0) = 0.8\mathrm{I}_{10*1}$, $\hat{\mathrm{W}}_{\mathbf{h}_{i,\iota}}(0) = 0.5\mathrm{I}_{10*1}$, and the others are zero, the tracking control performance of the proposed optimal control algorithm is shown in Fig.8. The 2-norm of the network weights for critic, actor and identifier are presented in Fig.9. Fig.10 displays the trajectory of the actuator input $\mathbf{u}_{i,\mathrm{k}}$ and output $\mathbf{u}^{\mathrm{F}}_{i,\mathrm{k}}$. Fig.11 further demonstrates that all the signals in the closed-loop system are not bound without FTC. From these graphs, it can be concluded that the optimized fault-tolerant controller can meet the control objective even if the fault occurs between 5-10s, 15-20s and 25-30s.

To further illustrate the superiority of the proposed optimal FTC approach, as depicted in Fig.12, the control input under the IBLF (the blue line), the tangent BLF in [27] ($\mathbf{y}^{\mathrm{T}}_i$ and $\mathbf{z}^{\mathrm{T}}_{i,1}$, the red line) and the logarithmic BLF in [29] ($\mathbf{y}^{\mathrm{L}}_i$ and $\mathbf{z}^{\mathrm{L}}_{i,1}$, the yellow line) are compared. Furthermore, the tracking control performance of the learning-based algorithm is compared with the algorithm with no optimization ($\mathbf{z}^{\mathrm{N}}_{i,1}$, the red line) in Fig.4, and the MSE results also highlight its optimality with respect to the one with no optimization.

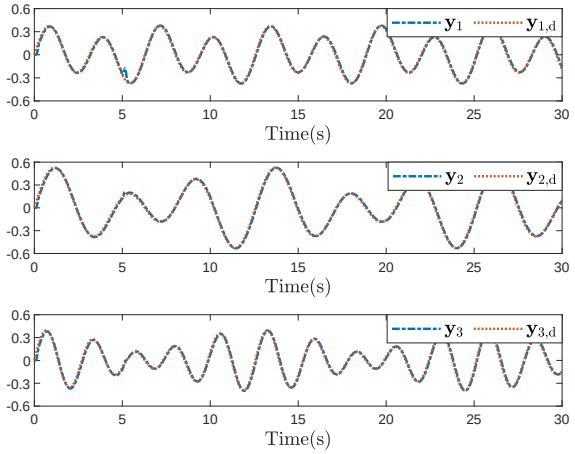

Fig. 8. Tracking trajectory results of $\mathbf{y}_i$ and $\mathbf{y}_{i,\mathrm{d}}$.

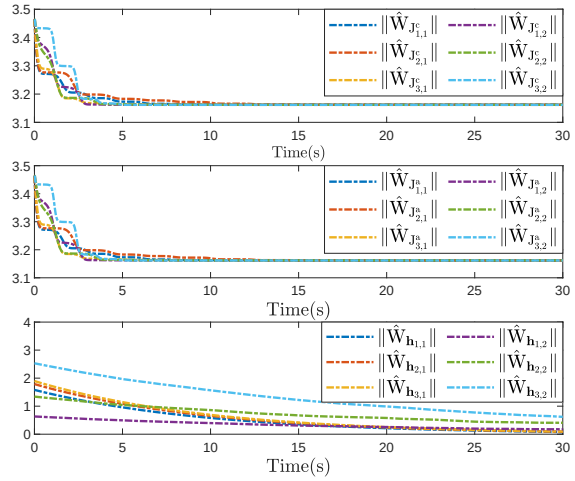

Fig. 9. The critic, actor and identifier neural network weight norms for Steps 1 and 2.

VI. Conclusion

This article introduced an optimized FTC strategy for the constrained LSIS via learning algorithm. By decomposing the learning process into the critic, the actor and the identifier networks to be estimated, the associated IBLF was incorporated into the decentralized backstepping control method to constrain the state-variables staying within an asymmetric region. On this basis, the restriction of converting state-constraints into error-constraints under the logarithmic and tangent BLFs

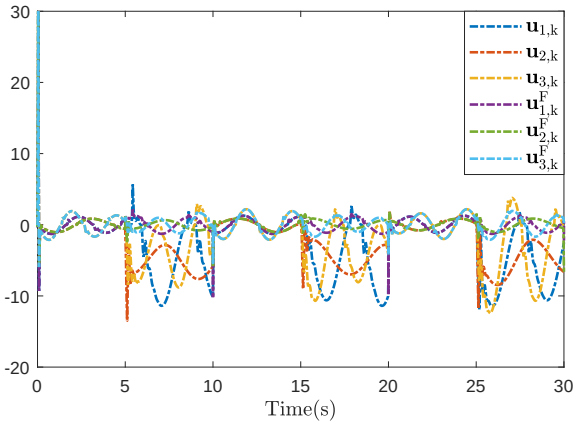

Fig. 10. Trajectories of control input $\mathbf{u}_{i,k}$ and control output $\mathbf{u}^{F}_{i,k}$.

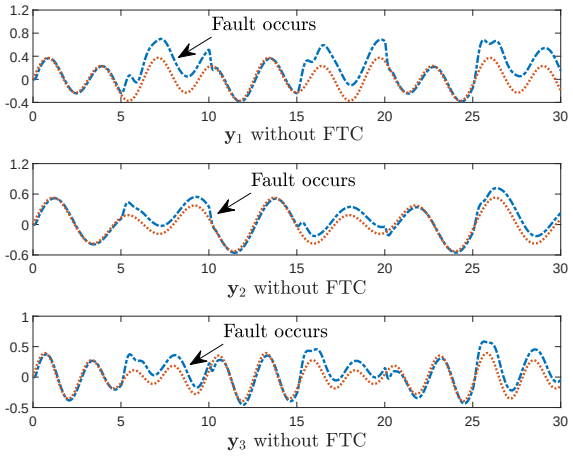

Fig. 11. Tracking trajectory result of $\mathbf{y}_i$ without FTC.

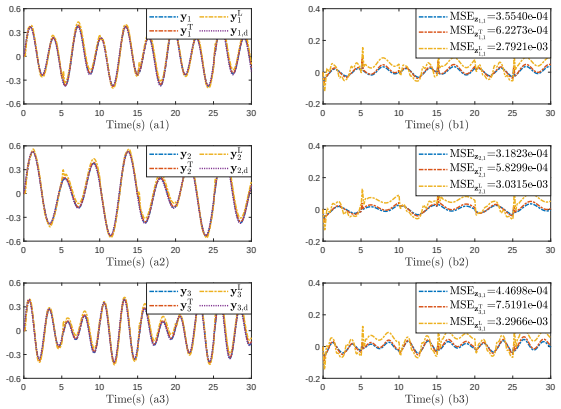

Fig. 12. The comparative tracking trajectories and the tracking errors of the asymmetric IBLF (the blue line), the tangent BLF in [27] ($\mathbf{y}^{T}_{i}$ and $\mathbf{z}^{T}_{i,1}$, the red line) and the logarithmic BLF in [29] ($\mathbf{y}^{L}_{i}$ and $\mathbf{z}^{L}_{i,1}$, the yellow line).

was relaxed. Considering the problem of intermittent actuator faults, the optimal controller derived from learning algorithm and the fault-tolerant controller were isolated by an intermediate controller. At the same time, the tracking errors were demonstrated to converge to a small neighborhood around the

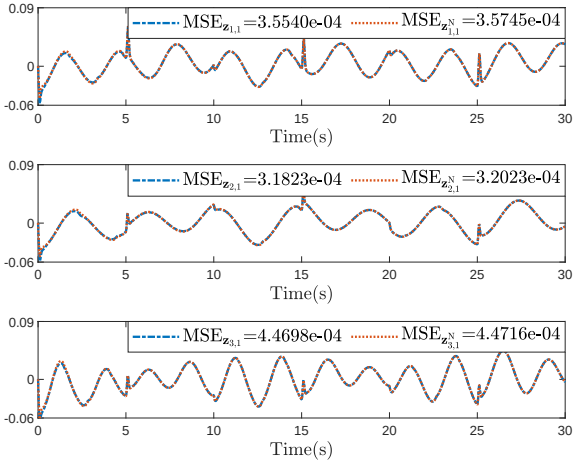

Fig. 13. The comparative tracking errors of the proposed algorithm and the algorithm with no optimization ($\mathbf{z}^{N}_{i,1}$, the red line).

zero. Finally, comparative results shown the effectiveness and superiority of the proposed method.

Here, the passive optimal FTC was investigated. Further, we will concentrate on the optimal active FTC case in the LSIS.

REFERENCES

[1] H. Zhang, C. Liu, H. Su, and K. Zhang, "Echo state network-based decentralized control of continuous-time nonlinear large-scale interconnected systems," *IEEE Transactions on Systems, Man, and Cybernetics: Systems*, vol. 51, no. 10, pp. 6293–6303, 2020.

[2] B. Niu, J. Liu, D. Wang, X. Zhao, and H. Wang, "Adaptive decentralized asymptotic tracking control for large-scale nonlinear systems with unknown strong interconnections," *IEEE/CAA Journal of Automatica Sinica*, vol. 9, no. 1, pp. 173–186, 2021.

[3] B. Zhao, D. Wang, G. Shi, D. Liu, and Y. Li, "Decentralized control for large-scale nonlinear systems with unknown mismatched interconnections via policy iteration," *IEEE Transactions on Systems, Man, and Cybernetics: Systems*, vol. 48, no. 10, pp. 1725–1735, 2017.

[4] H. Wang, P. X. Liu, J. Bao, X.-J. Xie, and S. Li, "Adaptive neural output-feedback decentralized control for large-scale nonlinear systems with stochastic disturbances," *IEEE Transactions on Neural Networks and Learning Systems*, vol. 31, no. 3, pp. 972–983, 2019.

[5] Y. H. Choi and S. J. Yoo, "Minimal-approximation-based decentralized backstepping control of interconnected time-delay systems," *IEEE Transactions on Cybernetics*, vol. 46, no. 12, pp. 3401–3413, 2016.

[6] J. Zhang, S. Li, C. K. Ahn, and Z. Xiang, "Decentralized event-triggered adaptive fuzzy control for nonlinear switched large-scale systems with input delay via command-filtered backstepping," *IEEE Transactions on Fuzzy Systems*, vol. 30, no. 6, pp. 2118–2123, 2021.

[7] S. Tong, Y. Li, and Y. Liu, "Observer-based adaptive neural networks control for large-scale interconnected systems with nonconstant control gains," *IEEE Transactions on Neural Networks and Learning Systems*, vol. 32, no. 4, pp. 1575–1585, 2020.

[8] S. Tong and M. Cui, "Fuzzy adaptive predefined-time decentralized fault tolerant control for fractional-order nonlinear large-scale systems with actuator faults," *IEEE Transactions on Fuzzy Systems*, vol. 32, no. 3, pp. 1000–1012, 2024.

[9] K. Zhang, B. Jiang, and M. Staroswiecki, "Dynamic output feedback-fault tolerant controller design for takagi–sugeno fuzzy systems with actuator faults," *IEEE Transactions on Fuzzy Systems*, vol. 18, no. 1, pp. 194–201, 2009.

[10] B. Jiang, K. Zhang, and P. Shi, "Integrated fault estimation and accommodation design for discrete-time takagi–sugeno fuzzy systems with actuator faults," *IEEE Transactions on Fuzzy Systems*, vol. 19, no. 2, pp. 291–304, 2010.

[11] F. Jia and X. He, "Active fault-tolerant control with adaptive estimation error compensation for nonlinear systems: Achieving asymptotic tracking," *IEEE Transactions on Industrial Informatics*, vol. 20, no. 4, pp. 6612–6621, 2024.

[12] V. Nithya, R. Sakthivel, F. Alzahrani, and Y.-K. Ma, "Decentralized fault-tolerant resilient control for fractional-order interconnected systems with input saturation," *International Journal of Control, Automation and Systems*, vol. 17, no. 11, pp. 2895–2905, 2019.

[13] W. Yang, Y. Jiang, X. He, Y. Zhu, and S. Wang, "Feasibility conditions-free prescribed performance decentralized fault-tolerant neural control of constrained large-scale systems," *IEEE Transactions on Systems, Man, and Cybernetics: Systems*, vol. 53, no. 5, pp. 3152–3164, 2022.

[14] T. Yang and H. Ma, "Decentralized adaptive finite-time fault-tolerant control for a class of high-power interconnected nonlinear systems via graph theory," *International Journal of Adaptive Control and Signal Processing*, vol. 37, no. 8, pp. 2097–2112, 2023.

[15] Q. Wan, Y. Pan, Y. Jing, and M. Zhao, "Decentralized fuzzy fixed-time fault-tolerant tracking control of nonlinear interconnected systems with dual performance," *International Journal of Fuzzy Systems*, vol. 24, no. 6, pp. 2873–2888, 2022.

[16] D. Wang, N. Gao, D. Liu, J. Li, and F. L. Lewis, "Recent progress in reinforcement learning and adaptive dynamic programming for advanced control applications," *IEEE/CAA Journal of Automatica Sinica*, vol. 11, no. 1, pp. 18–36, 2024.

[17] P. Elbert, S. Ebbesen, and L. Guzzella, "Implementation of dynamic programming for n-dimensional optimal control problems with final state constraints," *IEEE Transactions on Control Systems Technology*, vol. 21, no. 3, pp. 924–931, 2012.

[18] Y. Xu, B. Jiang, and H. Yang, "Two-level game-based distributed optimal fault-tolerant control for nonlinear interconnected systems," *IEEE Transactions on Neural Networks and Learning Systems*, vol. 31, no. 11, pp. 4892–4906, 2020.

[19] Z. Wang, L. Liu, Y. Wu, and H. Zhang, "Optimal fault-tolerant control for discrete-time nonlinear strict-feedback systems based on adaptive critic design," *IEEE Transactions on Neural Networks and Learning Systems*, vol. 29, no. 6, pp. 2179–2191, 2018.

[20] B. Kiumarsi, K. G. Vamvoudakis, H. Modares, and F. L. Lewis, "Optimal and autonomous control using reinforcement learning: A survey," *IEEE Transactions on Neural Networks and Learning Systems*, vol. 29, no. 6, pp. 2042–2062, 2017.

[21] H. Zhang, X. Zhao, H. Wang, G. Zong, and N. Xu, "Hierarchical sliding-mode surface-based adaptive actor–critic optimal control for switched nonlinear systems with unknown perturbation," *IEEE Transactions on Neural Networks and Learning Systems*, vol. 35, no. 2, pp. 1559–1571, 2024.

[22] M. E. Dehshalie, M. B. Menhaj, and M. Karrari, "Fault tolerant cooperative control for affine multi-agent systems: An optimal control approach," *Journal of the Franklin Institute*, vol. 356, no. 3, pp. 1360–1378, 2019.

[23] K. Li and Y. Li, "Adaptive NN optimal consensus fault-tolerant control for stochastic nonlinear multiagent systems," *IEEE Transactions on Neural Networks and Learning Systems*, vol. 34, no. 2, pp. 947–957, 2021.

[24] X. Min, S. Baldi, and W. Yu, "Finite-time distributed control of nonlinear multiagent systems via funnel technique," *IEEE Transactions on Systems, Man, and Cybernetics: Systems*, vol. 53, no. 2, pp. 1256–1267, 2022.

[25] X. Min, S. Baldi, W. Yu, and J. Cao, "Low-complexity control with funnel performance for uncertain nonlinear multi-agent systems," *IEEE Transactions on Automatic Control*, vol. 69, no. 3, pp. 1975–1982, 2024.

[26] A. Zahaf, S. Bououden, M. Chadli, and M. Chemachema, "Robust fault tolerant optimal predictive control of hybrid actuators with time-varying delay for industrial robot arm," *Asian Journal of Control*, vol. 24, no. 1, pp. 1–15, 2022.

[27] C.-C. Chen, Z.-Y. Sun, and S. S.-D. Xu, "Prescribed-time stabilization for high-order nonlinear systems with a pre-specified asymmetric output constraint," *Journal of the Franklin Institute*, vol. 360, no. 4, pp. 3545–3574, 2023.

[28] X. Tang, D. Zhai, and X. Li, "Adaptive fault-tolerance control based finite-time backstepping for hypersonic flight vehicle with full state constrains," *Information Sciences*, vol. 507, pp. 53–66, 2020.

[29] S. Singh and A. Jain, "Collision avoidance and connectivity preservation using asymmetric barrier lyapunov function with time-varying distance-constraints," *Systems & Control Letters*, vol. 183, p. 105672, 2024.

[30] Y. Wang, D. Li, and L. Liu, "Iblf-based adaptive finite-time control and modeling for continuous stirred tank reactor with output constraint," *Journal of the Franklin Institute*, vol. 359, no. 16, pp. 8669–8686, 2022.

[31] J. Zhang, "Integral barrier lyapunov functions-based neural control for strict-feedback nonlinear systems with multi-constraint," *International Journal of Control, Automation and Systems*, vol. 16, pp. 2002–2010, 2018.

[32] L. Liu, Y. Liu, A. Chen, S. Tong, and C. P. Chen, "Integral barrier lyapunov function-based adaptive control for switched nonlinear systems," *Science China Information Sciences*, vol. 63, pp. 1–14, 2020.

[33] Y. Liu, S. Tong, C. P. Chen, and D. Li, "Adaptive nn control using integral barrier lyapunov functionals for uncertain nonlinear block-triangular constraint systems," *IEEE Transactions on Cybernetics*, vol. 47, no. 11, pp. 3747–3757, 2016.

[34] F. Yuan, Y. Liu, L. Liu, J. Lan, D. Li, S. Tong, and C. P. Chen, "Adaptive neural consensus tracking control for nonlinear multiagent systems using integral barrier lyapunov functionals," *IEEE Transactions on Neural Networks and Learning Systems*, vol. 34, no. 8, pp. 4544–4554, 2021.

[35] D. Zhang, P. Ma, Y. Du, and T. Chao, "Integral barrier lyapunov function-based three-dimensional low-order integrated guidance and control design with seeker's field-of-view constraint," *Aerospace Science and Technology*, vol. 116, p. 106886, 2021.

[36] Z. Su, C. Li, and Z. Zhen, "Anti-disturbance constrained control of the air recovery carrier via an integral barrier lyapunov function," *Aerospace Science and Technology*, vol. 106, p. 106157, 2020.

[37] F. Jia and X. He, "Fault-tolerant control for uncertain nonstrict-feedback stochastic nonlinear systems with output constraints," *IEEE Transactions on Systems, Man, and Cybernetics: Systems*, vol. 53, no. 8, pp. 5212–5223, 2023.

[38] R. F. Araújo, L. A. Torres, and R. M. Palhares, "Distributed control of networked nonlinear systems via interconnected takagi–sugeno fuzzy systems with nonlinear consequent," *IEEE Transactions on Systems, Man, and Cybernetics: Systems*, vol. 51, no. 8, pp. 4858–4867, 2019.

[39] V. Narayanan, A. Sahoo, S. Jagannathan, and K. George, "Approximate optimal distributed control of nonlinear interconnected systems using event-triggered nonzero-sum games," *IEEE Transactions on Neural Networks and Learning Systems*, vol. 30, no. 5, pp. 1512–1522, 2018.

[40] G. Wen, L. Xu, and B. Li, "Optimized backstepping tracking control using reinforcement learning for a class of stochastic nonlinear strict-feedback systems," *IEEE Transactions on Neural Networks and Learning Systems*, vol. 34, no. 3, pp. 1291–1303, 2021.

[41] G. Wen, S. S. Ge, and F. Tu, "Optimized backstepping for tracking control of strict-feedback systems," *IEEE Transactions on Neural Networks and Learning Systems*, vol. 29, no. 8, pp. 3850–3862, 2018.

[42] Y. Liu, Q. Zhu, and G. Wen, "Adaptive tracking control for perturbed strict-feedback nonlinear systems based on optimized backstepping technique," *IEEE Transactions on Neural Networks and Learning Systems*, vol. 33, no. 2, pp. 853–865, 2020.

[43] B. Liu, M. Hou, J. Ni, Y. Li, and Z. Wu, "Asymmetric integral barrier lyapunov function-based adaptive tracking control considering full-state with input magnitude and rate constraint," *Journal of the Franklin Institute*, vol. 357, no. 14, pp. 9709–9732, 2020.

Authors' response to the Reviewers' comments on Paper Ref No. SMCA-23-09-2616

Qingyi Liu, Ke Zhang, Bin Jiang and Silvio Simani

April 29, 2024

The authors wish to thank the editor and the anonymous reviewers for their helpful comments and suggestions, which are invaluable for significant improvement of the readability and quality of the manuscript. We have considered these comments and suggestions carefully, and have revised the paper accordingly. Based on the reviewers comments, the article has been modified and further details have been added to it, including the followings:

1. Rewriting, rearranging, improving, and editing the **INTRODUCTION** section of the paper.
2. In the section **SIMULATION RESULTS**, some comparison results with those of the previous researches in this field have been added to illustrate the effectiveness of theoretical results.
3. Revising, improving the controller presentation, and adding a block diagram and some related explanations in the **OPTIMAL FTC SCHEME DESIGN** and **STABILITY ANALYSIS** sections, to illustrate the differences and novelties of design procedures clearly.
4. The symmetric integral barrier Lyapunov function in our previous manuscript has been extended to an asymmetric integral barrier Lyapunov function, and some corresponding sections have been modified.
5. Modifying the **CONCLUSION** section and adding the future work in this section.
6. Some expression and grammar errors are corrected to improve the quality of language in our paper.
7. A number of relevant references have been rearranged to improve the background, such as main motivations, contributions, simulation results and so on.

Furthermore, with thanks for the constructive comments of the editor and respected reviewers, the authors have tried to incorporate the comments in the revision and respond to the questions in order to improve the articles quality, clarity and presentation as follows:

1. Response to Associate Editor

First of all, we would like to thank you for your helpful comments and suggestions on our manuscript, and some responses of your comments are given as follows.

Comment 1: This manuscript has been evaluated by four reviewers who have unanimously provided positive evaluations. However, the reviewers also raised some issues, particularly regarding the richness of the introduction and background, the presentation of technical content, the validity of the simulation experiments, and language-related aspects. Based on the reviewers' comments, it is clear that the paper is not ready for publication. I suggest the authors study these comments carefully and then enhance the quality of the paper sufficiently.

Re:

Thanks for the beneficial suggestion of the respectable associate editor. The optimal fault-tolerant control problem has been investigated for a large-scale interconnected system with both intermittent loss of effectiveness and stuck faults, on the basis of a critic-actor-identifier architecture. From which, the actor is utilized to implement control actions, the critic is utilized to evaluate these actions from the environment and to return the evaluations to the actor so that the subsequent actions can be well, and the identifier is utilized to approximate the unknown dynamics. In the last round review, the reviewers mainly concentrate

on the problems including the background, the presentation of some sections, the comparative simulations, the quality of language, among others. For these major concerns of the reviewers about these problems, we have given the corresponding responses to these concerns and indicated in blue in the revised version. For the concerning of the richness of the introduction and background, the **INTRODUCTION** and **REFERENCES** sections have been entirely rewritten in the revised version, at the same time, we have tried to enhance and clarify the presentation of the original ideas, main features and objectives of this paper. Also, some brief explanations of optimal fault-tolerant control, barrier Lyapunov function and related recent references have been added to rich the introduction and background. In comparison with some previous literature, there are mainly three theoretical contributions and differences in our paper, which can be summarized in the following: 1) An asymmetric IBLF is incorporated into each backstepping step to maintain the state-variables in an asymmetric constrained region. This function can enable full state-constraints during the learning process directly, and avoid the complex tracking error-constraints conversion inherent in the conventional BLFs [27]-[29]; 2) The principle of Bellman optimality is exploited under a critic-actor-identifier architecture to achieve the optimal FTC. Different from the existing FTC schemes in [18], [21] and [22], the proposed strategy is free of exact knowledge of unknown dynamic that is estimated by identifier network; 3) In comparison with other FTC schemes in [14], [28], which only deal with a finite of actuator faults, the intermittent faults are studied here, and the optimal controller derived by actor network and the fault-tolerant controller are isolated by creating an intermediate controller. To better justification of the novelty over the existing ones, we have added some correlative explanations in this part (see the Remark 3.4 on page 4 and Remark 4.2 on page 7) and the comparative results of tracking control performance have been depicted in the **SIMULATION RESULTS** section.

Remark 3.4. The main advantages for the designed critic and actor training laws are: 1) it simplifies the design procedure in comparison to the existing optimal methods in [41], [42]; 2) it can reduce the computational complexity due to the unknown functions $\mathbf{f}_{i,1}(\bar{\mathbf{x}}_{i,1})$ and $\Delta_{i,1}(\bar{\mathbf{y}})$; 3) it enables to remove the PE condition commonly required in the optimal control.

Remark 4.2. In [27]-[29], it needs to compute the constraint bounds on the error variables $\mathrm{z}_{i,\mathfrak{l}}$. Therefore, it is essential to know the bounds of the virtual controllers. From the Eqs.(29), (35) and (39), it can be concluded that the constraint bounds are directly utilized in the control design. In this paper, this conservatism can be solved.

For the presentation of technical content, some formulas have been corrected in terms of typography, integrity and plausibility, and the authors have tried to explain them more precisely and completely in the revised manuscript. Furthermore, all the formulas have been corrected with the unified punctuation marks, such as the colons, parentheses and magnitudes. In order to present the optimal fault-tolerant control design procedure clearly, another section is added to illustrate the procedure clearly. That is, the optimized virtual controller, the optimized actual controller and the learning laws of network weights for the backstepping steps are presented in the section III, while the stability analysis for these three backstepping steps is shown in the section IV. Also, the numbers of the equations in these two sections are reduced correspondingly. Owing to the Step i,1 and Step $i,\hbar$ have some similarities in the control design and stability analysis, several formulas are omitted in the Step $i,\hbar$. Moreover, a brief block diagram of the proposed optimal fault-tolerant control scheme and some explanations of design procedure are added to exhibit the design procedures and the methodology clearer, see the Fig.1 (i.e., the figure 1 in the response) and Remark 3.5 in the revised article.

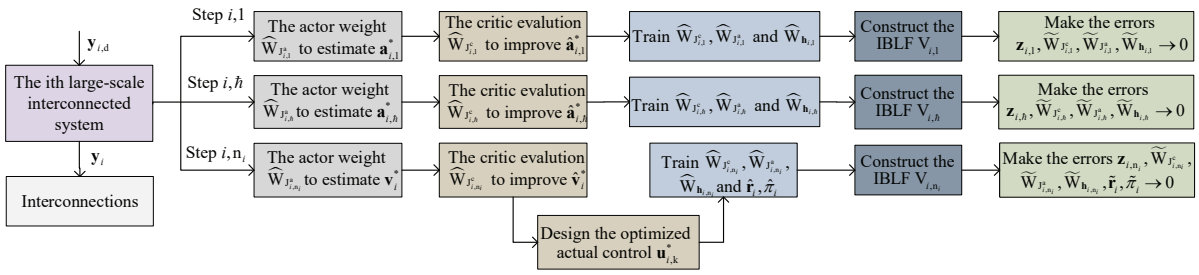

Figure 1: The block diagram of the proposed learning-based optimal FTC design.

Remark 3.5 The proposed design algorithm includes the following procedures: 1) the formulated system controlled by optimizing the virtual input in each $\mathrm{n}_i - 1$ dimension and the actual input in the n_i dimension with asymmetric constraints; 2) the critic-actor-identifier framework is used to approximate the control

policy, the value index and the nonlinear function, respectively; 3) with the defined condition for the principle of Bellman optimality, the actor/critic/identifier training laws are designed in accordance with the stability analysis; 4) by iterative updating the neural networks, the HJB equation and the optimality are finally satisfied.

For the validity of the simulation experiments, some additional figures (including the tracking control performance with no fault-tolerant control, the control input and the approximated network weights) and comparative results have been shown correspondingly. The tracking performance of the faulty system without the fault-tolerant control has been added to accomplish the same control objective, see the **Fig.5** on page 8 and **Fig.11** on page 10 (i.e., the figure 2 in the response). From which, it can be observed that the system output cannot track the reference trajectory, and the tracking error is very large when the intermittent actuator faults occur. Therefore, it is concluded that the proposed optimized fault-tolerant control approach without the compensation algorithm (27) and (28) cannot guarantee the boundedness of all the variables, i.e., the subsystems are unstable without using fault-tolerant control. Also, the control input $\mathbf{u}_{i,\mathrm{k}}$ and actuator output $\mathbf{u}_{i,\mathrm{k}}^{\mathrm{F}}$ are also depicted in **Fig.4** and **Fig.10** on page 8 and 10, i.e., the figure 3 in our response. From which, we can conclude that the control input signals are bounded regardless of whether there are intermittent actuator faults when applying our proposed optimal fault-tolerant control scheme, and the optimal fault-tolerant controller can stabilize the whole system well. The norm-bound of the estimated critic weight $\hat{\mathrm{W}}_{\mathrm{J}_{i,\iota}^{\mathrm{c}}}$, $\iota = 1, 2, \ldots, \mathrm{n}_i$, actor weight $\hat{\mathrm{W}}_{\mathrm{J}_{i,\iota}^{\mathrm{a}}}$ and identifier weight $\hat{\mathrm{W}}_{\mathbf{h}_{i,\iota}}$ vectors are shown in **Fig.3 (a)-(c)** and **Fig.9 (a)-(c)**. As is described before, the actor performs certain actions by interacting with the environment, and the critic evaluates the actions and returns feedback to the actor so that the performance of subsequent actions can be improved. From the updating laws of the critic, the actor and the identifier network weights (13), (20) and (26), we know that the actor and the critic weights are tuned to satisfy the principle of Bellman optimality of Hamilton-Jacobi-Bellman equation, while the identifier weight is utilized to approximate the unknown function $\mathbf{h}_{i,1}(\zeta_{i,1})$. From the above-mentioned figures, it can be further concluded that the presented method can not only guarantee that all the signals in closed-loop systems are uniformly ultimately bounded, but also achieve the optimal control objective. To illustrate the advantage and superiority of the proposed optimal fault-tolerant control scheme, the simulation results are compared with some relevant researches from the aspects of BLF and optimization. The control performance of the asymmetric IBLF, the tangent BLF in [27] and the logarithmic BLF in [29] are displayed in **Fig.6** and **Fig.12** (see the figure 5 in our response), i.e., (a1)-(a2) and (a1)-(a3) are tracking trajectories, and (b1)-(b2) and (b1)-(b3) are tracking errors. These three types BLFs have seen similar performance in tracking control, however, the output-variable with the proposed asymmetric IBLF is closer to the actual trajectories than the others due to its smaller tracking error. Through the selected mean square error performance criteria $\mathrm{MSE} = (1/\mathrm{T})\sum_{\mathrm{t}=0}^{\mathrm{T}}(\mathbf{y}_i(\mathrm{t}) - \mathbf{y}_{i,\mathrm{d}}(\mathrm{t}))^2$, it is possible to verify the well tracking performance and less conservative features of the proposed algorithm. Additionally, **Fig.7** and **Fig.13** (see the figure 6 in our response) show the comparisons of the tracking performance between the proposed algorithm and the algorithm with no optimization, also, the MSE results of the proposed algorithm illustrate its efficiency than the one with no optimization.

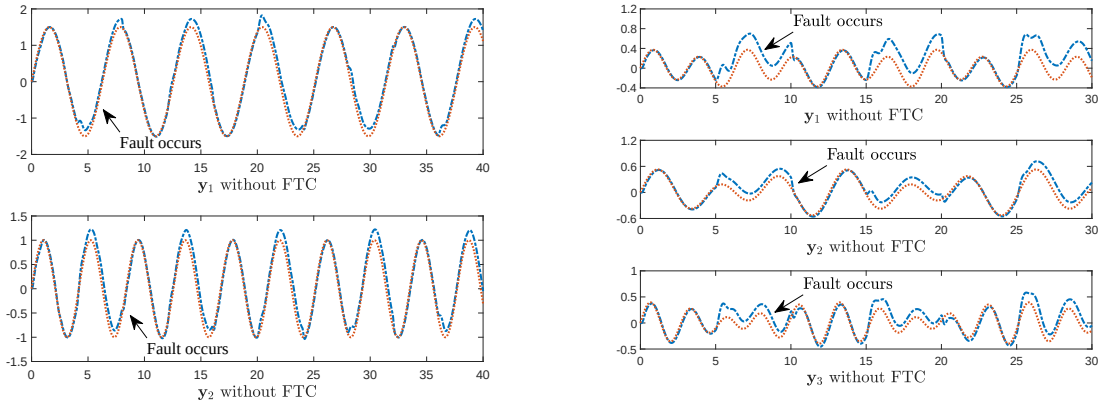

(a) Tracking trajectory result of $\mathbf{y}_i$ without FTC in Example 5.1.

(b) Tracking trajectory result of $\mathbf{y}_i$ without FTC in Example 5.2.

Figure 2: The tracking trajectory result of $\mathbf{y}_i$ without FTC.

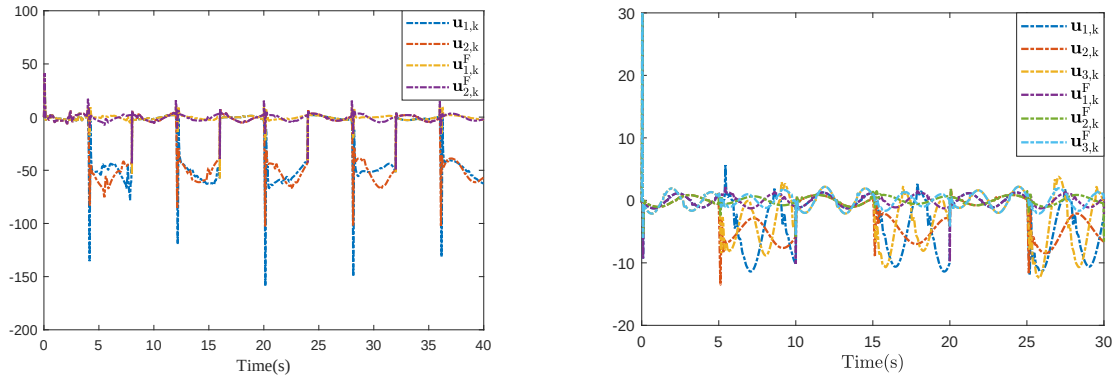

(a) Trajectories of control input $\mathbf{u}_{i,\mathrm{k}}$ and control output $\mathbf{u}^{\mathrm{F}}_{i,\mathrm{k}}$ in Example 5.1.

(b) Trajectories of control input $\mathbf{u}_{i,\mathrm{k}}$ and control output $\mathbf{u}^{\mathrm{F}}_{i,\mathrm{k}}$ in Example 5.2.

Figure 3: The trajectories of control input $\mathbf{u}_{i,\mathrm{k}}$ and control output $\mathbf{u}^{\mathrm{F}}_{i,\mathrm{k}}$.

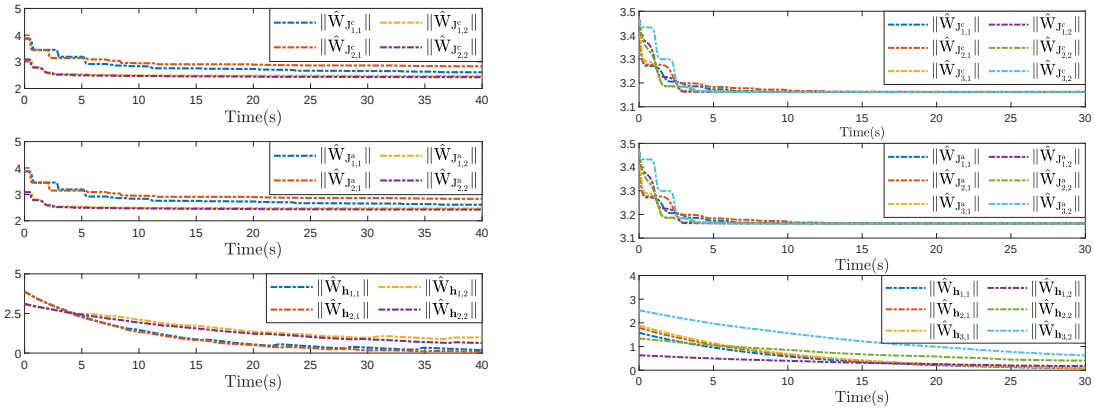

(a) The critic, actor and identifier neural network weight norms for Steps 1 and 2 in Example 5.1.

(b) The critic, actor and identifier neural network weight norms for Steps 1 and 2 in Example 5.2.

Figure 4: The critic, actor and identifier neural network weight norms for Steps 1 and 2.

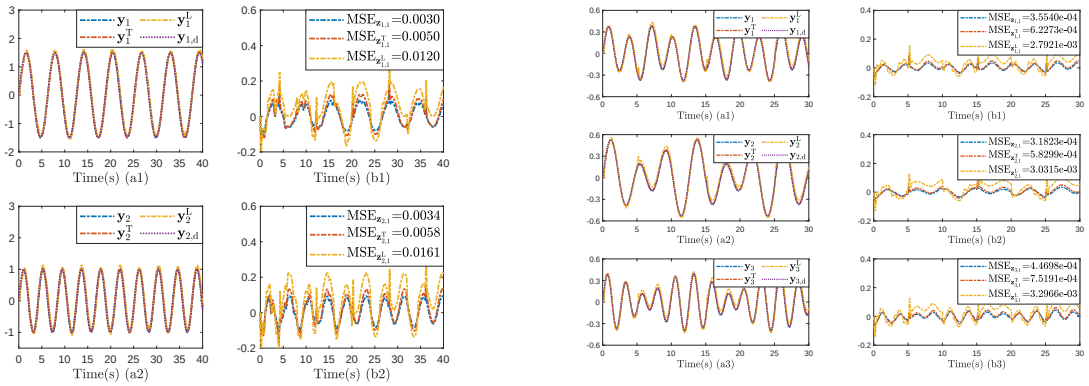

(a) The comparative results of different asymmetric BLF in Example 5.1.

(b) The comparative results of different asymmetric BLF in Example 5.2.

Figure 5: The comparative tracking trajectories and the tracking errors of the asymmetric IBLF (the blue line), the tangent BLF in [27] ($\mathbf{y}^{\mathrm{T}}_i$ and $\mathbf{z}^{\mathrm{T}}_{i,1}$, the red line) and the logarithmic BLF in [29] ($\mathbf{y}^{\mathrm{L}}_i$ and $\mathbf{z}^{\mathrm{L}}_{i,1}$, the yellow line).

For the language-related aspect, the authors have thoroughly rewritten the language and tried to resolve the variable definitions and demonstrations as many as possible, which are indicated in blue in the revised version. These changes will not influence the content and framework of the article. Now, we are confident to say that this paper is much more readable than before.

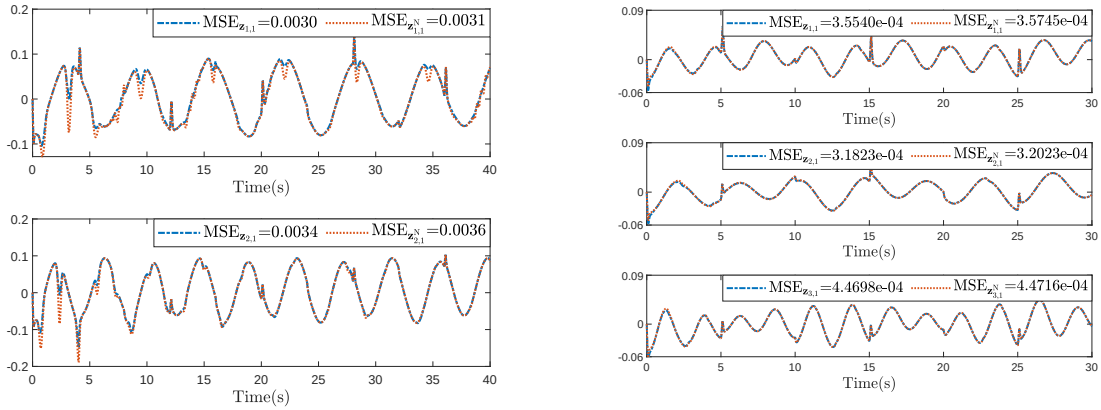

(a) The comparative results with no optimization in Example 5.1.

(b) The comparative results with no optimization in Example 5.2.

Figure 6: The comparative tracking errors of the proposed algorithm and the algorithm with no optimization ($\mathbf{z}^{\mathrm{N}}_{i,1}$, the red line).

Once again, the authors would like to express their appreciation and sincere thanks for the respectable editor's encouraging, approving, constructive, fruitful and inspiring remarks and comments.

2. Response to Reviewer 1

First of all, we would like to thank you for your helpful comments and suggestions on our manuscript, and some responses of your comments are given as follows.

Comment 1: Can the authors propose a comparison of a fault system, controlled by a controller without fault compensation? Then compare it with the presence of fault compensation. This would provide a convincing case of the effectiveness of fault compensation.

Re:

Thanks for the careful consideration of the respectable reviewer. This manuscript investigates the optimal fault-tolerant control problem for a series of state-constrained large-scale interconnected systems with intermittent actuator faults, in which the critic-actor-identifier framework in each backstepping procedure to evaluate the performance index, the optimized controller and the unknown functions, respectively. In accordance with the theoretical results, an electrical power system and a walking robot are presented to illustrate the superiority and the validity of the learning-based optimized fault-tolerant controller. To further verify the proposed control scheme, the tracking performance of the faulty system without the fault-tolerant control has been added to accomplish the same control objective, see the **Fig.5** on page 8 and **Fig.11** on page 10, i.e., the figure 7 in the response. In the simulations of no fault-tolerance control, the initial conditions of the variables and parameters are selected similar to the fault-tolerance case, and as a result, the structure of the **SIMULATION RESULTS** section, numbering of the figures, also have been changed. From which, it can be observed that the system output cannot track the reference trajectory, and the tracking error is very large when the intermittent actuator faults occur. Therefore, it is concluded that the proposed optimized fault-tolerant control approach without the compensation algorithm (27) and (28) cannot guarantee the boundedness of all the variables, i.e., the subsystems are unstable without using fault-tolerant control.

Comment 2: Also, from the simulations the authors report only the tracking errors which is not enough, it is suggested to give the control input as well. This would provide a convincing case of the reasonable control input.

Re:

The authors of this paper welcome the valuable comment. In the stage of simulations, the intermittent actuator faults are chosen as $\mathbf{u}^{\mathrm{F}}_{1,\mathrm{k}} = 0.2\mathbf{u}_{1,\mathrm{k}} + 1$ and $\mathbf{u}^{\mathrm{F}}_{2,\mathrm{k}} = 0.3\mathbf{u}_{2,\mathrm{k}} + 1.5$ when $\mathrm{t} \in [\mathrm{hT}^*, (\mathrm{h}+1)\mathrm{T}^*)$, for $\mathrm{h} = 1, 3, 5, \ldots$, and $\mathrm{T}^* = 4\mathrm{s}$ in the first example, while $\mathbf{u}^{\mathrm{F}}_{1,\mathrm{k}} = 0.2\mathbf{u}_{1,\mathrm{k}} + 1.3$, $\mathbf{u}^{\mathrm{F}}_{2,\mathrm{k}} = 0.3\mathbf{u}_{2,\mathrm{k}} + 1.25$ and $\mathbf{u}^{\mathrm{F}}_{3,\mathrm{k}} = 0.25\mathbf{u}_{2,\mathrm{k}} + 1.2$ when $\mathrm{t} \in [\mathrm{hT}^*, (\mathrm{h}+1)\mathrm{T}^*)$, for $\mathrm{h} = 1, 3, 5, \ldots$, and $\mathrm{T}^* = 5\mathrm{s}$ in the second example.

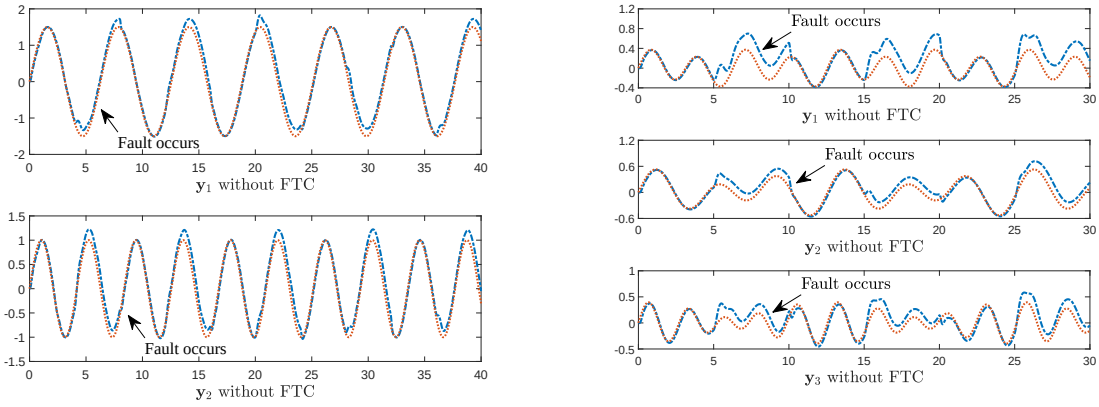

(a) Tracking trajectory result of $\mathbf{y}_i$ without FTC in Example 5.1.

(b) Tracking trajectory result of $\mathbf{y}_i$ without FTC in Example 5.2.

Figure 7: The tracking trajectory result of $\mathbf{y}_i$ without FTC.

Accordingly, the satisfactory the fault-tolerant tracking control performance is reflected on the tracking errors and the selected criteria MSE $= (1/\mathrm{T})\sum_{\mathrm{t}=1}^{\mathrm{T}}(\mathbf{y}_i(\mathrm{t}) - \mathbf{y}_{i,\mathrm{d}}(\mathrm{t}))^2$. To carry out this constructive comment and suggestion, the control input $\mathbf{u}_{i,\mathrm{k}}$ and actuator output $\mathbf{u}_{i,\mathrm{k}}^{\mathrm{F}}$ are also depicted in **Fig.4** and **Fig.10** on page 8 and 10, i.e., the figure 8 in our response. From which, we can conclude that the control input signals are bounded regardless of whether there are intermittent actuator faults when applying our proposed optimal fault-tolerant control scheme, and the optimal fault-tolerant controller can stabilize the whole system well.

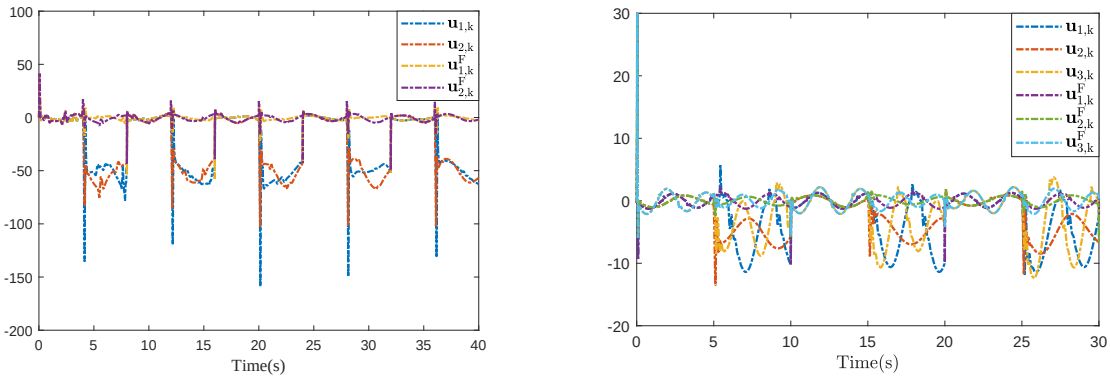

(a) Trajectories of control input $\mathbf{u}_{i,\mathrm{k}}$ and control output $\mathbf{u}_{i,\mathrm{k}}^{\mathrm{F}}$ in Example 5.1.

(b) Trajectories of control input $\mathbf{u}_{i,\mathrm{k}}$ and control output $\mathbf{u}_{i,\mathrm{k}}^{\mathrm{F}}$ in Example 5.2.

Figure 8: The trajectories of control input $\mathbf{u}_{i,\mathrm{k}}$ and control output $\mathbf{u}_{i,\mathrm{k}}^{\mathrm{F}}$.

Comment 3: This would be especially relevant in the platooning example (Example 4.2), where is important to assess if the acceleration of the vehicle is in reasonable range, if the velocity is positive, ... and other reasonable setting for a vehicle.

Re:

Thank you for pointing out this. The driving behavior of an individual vehicle within the platoon can be described by a generalized third-order nonlinear model as $\dot{\mathrm{d}}_i = \mathrm{v}_i - \mathrm{v}_{i-1}$, $\dot{\mathrm{v}}_i = \mathrm{a}_{\mathrm{c}i}$ and $\dot{\mathrm{a}}_{\mathrm{c}i} = \iota_i^{-1}\mathrm{u}_i - \iota_i^{-1}\mathrm{a}_{\mathrm{c}i}$, $i = 1, 2, \ldots, \mathrm{N}$, where $\mathrm{d}_i = \mathrm{x}_{i-1} - \mathrm{x}_i$ is the distance between two consecutive vehicles with x_{i-1} and x_i being their positions, v_i and $\mathrm{a}_{\mathrm{c}i}$ are the velocity and acceleration of the ith vehicle, u_i is the input signal chosen to make the whole system satisfy certain performance criteria, and ι_i is the time constant of the engine. For a platoon of N vehicles running on a straight flat road, it is reasonable to assume the relative distance d_i and the velocity v_i are positive, and the velocity v_i and acceleration $\mathrm{a}_{\mathrm{c}i}$ are in a limited range. Nevertheless, we found that this dynamic system cannot be modeled by the proposed large-scale interconnected system (1) with the system output $\mathrm{y}_i = \mathrm{x}_{i,1}$, due to the state vector of the ith vehicle is $\mathrm{x}_i = [\mathrm{v}_{i-1} - \mathrm{v}_{i,\mathrm{d}}, \mathrm{a}_{\mathrm{c}i-1} - \mathrm{a}_{\mathrm{c}i,\mathrm{d}}, \mathrm{d}_i - \mathrm{d}_{i,\mathrm{d}}, \mathrm{v}_i - \mathrm{v}_{i,\mathrm{d}}, \mathrm{a}_{\mathrm{c}i} - \mathrm{a}_{\mathrm{c}i,\mathrm{d}}]^{\mathrm{T}}$ and the system output is $\mathrm{y}_i = \mathrm{C}_i\mathrm{x}_i$.

Moreover, it is reasonable to utilize the distributed control strategy to stabilize the N vehicles rather than using the decentralized control. Hence, this practical example is not suitable to verify the effectiveness of the proposed optimal fault-tolerant controller in the simulations. This is our negligence to use this inappropriate example in the last round review. We were really sorry for our careless mistakes, and now, we have replaced this example with an electrical power system composed of two-machine subsystems.
As shown in the example 4.1, the dynamic model of the electrical power system is formulated in (44a) and (44b), where $\mathbf{x}_{i,1}$ and $\mathbf{x}_{i,2}$ denote the absolute rotor angle and the angular velocity of the ith machine. M_i, D_i and E_i separately represent the inertia coefficient, the damping coefficient and the internal voltage. Also, $\mathrm{Y}_{i,j}$, $\delta^0_{i,j}$ and $\theta_{i,j}$ are the constants depending on the topology, the physical properties of the network and the loads (admittance matrix) between the ith and jth machine. By selecting the reasonable parameters and under the zero initial conditions, the simulation results are exhibited in **Fig.2-7**. **Fig.2** depicts the trajectory of the output-variable $\mathbf{y}_i$ and the tracking reference signal $\mathbf{y}_{i,\mathrm{d}}$, i.e., the figure 9(a) in the response. **Fig.3** shows the 2-norm of the critic, actor and identifier network weights, i.e., $\|\hat{\mathrm{W}}_{\mathrm{J}^{\mathrm{c}}_{i,\iota}}\|$, $\|\hat{\mathrm{W}}_{\mathrm{J}^{\mathrm{a}}_{i,\iota}}\|$ and $\|\hat{\mathrm{W}}_{\mathbf{h}_{i,\iota}}\|$, $\iota = 1, 2, \ldots, \mathrm{n}_i$, i.e., the figure 10(a) in the response. **Fig.4** and **Fig.5** (i.e., the figure 8(a) and figure 7(a) in the response) present the boundedness of $\mathbf{u}_{i,\mathrm{k}}$, $\mathbf{u}^{\mathrm{F}}_{i,\mathrm{k}}$ and the tracking trajectories of $\mathbf{y}_i$ without fault-tolerant control, respectively. Moreover, the comparative results on barrier Lyapunov function and optimization are separately displayed in **Fig.6** and **Fig.7** (i.e., the figure 9(b) and (c) in the response). From these figures, we can know that the proposed algorithm can stabilize the whole system and track the actual trajectories more accurately.

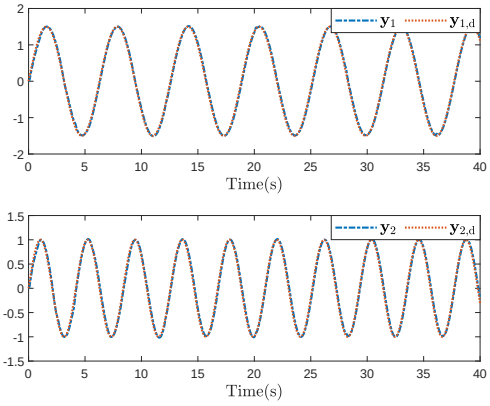

(a) Tracking trajectory results of $\mathbf{y}_i$ and $\mathbf{y}_{i,\mathrm{d}}$.

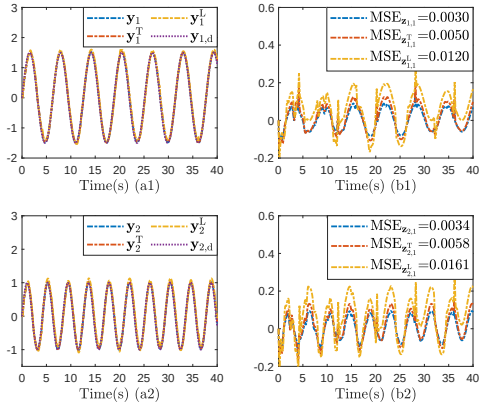

(b) The comparative tracking trajectories and the tracking errors of the asymmetric IBLF (the blue line), the tangent BLF (the red line) and the logarithmic BLF (the yellow line).

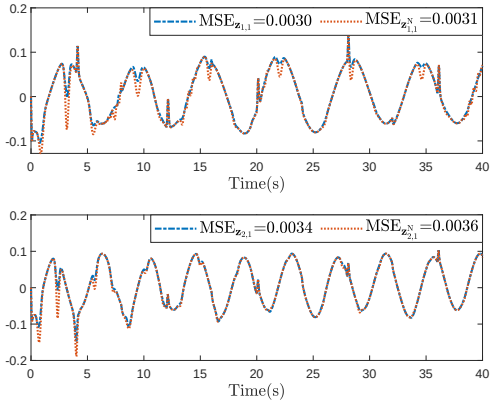

(c) The comparative tracking errors of the proposed algorithm and the algorithm with no optimization.

Figure 9: The tracking results and the comparative results in Example 5.1.

Comment 4: In many learning-based methods in the literature, a probing noise is required to guarantee convergence to the rule parameters. I did not see this mentioned in the manuscript, although I suspect

that some probing noise is needed as the authors select the signals in a sinusoidal form, expected to guarantee persistence of excitation. Please clarify if persistence of excitation is required or not. If it is required, please clarify where. If it is not required, please clarify why.

Re:

Thanks for the beneficial suggestion of the respectable reviewer. The design of an optimal controller is often troublesome because the analytical solution of the Hamilton-Jacobi-Bellman equation is difficult to obtain. This motivates the application of neural networks or fuzzy logic systems as an important supplement of the adaptive dynamic programming technique due to their global approximation ability, which has been considered an effective online and forward optimal controller design strategy. Note that the neural networks or the fuzzy logic systems require iterative optimization algorithms for training to obtain the optimized weighting parameters. During this process, the persistent of excitation (PE) condition is a commonly used precondition to avoid the disappearance of the gradient of the value function, such that the parameters can be continuously updated until they converge to the optimum. For the learning-based optimal control design, by defining a function $\Phi_i = \frac{1}{2}\mathrm{B}_{\mathrm{e}i,\mathrm{l}}^2$ with the Bellman residual error as $\mathrm{B}_{\mathrm{e}i,\mathrm{l}} = \mathrm{H}_{i,\mathrm{l}}(\mathbf{z}_{i,\mathrm{l}}, \mathbf{a}_{i,\mathrm{l}}, \mathrm{J}_{\mathbf{z}_{i,\mathrm{l}}}) - \mathrm{H}_{i,\mathrm{l}}(\mathbf{z}_{i,\mathrm{l}}, \mathbf{a}_{i,\mathrm{l}}^*, \mathrm{J}_{\mathbf{z}_{i,\mathrm{l}}}^*) = \mathrm{H}_{i,\mathrm{l}}(\mathbf{z}_{i,\mathrm{l}}, \mathbf{a}_{i,\mathrm{l}}, \mathrm{J}_{\mathbf{z}_{i,\mathrm{l}}})$, $\mathrm{l} = 1, 2, \ldots, \mathrm{n}_i$, the critic updating law can be yielded based on the gradient descent algorithm for minimizing the Bellman residual error:

$$\begin{aligned}\dot{\hat{\mathrm{W}}}_{\mathrm{J}_{i,\mathrm{l}}^{\mathrm{c}}} &= -\frac{\lambda_{i,\mathrm{l}}^{\mathrm{c}}}{1+\|\xi_{i,\mathrm{l}}\|^2}\frac{\partial \Phi_i}{\partial \hat{\mathrm{W}}_{\mathrm{J}_{i,\mathrm{l}}^{\mathrm{c}}}} \\ &= -\frac{\lambda_{i,\mathrm{l}}^{\mathrm{c}}}{1+\|\xi_{i,\mathrm{l}}\|^2}\xi_{i,\mathrm{l}}\big(\xi_{i,\mathrm{l}}^{\mathrm{T}}\hat{\mathrm{W}}_{\mathrm{J}_{i,\mathrm{l}}^{\mathrm{c}}} - (\mathrm{K}_{i,\mathrm{l}}^2 - 1)\mathrm{z}_{i,\mathrm{l}}^2 \\ &\quad + 2\mathrm{K}_{i,\mathrm{l}}\mathrm{z}_{i,\mathrm{l}}(\hat{\mathrm{W}}_{\mathbf{h}_{i,\mathrm{l}}}\mathrm{S}_{\mathbf{h}_{i,\mathrm{l}}} - \dot{\hat{\mathrm{a}}}_{i,\mathrm{l}-1}^*) + \frac{1}{4}\hat{\mathrm{W}}_{\mathrm{J}_{i,\mathrm{l}}^{\mathrm{a}}}^{\mathrm{T}}\bar{\mathrm{S}}_{\mathrm{J}_{i,\mathrm{l}}}\hat{\mathrm{W}}_{\mathrm{J}_{i,\mathrm{l}}^{\mathrm{a}}}\big)\end{aligned} \tag{1}$$

where $\dot{\hat{\mathrm{a}}}_{i,0}^* = \dot{\mathbf{y}}_{i,\mathrm{d}}$ and $\xi_{i,\mathrm{l}} = \mathrm{S}_{\mathrm{J}_{i,1}}(\hat{\mathrm{W}}_{\mathbf{h}_{i,\mathrm{l}}}\mathrm{S}_{\mathbf{h}_{i,\mathrm{l}}} - \dot{\hat{\mathrm{a}}}_{i,\mathrm{l}-1}^* - \mathrm{K}_{i,\mathrm{l}}\mathrm{z}_{i,\mathrm{l}} - \frac{1}{2}\hat{\mathrm{W}}_{\mathrm{J}_{i,\mathrm{l}}^{\mathrm{a}}}^{\mathrm{T}}\mathrm{S}_{\mathrm{J}_{i,1}})$.

Also, the actor network weight law is designed based on the stability analysis:

$$\dot{\hat{\mathrm{W}}}_{\mathrm{J}_{i,\mathrm{l}}^{\mathrm{a}}} = \frac{1}{2}\mathrm{S}_{\mathrm{J}_{i,1}}\mathrm{z}_{i,\mathrm{l}} - \lambda_{i,\mathrm{l}}^{\mathrm{a}}\bar{\mathrm{S}}_{\mathrm{J}_{i,\mathrm{l}}}\hat{\mathrm{W}}_{\mathrm{J}_{i,\mathrm{l}}^{\mathrm{a}}} + \frac{\lambda_{i,\mathrm{l}}^{\mathrm{c}}}{4(1+\|\xi_{i,\mathrm{l}}\|^2)}\bar{\mathrm{S}}_{\mathrm{J}_{i,\mathrm{l}}}\hat{\mathrm{W}}_{\mathrm{J}_{i,\mathrm{l}}^{\mathrm{a}}}^{\mathrm{T}}\xi_{i,\mathrm{l}}\hat{\mathrm{W}}_{\mathrm{J}_{i,\mathrm{l}}^{\mathrm{c}}} \tag{2}$$

For obtaining the desired control performance, the term $\xi_{i,\mathrm{l}}\xi_{i,\mathrm{l}}^{\mathrm{T}}$ should satisfy the PE condition.

However, the PE condition is difficult to verify during the learning process and in practical applications. To relax the PE condition, some additional assumptions have been introduced to ensure the stability of the control system. Motivated by the aforementioned limitations, this article proposes an optimized fault-tolerant control algorithm with neural networks for the large-scale interconnected systems on the basis of a critic-actor-identifier architecture, in which the critic, actor and identifier are utilized for evaluating the system performance, implementing the control action and estimating the unknown dynamic, respectively. In particular, the updating laws of the critic-actor-identifier architecture are derived from the Bellman residual error, such that the gradient of the Bellman residual error is always less than zero. This leads to a simple updating law making the adaptive dynamic programming technique not rely on the assumption of the PE condition, or on additional constraints. Note that the optimal control (12b), (18b) and (24b) derive $\mathrm{B}_{\mathrm{e}i,\mathrm{l}} \to 0$. If $\mathrm{H}_{i,\mathrm{l}}(\mathbf{z}_{i,\mathrm{l}}, \mathbf{a}_{i,\mathrm{l}}, \mathrm{J}_{\mathbf{z}_{i,\mathrm{l}}}) = 0$ holds, the following equation can be derived $\partial \mathrm{H}_{i,\mathrm{l}}(\mathbf{z}_{i,\mathrm{l}}, \mathbf{a}_{i,\mathrm{l}}, \mathrm{J}_{\mathbf{z}_{i,\mathrm{l}}})/\partial \hat{\mathrm{W}}_{\mathrm{J}_{i,\mathrm{l}}^{\mathrm{a}}} = \frac{1}{2}\bar{\mathrm{S}}_{\mathrm{J}_{i,\mathrm{l}}}(\hat{\mathrm{W}}_{\mathrm{J}_{i,\mathrm{l}}^{\mathrm{a}}} - \hat{\mathrm{W}}_{\mathrm{J}_{i,\mathrm{l}}^{\mathrm{c}}}) = 0$. Subsequently, by denoting a function as $\mathrm{E}_i = \mathrm{Tr}\{(\hat{\mathrm{W}}_{\mathrm{J}_{i,\mathrm{l}}^{\mathrm{a}}} - \hat{\mathrm{W}}_{\mathrm{J}_{i,\mathrm{l}}^{\mathrm{c}}})^{\mathrm{T}}(\hat{\mathrm{W}}_{\mathrm{J}_{i,\mathrm{l}}^{\mathrm{a}}} - \hat{\mathrm{W}}_{\mathrm{J}_{i,\mathrm{l}}^{\mathrm{c}}})\}$, it is easy to verify that $\partial \mathrm{H}_{i,\mathrm{l}}(\mathbf{z}_{i,\mathrm{l}}, \mathbf{a}_{i,\mathrm{l}}, \mathrm{J}_{\mathbf{z}_{i,\mathrm{l}}})/\partial \hat{\mathrm{W}}_{\mathrm{J}_{i,\mathrm{l}}^{\mathrm{a}}} = 0$ and $\mathrm{E}_i = 0$ are equivalent. Since $\partial \mathrm{E}_i/\partial \hat{\mathrm{W}}_{\mathrm{J}_{i,\mathrm{l}}^{\mathrm{a}}} = -\partial \mathrm{E}_i/\partial \hat{\mathrm{W}}_{\mathrm{J}_{i,\mathrm{l}}^{\mathrm{c}}} = 2(\hat{\mathrm{W}}_{\mathrm{J}_{i,\mathrm{l}}^{\mathrm{a}}} - \hat{\mathrm{W}}_{\mathrm{J}_{i,\mathrm{l}}^{\mathrm{c}}})$, the time-derivative of E_i can be calculated as:

$$\begin{aligned}\dot{\mathrm{E}}_i &= \mathrm{Tr}\{\frac{\partial \mathrm{E}_i}{\partial \hat{\mathrm{W}}_{\mathrm{J}_{i,\mathrm{l}}^{\mathrm{a}}}}\dot{\hat{\mathrm{W}}}_{\mathrm{J}_{i,\mathrm{l}}^{\mathrm{a}}} + \frac{\partial \mathrm{E}_i}{\partial \hat{\mathrm{W}}_{\mathrm{J}_{i,\mathrm{l}}^{\mathrm{c}}}}\dot{\hat{\mathrm{W}}}_{\mathrm{J}_{i,\mathrm{l}}^{\mathrm{c}}}\} \\ &= \mathrm{Tr}\{\frac{\partial \mathrm{E}_i}{\partial \hat{\mathrm{W}}_{\mathrm{J}_{i,\mathrm{l}}^{\mathrm{a}}}}(-\lambda_{i,\mathrm{l}}^{\mathrm{a}}\bar{\mathrm{S}}_{\mathrm{J}_{i,\mathrm{l}}}\hat{\mathrm{W}}_{\mathrm{J}_{i,\mathrm{l}}^{\mathrm{a}}} + \bar{\lambda}_{i,\mathrm{l}}\bar{\mathrm{S}}_{\mathrm{J}_{i,\mathrm{l}}}\hat{\mathrm{W}}_{\mathrm{J}_{i,\mathrm{l}}^{\mathrm{c}}}) - \frac{\partial \mathrm{E}_i}{\partial \hat{\mathrm{W}}_{\mathrm{J}_{i,\mathrm{l}}^{\mathrm{c}}}}\lambda_{i,\mathrm{l}}^{\mathrm{c}}\bar{\mathrm{S}}_{\mathrm{J}_{i,\mathrm{l}}}\hat{\mathrm{W}}_{\mathrm{J}_{i,\mathrm{l}}^{\mathrm{c}}}\} \\ &= -\frac{\lambda_{i,\mathrm{l}}^{\mathrm{a}}}{2}\mathrm{Tr}\{\frac{\partial \mathrm{E}_i}{\partial \hat{\mathrm{W}}_{\mathrm{J}_{i,\mathrm{l}}^{\mathrm{a}}}^{\mathrm{T}}}\bar{\mathrm{S}}_{\mathrm{J}_{i,1}}\frac{\partial \mathrm{E}_i}{\partial \hat{\mathrm{W}}_{\mathrm{J}_{i,\mathrm{l}}^{\mathrm{a}}}}\} \le 0\end{aligned} \tag{3}$$

which indicates that the updating laws (13), (19) and (25) can ensure the satisfaction of the above inequality, and the Bellman residual error can be near to 0 without the PE condition. To better justification

of the difference over the existing ones, we have added some correlative explanations in this part, see the **Remark 3.3** and **3.4** on page 4.

Remark 3.3. The existing results in [41], [42] need the persistent excitation (PE) condition to stabilize the control system. In contrast, we show that the Bellman residual error converges to zero without the PE condition. This can also be verified by defining a function $\mathrm{E}_i = \mathrm{Tr}\{(\hat{\mathrm{W}}_{\mathrm{J}^{\mathrm{a}}_{i,1}} - \hat{\mathrm{W}}_{\mathrm{J}^{\mathrm{c}}_{i,1}})^{\mathrm{T}}(\hat{\mathrm{W}}_{\mathrm{J}^{\mathrm{a}}_{i,1}} - \hat{\mathrm{W}}_{\mathrm{J}^{\mathrm{c}}_{i,1}})\}$. It can be verified that $\mathrm{E}_i = 0$ and $\frac{\partial \mathrm{H}_{i,1}(\mathbf{z}_{i,1},\mathbf{a}_{i,1},\mathrm{J}_{\mathbf{z}_{i,1}})}{\partial \hat{\mathrm{W}}_{\mathrm{J}^{\mathrm{a}}_{i,1}}} = 0$ are equivalent. Since $\frac{\partial \mathrm{E}_i}{\partial \hat{\mathrm{W}}_{\mathrm{J}^{\mathrm{a}}_{i,1}}} = -\frac{\partial \mathrm{E}_i}{\partial \hat{\mathrm{W}}_{\mathrm{J}^{\mathrm{c}}_{i,1}}} = 2(\hat{\mathrm{W}}_{\mathrm{J}^{\mathrm{a}}_{i,1}} - \hat{\mathrm{W}}_{\mathrm{J}^{\mathrm{c}}_{i,1}})$, the time-derivative of E_i can be calculated as:

$$\begin{aligned}\dot{\mathrm{E}}_i &= \mathrm{Tr}\{\frac{\partial \mathrm{E}_i}{\partial \hat{\mathrm{W}}_{\mathrm{J}^{\mathrm{a}}_{i,1}}}\dot{\hat{\mathrm{W}}}_{\mathrm{J}^{\mathrm{a}}_{i,1}} + \frac{\partial \mathrm{E}_i}{\partial \hat{\mathrm{W}}_{\mathrm{J}^{\mathrm{c}}_{i,1}}}\dot{\hat{\mathrm{W}}}_{\mathrm{J}^{\mathrm{c}}_{i,1}}\} \\ &= -\frac{\lambda^{\mathrm{a}}_{i,1}}{2}\mathrm{Tr}\{\frac{\partial \mathrm{E}_i}{\partial \hat{\mathrm{W}}^{\mathrm{T}}_{\mathrm{J}^{\mathrm{a}}_{i,1}}}\bar{\mathrm{S}}_{\mathrm{J}_{i,1}}\frac{\partial \mathrm{E}_i}{\partial \hat{\mathrm{W}}_{\mathrm{J}^{\mathrm{a}}_{i,1}}}\} \leq 0\end{aligned} \tag{4}$$

which implies that the learning laws (13a) and (13b) can ensure the satisfaction of (14), and the Bellman residual error can converge to zero without the PE condition.

Remark 3.4. The main advantages for the designed critic and actor training laws are: 1) it simplifies the design procedure in comparison to the existing optimal methods in [41], [42]; 2) it can reduce the computational complexity due to the unknown functions $\mathbf{f}_{i,1}(\bar{\mathbf{x}}_{i,1})$ and $\Delta_{i,1}(\bar{\mathbf{y}})$; 3) it enables to remove the PE condition commonly required in the optimal control.

Comment 5: By the way, it is also appropriate to provide the performance of the learning algorithm, the convergence of the parameters and so on.

Re:

With thanks for the careful attention of the respectable reviewer, the norm-bound of the estimated critic weight $\hat{\mathrm{W}}_{\mathrm{J}^{\mathrm{c}}_{i,\iota}}$, $\iota = 1, 2, \ldots, \mathrm{n}_i$, actor weight $\hat{\mathrm{W}}_{\mathrm{J}^{\mathrm{a}}_{i,\iota}}$ and identifier weight $\hat{\mathrm{W}}_{\mathbf{h}_{i,\iota}}$ vectors are shown in **Fig.3 (a)-(c)** and **Fig.9 (a)-(c)**. As is described before, the actor performs certain actions by interacting with environment, and the critic evaluates the actions and returns feedback to the actor so that the performance of subsequent actions can be improved. From the critic, the actor and the identifier updating laws (13), (20) and (26), we know that the actor and the critic weights are tuned to satisfy the principle of Bellman optimality of Hamilton-Jacobi-Bellman equation, while the identifier weight is utilized to approximate the unknown function $\mathbf{h}_{i,1}(\zeta_{i,1})$. From the above-mentioned figures, it can be further concluded that the presented method can not only guarantee that all the signals in closed-loop systems are uniformly ultimately bounded, but also achieve the optimal control objective.

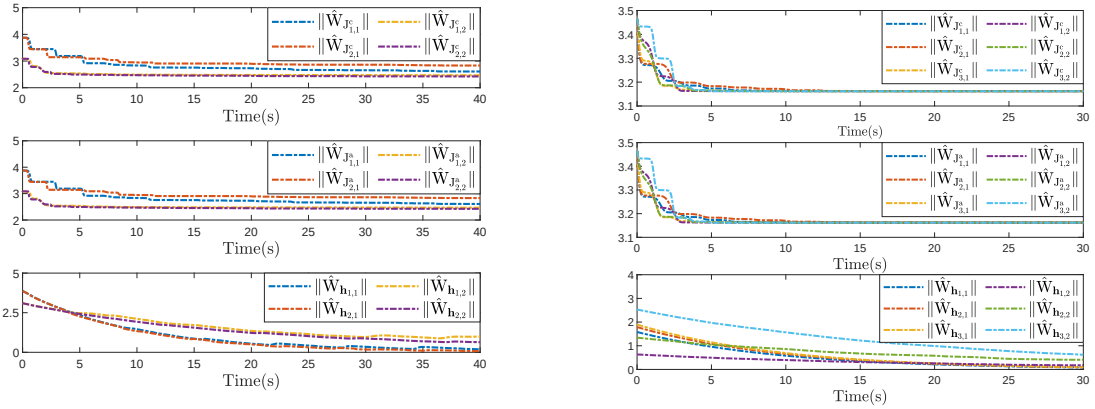

(a) The critic, actor and identifier neural network weight norms for Steps 1 and 2 in Example 5.1.

(b) The critic, actor and identifier neural network weight norms for Steps 1 and 2 in Example 5.2.

Figure 10: The critic, actor and identifier neural network weight norms for Steps 1 and 2.

Comment 6: In general, English language is sometimes poor, please consider polishing it. Some expression are also not rigorous, such as 'achieve an exceptional system performance', please consider polishing it.

Re:
Thank you for your useful advice. To address these deficiencies in the article, the authors have thoroughly rewritten the language and tried to resolve the variable definitions and demonstrations as many as possible, which are indicated in blue in the revised version. These changes will not influence the content and framework of the article. Now, we are confident to say that this paper is much more readable than before.

Once again, the authors would like to express their appreciation and sincere thanks for the respectable reviewer's encouraging, approving, constructive, fruitful and inspiring remarks and comments.

3. Response to Reviewer 2

First of all, we would like to thank you for your helpful comments and suggestions on our manuscript, and some responses of your comments are given as follows.

Comment 1: The language of some sentences need to be modified. (e.g., the actuator faults including the loss of effectiveness and stuck faults, which are modeled as. This sentence lacks the predicate.)
Re:
Thanks for the beneficial suggestion of the respectable reviewer. On the basis of your suggestion, we have checked the language of this paper carefully, and we have corrected some grammatical, editorial and even conceptual errors as much as possible. These changes will not influence the content and framework of the paper. And here, we did not list the changes but indicated in blue in the revised version.

Comment 2: What is the Young's inequality? In this paper, the Young's inequality is directly introduced. Please provide an appropriate introduction about the Young's inequality.
Re:
Thanks for the careful attention of the respectable reviewer. In the manuscript, the Young's inequality is introduced to amplify the terms $\phi_{i,1}\Delta_{i,1}$, $\phi_{i,\hbar}\Delta_{i,\hbar}$ and $\phi_{i,\mathrm{n}_i}\Delta_{i,\mathrm{n}_i}$ in (30), (35) and (39). The specific form of the Young's inequality is presented in **Lemma 2.2** on page 3, i.e, for any vectors $\mathrm{x}, \mathrm{y} \in \mathcal{R}^{\mathrm{n}}$, there is an inequality $\mathrm{xy} \leq \frac{\eta^{\mathrm{a}}}{\mathrm{a}}|\mathrm{x}|^{\mathrm{a}} + \frac{1}{\mathrm{b}\eta^{\mathrm{b}}}|\mathrm{y}|^{\mathrm{b}}$ holds with $\eta > 0$, $\mathrm{a} > 1$, $\mathrm{b} > 1$ and $(\mathrm{a}-1)(\mathrm{b}-1) = 1$. As for the inequalities (30), (35) and (39), if we choose $\mathrm{a} = \mathrm{b} = 2$ and $\eta = 1/\sqrt{2}$, and combine the Assumption 2.2, it derives that

$$\phi_{i,\mathrm{l}}\Delta_{i,\mathrm{l}} \leq \frac{1}{4}\phi_{i,\mathrm{l}}^2 + (\sum_{\mathrm{s}=1}^{\mathrm{p}_{i,\mathrm{l}}}\sum_{l=1}^{\mathrm{N}} \mathrm{q}_{i,\mathrm{l},l}^{\mathrm{s}}|\mathbf{y}_l|^{\mathrm{s}})^2,\ \mathrm{l} = 1, 2, \ldots, \mathrm{n}_i \tag{5}$$

By using the Cauchy-Schwartz inequality $(\sum_{\mathrm{s}=1}^{\mathrm{p}_{i,\mathrm{l}}} \mathrm{a}_{\mathrm{s}}\mathrm{b}_{\mathrm{s}})^2 \leq (\sum_{\mathrm{s}=1}^{\mathrm{p}_{i,\mathrm{l}}} \mathrm{a}_{\mathrm{s}}^2)(\sum_{\mathrm{s}=1}^{\mathrm{p}_{i,\mathrm{l}}} \mathrm{b}_{\mathrm{s}}^2)$, we can obtain

$$\begin{aligned}(\sum_{\mathrm{s}=1}^{\mathrm{p}_{i,\mathrm{l}}}\sum_{l=1}^{\mathrm{N}} \mathrm{q}_{i,\mathrm{l},l}^{\mathrm{s}}|\mathbf{y}_l|^{\mathrm{s}})^2 &\leq \big(\sum_{\mathrm{s}=1}^{\mathrm{p}_{i,\mathrm{l}}}(\sum_{l=1}^{\mathrm{N}} \mathrm{q}_{i,\mathrm{l},l}^{\mathrm{s}}|\mathbf{y}_l|^{\mathrm{s}})^2 \times \sum_{\mathrm{s}=1}^{\mathrm{p}_{i,\mathrm{l}}} 1^2\big) \\ &\leq \mathrm{p}_{i,\mathrm{l}}\sum_{\mathrm{s}=1}^{\mathrm{p}_{i,\mathrm{l}}}(\sum_{l=1}^{\mathrm{N}}(\mathrm{q}_{i,\mathrm{l},l}^{\mathrm{s}}|\mathbf{y}_l|^{\mathrm{s}})^2 \times \sum_{l=1}^{\mathrm{N}} 1^2)\end{aligned} \tag{6}$$

For the large-scale interconnected system with N subsystem, there is $\mathrm{Np}_{i,\mathrm{l}}\sum_{i=1}^{\mathrm{N}}\sum_{\mathrm{s}=1}^{\mathrm{p}_{i,\mathrm{l}}}(\sum_{l=1}^{\mathrm{N}}(\mathrm{q}_{i,\mathrm{l},l}^{\mathrm{s}}|\mathbf{y}_l|^{\mathrm{s}})^2 \leq \mathrm{Np}_{i,\mathrm{l}}\sum_{i=1}^{\mathrm{N}}\sum_{\mathrm{s}=1}^{\mathrm{p}_{i,\mathrm{l}}}\sum_{l=1}^{\mathrm{N}}(\mathrm{q}_{l,\mathrm{l},i}^{\mathrm{s}}|\mathbf{y}_i|^{\mathrm{s}})^2$. By substituting $\mathbf{y}_i = \mathbf{x}_{i,1}$ and $\mathbf{x}_{i,1} = \mathbf{z}_{i,1} + \mathbf{y}_{i,\mathrm{d}}$ into the above inequality, and utilising Cauchy-Schwartz inequality $(\sum_{i=1}^{2} \mathrm{a}_i)^{2\mathrm{k}} \leq 2^{2\mathrm{k}}(\sum_{i=1}^{2} \mathrm{a}_i^{2\mathrm{k}})$, one has

$$\mathrm{Np}_{i,\mathrm{l}}\sum_{\mathrm{s}=1}^{\mathrm{p}_{i,\mathrm{l}}}\sum_{l=1}^{\mathrm{N}}(\mathrm{q}_{l,\mathrm{l},i}^{\mathrm{s}}|\mathbf{y}_i|^{\mathrm{s}})^2 \leq \sum_{\mathrm{s}=1}^{\mathrm{p}} 2^{2\mathrm{s}}\mathbf{q}_{l,\mathrm{l},i}(|\mathbf{z}_{i,1}|^{2\mathrm{s}} + |\mathbf{y}_{i,\mathrm{d}}|^{2\mathrm{s}}) \tag{7}$$

where $\mathbf{q}_{l,\mathrm{l},i} = \mathrm{Np}\sum_{l=1}^{\mathrm{N}} \mathrm{q}_{l,\mathrm{l},i}^{2\mathrm{s}}$, $\mathrm{l} = 1, 2, \ldots, \mathrm{n}_i$. These computational procedures are omitted in the inequalities (30), (35) and (39) for simplifications.
Lemma 2.2 (Young's inequality [4]). For any vectors $\mathrm{x}, \mathrm{y} \in \mathcal{R}^{\mathrm{n}}$, the following inequality holds:

$$\mathrm{xy} \leq \frac{\eta^{\mathrm{a}}}{\mathrm{a}}|\mathrm{x}|^{\mathrm{a}} + \frac{1}{\mathrm{b}\eta^{\mathrm{b}}}|\mathrm{x}|^{\mathrm{b}} \tag{8}$$

where $\eta > 0$, $\mathrm{a} > 1$, $\mathrm{b} > 1$ and $(\mathrm{a}-1)(\mathrm{b}-1) = 1$.

Comment 3: Please unify the use of punctuation marks. All formulas are preceded by colons, but the formula (47) does not use colons.

Re:

The authors of this paper welcome the valuable comment. Based on your comment, all the formulas have been reviewed and corrected in terms of typography, integrity and plausibility, and the authors have tried to explain them more precisely and completely in the revised manuscript. Furthermore, all the formulas have been corrected with the unified punctuation marks, such as the colons, parentheses, magnitudes and so on.

Comment 4: Please highlight the contribution of the paper. Besides, the research background can be enriched by considering the related work: Recent progress in reinforcement learning and adaptive dynamic programming for advanced control applications; Optimal and autonomous control using reinforcement learning: A survey. The reviewer thinks that such publications can greatly improve the coverage of the paper.

Re:

Thank you for your useful advice. As is well known that, the increasing complexity makes components and equipments be more susceptible to diverse faults, which may cause unexpected reactions and even catastrophes in the automated process. Therefore, the fault-tolerant control techniques have been investigated intensively over the past few decades. Note that most results achieved the stabilization only for faulty nonlinear systems, rather than both stabilization and optimization simultaneously, thus, the optimal fault-tolerant control method is imperative and challenge to balance the stability and the optimality of faulty systems. From the viewpoint of most previous studies, there are still no results on reporting the optimal fault-tolerant control design for both multiplicative and additive faults cases (most results only focus on additive faults or the actuator faults under a single occurrence time), even in the large-scale interconnected systems, which are the main motivations of our paper. In light of the mentioned benefits and limitations, we intend to introduce the optimal fault-tolerant control problem for a class of large-scale interconnected systems with both intermittent loss of effectiveness and stuck actuator faults, with the help of a critic-actor-identifier architecture. Among which, the actor is utilized to implement control actions, the critic is utilized to evaluate these actions from the environment and to return the evaluations to the actor so that the subsequent actions can be well, and the identifier is utilized to approximate the unknown dynamic.

To address this concern of the honorable reviewer, the **INTRODUCTION** and **REFERENCES** sections have been entirely rewritten in the revised version, at the same time, we have tried to enhance and clarify the presentation of the original ideas, main features and objectives of this paper. Further, a number of related reference and explanations and new evaluations have been added to the introduction. These descriptions are indicated in blue in the revised manuscript. In comparison to some previous literature, there are mainly three theoretical contributions and differences in our paper, which can be summarized as the following aspects: 1) An asymmetric IBLF is incorporated into each backstepping step to maintain the state-variables in an asymmetric constrained region. This function can enable full state-constraints during the learning process directly, and avoid the complex tracking error-constraints conversion inherent in the conventional BLFs [27]-[29]; 2) The principle of Bellman optimality is exploited under a critic-actor-identifier architecture to achieve the optimal FTC. Different from the existing FTC schemes in [18], [21] and [22], the proposed strategy is free of exact knowledge of unknown dynamic that is estimated by identifier network; 3) In comparison with other FTC schemes in [14], [28], which only deal with a finite of actuator faults, the intermittent faults are studied here, and the optimal controller derived by actor network and the fault-tolerant controller are isolated by creating an intermediate controller. To better justification of the novelty over the existing ones, we have added some correlative explanations in this part (see the Remark 3.4 on page 4 and Remark 4.2 on page 7) and the comparative results of tracking control performance have been depicted in the **SIMULATION RESULTS** section.

Remark 3.4. The main advantages for the designed critic and actor training laws are: 1) it simplifies the design procedure in comparison to the existing optimal methods in [41], [42]; 2) it can reduce the computational complexity due to the unknown functions $\mathbf{f}_{i,1}(\bar{\mathbf{x}}_{i,1})$ and $\Delta_{i,1}(\bar{\mathbf{y}})$; 3) it enables to remove the PE condition commonly required in the optimal control.

Remark 4.2. In [27]-[29], it needs to compute the constraint bounds on the error variables $z_{i,\iota}$. Therefore, it is essential to know the bounds of the virtual controllers. From the Eqs.(29), (35) and (39), it can be concluded that the constraint bounds are directly utilized in the control design. In this paper, this

conservatism can be solved.

Comment 5: The parentheses in some formulas are small. A suitable parenthesis can wrap the entire content inside. (e.g., The parentheses of the formulas (23) and (29) are obviously too small.)
Re:
We appreciate the useful advice made by the respectable reviewer. Owing to the changes made in the article, the structure of some sections, and as a result, numbering of the formula has been changed, and omissions and inconsistencies have been corrected in the revised manuscript correspondingly. In addition, the suitable parentheses, punctuation marks and font sizes have been added in each formula.

Comment 6: How are the actuator faults established? Is it accurate to only consider the loss of effectiveness and the stuck faults? Please provide the detailed response from the authors.
Re:
Thanks for the careful consideration of the respectable reviewer. Intermittent faults are that the actuator states change frequently between normally working mode and faulty mode or between various faulty modes during operation. Such faults will inevitably lead to the intermittent jumps of unknown parameters, and the number of jumps may tend to be infinite. Due to the effects of intermittent jumps, the estimated parameters in the controller may increase ceaselessly, and the possible increase of the Lyapunov function may accumulate ceaselessly, as the number of jumps increases. Finally, the boundedness property is lost as the number of jumps tends to infinity. Nevertheless, the existing fault-tolerant control schemes cannot be applied to deal with the problems on the infinite number of actuator failures. Therefore, under the case of intermittent actuator faults, effectively guaranteeing the boundedness of parameter estimates in the controller and closed-loop stability is very challenging; in turn, establishing the optimal fault-tolerant control strategy and the system tracking performance are also difficult.
It is well known that, the actuator faults $\mathbf{u}_i^{\mathrm{F}} = \psi_i(\mathrm{t})\mathbf{u}_i + \zeta_i(\mathrm{t})$ including both the loss of effectiveness and stuck-type actuator faults have been considered in [13], [27] under single occurrence time, where $\psi_i(\mathrm{t})$ represent the unknown efficiency factor satisfying $0 \leq \psi_i(\mathrm{t}) < 1$ and $\zeta_i(\mathrm{t})$ is a bounded signal (bounded function). In contrast to this, we consider an actuator fault that may be recovered to a normally working mode or changes from one fault mode to another fault mode intermittently. As described in the Eq.(2), $0 \leq \underline{\psi}_{i,\mathrm{k}} \leq \psi_{i,\mathrm{k}}^{\mathrm{h}} \leq 1$ with $\underline{\psi}_{i,\mathrm{k}}$ and $\psi_{i,\mathrm{k}}^{\mathrm{h}}$ being unknown constants, $\zeta_{i,\mathrm{k}}^{\mathrm{h}}$ is the stuck value. $\mathrm{t} \in [\mathrm{t}_{i,\mathrm{h}}, \mathrm{t}_{i,\mathrm{h}+1})$ for $\mathrm{h} \in \mathrm{Z}^+$, and $\mathrm{t}_{i,\mathrm{h}}$ represents the unknown failure time constant, which indicates the actuator faults are completely unpredictable in time, pattern, and value. From the Eq.(2), four types of states of the kth actuator are described as follows: i) $\psi_{i,\mathrm{k}}^{\mathrm{h}} \in (0,1)$ and $\zeta_{i,\mathrm{k}}^{\mathrm{h}} \neq 0$ indicate that the kth actuator has the loss of control effectiveness and stuck faults at the same time; ii) $\psi_{i,\mathrm{k}}^{\mathrm{h}} \in (0,1)$ and $\zeta_{i,\mathrm{k}}^{\mathrm{h}} = 0$ imply that it can only output a fraction of the control input; iii) $\psi_{i,\mathrm{k}}^{\mathrm{h}} = 1$ and $\zeta_{i,\mathrm{k}}^{\mathrm{h}} \neq 0$ signify stuck faults only; iv) $\psi_{i,\mathrm{k}}^{\mathrm{h}} = 1$ and $\zeta_{i,\mathrm{k}}^{\mathrm{h}} = 0$ means the fault-free case. Concise descriptions of the intermittent actuator faults are further explained in the revised article as a response to this comment (see the **Remark 2.1** and **2.2** on page 2).
There are many types of faults (the actuator/sensor or the component faults) that occur in the engineering systems that are modeled the studied system described in (1), wherein the loss of effectiveness and the stuck actuator faults are common types. For the electrical power system composed of two-machines, the pressure drop across the valve changes depending on its opening (i.e., the flow rate value), and the control voltage signals are sent from the controller to the valve, and control the needle valves opening to achieve the required constant pressure drop across the valve. The faults that are considered in this paper including multiplicative and additive actuator faults, the partial loss (multiplicative) and bias (additive) failures of electromechanical components including motor and generator may cause unstable voltages during the long-time running or working in the remote and harsh environments. And for a walking robot, the multiplicative term refers to a fault that maybe caused by partial loss of actuator torque, electrical power or partial brakes of a joint, while the additive term means that a joint is gradually drifting from the actual torque command caused by the damage in the motor windings or faulty electronics.
Remark 2.1. The ith actuator mainly can experiment with the following four cases: i) $\psi_{i,\mathrm{k}}^{\mathrm{h}} \in (0,1)$ and $\zeta_{i,\mathrm{k}}^{\mathrm{h}} \neq 0$ indicate that the ith subsystem has the loss of control effectiveness and stuck faults at the same time; ii) $\psi_{i,\mathrm{k}}^{\mathrm{h}} \in (0,1)$ and $\zeta_{i,\mathrm{k}}^{\mathrm{h}} = 0$ imply that it can only output a fraction of the control input; iii) $\psi_{i,\mathrm{k}}^{\mathrm{h}} = 1$ and $\zeta_{i,\mathrm{k}}^{\mathrm{h}} \neq 0$ signify stuck faults only; iv) $\psi_{i,\mathrm{k}}^{\mathrm{h}} = 1$ and $\zeta_{i,\mathrm{k}}^{\mathrm{h}} = 0$ means the fault-free case.
Remark 2.2. The fault number h in [14], [28] is limited to finite under a single occurrence time. In contrast to this, the more general case is considered as Eq.(2), which indicates that the actuator can be intermittently revert to normal operation, or alternate intermittently between different fault modes. It is

applicable not only to the actuator faults with uniform interval periods but to those with non-uniform interval periods.

Once again, the authors would like to express their appreciation and sincere thanks for the respectable reviewer's encouraging, approving, constructive, fruitful and inspiring remarks and comments.

4. Response to Reviewer 3

First of all, we would like to thank you for your helpful comments and suggestions on our manuscript, and some responses of your comments are given as follows.

Comment 1: In this paper, under equation (1), the authors propose the assumption on the dynamics of the system. For example limitation on $\mathbf{g}_{i,j}(\mathbf{x}_{i,j})$ and $\Delta_{i,j}(\bar{\mathbf{y}})$ are not acceptable assumptions. I think that it is essential to derive new assumption on $\mathbf{f}_{i,j}(\mathbf{x}_{i,j})$.
Re:
Thanks for the beneficial suggestion of the respectable reviewer. As for the considered large-scale interconnected system (1) with N subsystems, $\mathbf{f}_{i,\iota}(\bar{\mathbf{x}}_{i,\iota})$ and $\mathbf{g}_{i,\iota}(\bar{\mathbf{x}}_{i,\iota})$, $\iota = 1, 2, \ldots, \mathrm{n}_i$ depict the unknown functions, and $\Delta_{i,\iota}(\bar{\mathbf{y}})$ is the interconnection among subsystems with $\bar{\mathbf{y}} = [\mathbf{y}_1, \mathbf{y}_2, \ldots, \mathbf{y}_{\mathrm{N}}]^{\mathrm{T}}$. Subsequently, the optimal fault-tolerant control strategy is designed to track the desired reference signal $\mathbf{y}_{i,\mathrm{d}}$, on the basis of the backstepping control technique and a critic-actor-identifier learning-based framework. To achieve this purpose, there are some assumptions and lemmas employed for the large-scale interconnected system. Some assumptions are utilized to achieve this purpose, see the Assumption 2.1-2.3. The Assumption 2.1 implies that the control coefficient $\mathbf{g}_{i,1}(\bar{\mathbf{x}}_{i,\iota})$ is bounded and not equal to zero, and the sign function of $\mathbf{g}_{i,\mathrm{n}_i}^{\mathrm{k}}$ is known, which are the standard controllable condition in dynamic system and can be found in [37]. This assumption of coefficient is guarantee that the fault-tolerant controller is exist and can be designed by applying the proposed strategy. The Assumption 2.2 is a bounded restriction for the interconnected term $\Delta_{i,\iota}(\bar{\mathbf{y}})$, which is utilized in stability analysis of the inequalities (31), (36) and (41), with the help of the Youngs inequality (i.e., the Lemma 2.2). Besides, the Assumption 2.3 is a bounded condition for the desired trajectory $\mathbf{y}_{i,\mathrm{d}}$ and its ιth order derivative, that making the optimized virtual control inputs $\hat{\mathbf{a}}_{i,\hbar-1}^{*}$, $\hat{\mathbf{a}}_{i,\mathrm{n}_i-1}^{*}$ and optimized actual control input $\mathbf{u}_{i,\mathrm{k}}^{*}$ are bounded. To estimate the unknown function $\mathbf{f}_{i,\iota}(\bar{\mathbf{x}}_{i,\iota})$, the neural network in Lemma 2.1 is utilized to solve this problem due to its global approximation ability. In this article, the unknown dynamic $\mathbf{h}_{i,\iota}(\zeta_{i,\iota})$ containing $\mathbf{f}_{i,\iota}(\bar{\mathbf{x}}_{i,\iota})$ and other unknown terms is approximated by neural network, and the training law of identifier weight is given correspondingly.
Note that in some practical applications of the large-scale interconnected systems, e.g., an electrical power system composed of two-machine subsystems [38], a walking robot composed by three interconnected subsystems [39], the inverted pendulums [14], etc. The control coefficients are also bounded and not close to zero, and the interconnected terms in these practical examples are bounded by a function in state variables. These examples can reflect that the Assumption 2.1-2.3 are reasonable and meet in practice. To address this concern of the honorable referee, the description of all assumptions and lemmas have been changed, and some explanations about the assumptions and lemmas have been added, see the **Remark 2.3** on page 3 in the revised paper.
Remark 2.3. As a kind of typical LSIS, the form of Eq.(1) can be found in several practical applications [14], [38], [39]. It should be underlined that Assumptions 2.1-2.3 are the standard and necessary requirements in the optimal FTC design during the subsequent section.

Once again, the authors would like to express their appreciation and sincere thanks for the respectable reviewer's encouraging, approving, constructive, fruitful and inspiring remarks and comments.

5. Response to Reviewer 4

First of all, we would like to thank you for your helpful comments and suggestions on our manuscript, and some responses of your comments are given as follows.

Comment 1: The fault-tolerant control problem in large-scale and networked systems has been of interest at least for the last three decades. That means any contribution in the field should be well justified

and supported by the available literature. I see some very important and relevant articles that have not been reviewed in the paper. For example:
[1] Tang, X., Zhai, D. and Li, X., 2020. Adaptive fault-tolerance control based finite-time backstepping for hypersonic flight vehicle with full state constrains. Information Sciences, 507, pp.53-66.
addresses a very similar problem and even use the Barrier Lyapunov Function method (the same as this paper). I am really keen to see where the weakness of the method, proposed in [1], is and how the current paper is going to fix it. Or, the following paper is very relevant, but is not cited:
[2] Yang, W., Jiang, Y., He, X., Zhu, Y. and Wang, S., 2022. Feasibility conditions-free prescribed performance decentralized fault-tolerant neural control of constrained large-scale systems. IEEE Transactions on Systems, Man, and Cybernetics: Systems, 53(5), pp.3152-3164.
Authors are kindly asked to:
a. Complete the literature review, and clearly show the gap of knowledge that none of the previous literature has filled.
b. Compare the performance of the proposed controller with one or two most relevant articles in the literature to prove the gap is filled.

Re:

Thanks for the careful consideration of the respectable reviewer. Note that the optimal controller can ensure that the closed-loop system is bounded, and achieves an adequate level of performance as well, the optimal fault-tolerant control problem is investigated for the large-scale interconnected systems with the intermittent actuator faults and state-constraints. To illustrate the differences and the contributions with the existing literature, the **INTRODUCTION** and **SIMULATION RESULTS** sections are completely rewritten and their organizations are modified accordingly. Also, the related recent articles and comparative results are added to better justification of the novelty over the existing ones.

a). For the gaps and contributions of the manuscript, some corresponding works are supplied to elaborate the specificities and the differences. In comparison with the previous literature, there are mainly two aspects are illustrated as follows, including the optimal fault-tolerant control and the integral barrier Lyapunov function. It is well known that the optimal fault-tolerant control has an extensive application prospect in control fields, aiming at finding a controller during an interval while optimizing the objective function, then the energy consumption is reduced in the case of faults. From the viewpoint of most previous studies, there are still no results on reporting the optimal fault-tolerant control design for both intermittent multiplicative and additive faults case (most results only focus on additive faults or the actuator faults under a single occurrence time), even in the large-scale interconnected systems, which are the main motivations of our paper. In light of the mentioned benefits and limitations, we intend to introduce the optimal fault-tolerant control problem for a class of large-scale interconnected systems with both intermittent loss of effectiveness and stuck actuator faults, with the help of a critic-actor-identifier architecture. From which, the actor is utilized to implement control actions, the critic is utilized to evaluate these actions from the environment and to return the evaluations to the actor so that the subsequent actions can be well, and the identifier is utilized to approximate the unknown dynamic.
As for the constrained system, the processing of constraints using integral barrier Lyapunov function have been greatly simplified and relaxed the feasibility conditions, i.e., it has a well-calculated capability of not requiring to convert state-constraints into transformed error-constraints, but help to restrict a system state directly. Thus, the conservatism of tangent-type and logarithmic-type barrier Lyapunov functions-based control in the existing literature can be reduced. Also, the integral barrier Lyapunov functions studied in most works are only available for constrained problems with the symmetric limitations. On this basis, the asymmetric integral barrier Lyapunov function can handle the optimal fault-tolerant control design with an asymmetric state-constrained problem.
Throughout the whole article, we intend to summarize and enhance the innovations and contributions specifically in terms of these two aspects. These descriptions are indicated in blue. Compared with some previous literature, there are three theoretical contributions and differences in our paper, which can be summarized in following: 1) An asymmetric IBLF is incorporated into each backstepping step to maintain the state-variables in an asymmetric constrained region. This function can enable full state-constraints during the learning process directly, and avoid the complex tracking error-constraints conversion inherent in the conventional BLFs [27]-[29]; 2) The principle of Bellman optimality is exploited under a critic-actor-identifier architecture to achieve the optimal FTC. Different from the existing FTC schemes in [18], [21] and [22], the proposed strategy is free of exact knowledge of unknown dynamic that is estimated by identifier network; 3) In comparison with other FTC schemes in [14], [28], which only deal with a finite

of actuator faults, the intermittent faults are studied here, and the optimal controller derived by actor network and the fault-tolerant controller are isolated by creating an intermediate controller. To better justification of the novelty over the existing ones, we have added some correlative explanations in this part (see the Remark 3.4 and Remark 4.2) and the comparative results of tracking control performance have been depicted in the **SIMULATION RESULTS** section.

Remark 3.4. The main advantages for the designed critic and actor training laws are: 1) it simplifies the design procedure in comparison to the existing optimal methods in [41], [42]; 2) it can reduce the computational complexity due to the unknown functions $\mathbf{f}_{i,1}(\bar{\mathbf{x}}_{i,1})$ and $\Delta_{i,1}(\bar{\mathbf{y}})$; 3) it enables to remove the PE condition commonly required in the optimal control.

Remark 4.2. In [27]-[29], it needs to compute the constraint bounds on the error variables $\mathrm{z}_{i,\iota}$. Therefore, it is essential to know the bounds of the virtual controllers. From the Eqs.(29), (35) and (39), it can be concluded that the constraint bounds are directly utilized in the control design. In this paper, this conservatism can be solved.

b). In order to show the superiority of the proposed optimal fault-tolerant control scheme, the simulation results are compared with some relevant researches from the aspects of barrier Lyapunov function and optimization. The tracking control performance of the asymmetric IBLF, the asymmetric tangent BLF in [27] and the asymmetric logarithmic BLF in [29] are displayed in **Fig.6** and **Fig.12** (see the figure 11 in our response), i.e., (a1)-(a2) and (a1)-(a3) are tracking trajectories, and (b1)-(b2) and (b1)-(b3) are tracking errors. These three types BLFs have seen similar performance in tracking control, however, the output-variable with the proposed asymmetric IBLF is closer to the actual trajectories than the others due to its a smaller tracking error. Through the selected mean square error performance criteria $\mathrm{MSE} = (1/\mathrm{T})\sum_{\mathrm{t}=0}^{\mathrm{T}}(\mathbf{y}_i(\mathrm{t}) - \mathbf{y}_{i,\mathrm{d}}(\mathrm{t}))^2$, it is possible to verify the well tracking performance and less conservative features of the proposed algorithm. Additionally, **Fig.7** and **Fig.13** (see the figure 12 in our response) show the comparisons of the tracking performance between the proposed algorithm and the algorithm without optimization, also, the MSE results of the proposed algorithm illustrate its efficiency than the one with no optimization.

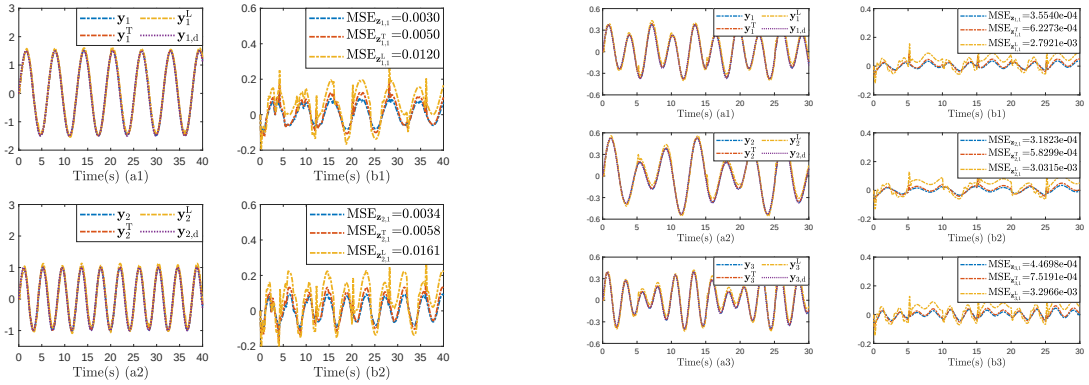

(a) The comparative results of different asymmetric BLF in Example 5.1.

(b) The comparative results of different asymmetric BLF in Example 5.2.

Figure 11: The comparative tracking trajectories and the tracking errors of the asymmetric IBLF (the blue line), the tangent BLF in [27] ($\mathbf{y}_i^{\mathrm{T}}$ and $\mathbf{z}_{i,1}^{\mathrm{T}}$, the red line) and the logarithmic BLF in [29] ($\mathbf{y}_i^{\mathrm{L}}$ and $\mathbf{z}_{i,1}^{\mathrm{L}}$, the yellow line).

Comment 2: The paper is structurally very difficult to follow. That is mainly because,

a. The notation of the paper is sometimes vague and not consistent. For example in Eq.(1), the subscript j in $\mathbf{x}_{i,j}$ means jth element of $\mathbf{x}_i$, while in $\Delta_{i,j}$ it means jth subsystem, and in $\mathbf{a}_{i,j}$ (in Eq.(10)) it refers to jth step. Also, in Eq.(1), many papers use $\mathbf{x}_i$ ($\mathbf{x}$ in boldface) to show the state vector of subsystem i. What is the point of using $\mathbf{x}_{i,j}$ instead? I suggest using consistent notation and symbols throughout the paper and, most importantly, defining all of them clearly in a nomenclature.

b. Parameters, used in equations, need to be clearly defined. For example, what is n_i in Eq.(1)? What is p in Assumption 2.2, and where it has been used? What is $\mathbf{a}_{i1}$ in Eq.(3) and what is its difference with $\mathbf{a}_{i,j}$ in Eq.(7)?

c. Section III, the main contribution of the paper, is a very long section without any subsections or

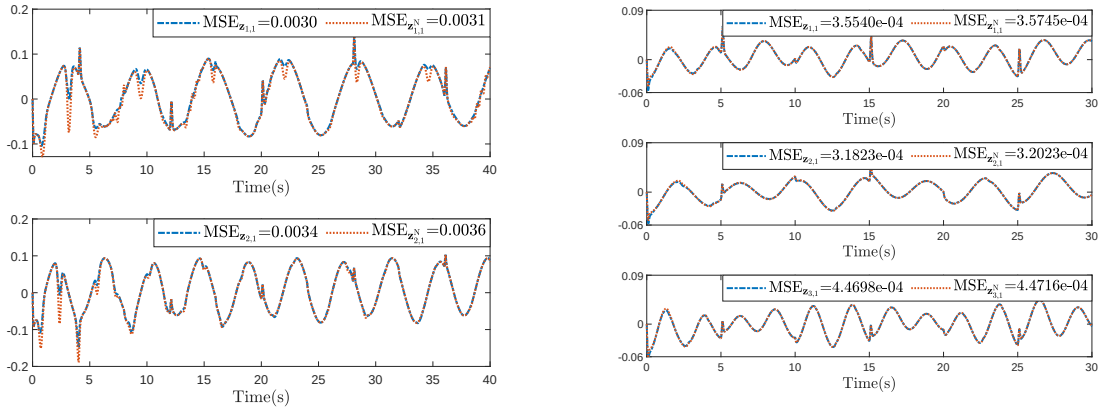

(a) The comparative results with no optimization in Example 5.1.

(b) The comparative results with no optimization in Example 5.2.

Figure 12: The comparative tracking errors of the proposed algorithm and the algorithm with no optimization ($\mathbf{z}^{\mathrm{N}}_{i,1}$, the red line).

general explanations of what is happening. Three steps, called Step $i,1$, Step i,h, and Step i,n_i have been introduced. When one goes through them, Step $i,1$ and Step i,h are so similar in procedure. Authors are requested to:

• Add appropriate subsections to section III.

• Reduce the number of equations by augmenting pre-defined Steps (Step $i,1$, Step i,h, and Step i,n_i), or transferring either of them to the appendix.

• Add a control block diagram to clearly show how the combination of this backstepping and learning works.

• A brief explanation of 'Barrier Lyapunov Function' should be added in the preliminary section.

• On page 4, line 40, it is claimed that the proposed method 'is significantly simple in comparison to the existing optimal methods in [25],[27]'. What is the authors' justification for this simplicity? How is it measured and proved?

Re:

Thanks for the beneficial suggestion of the respectable reviewer. Due to the changes made in the article, the structure of the sections II-IV, and as a result, the numbering of the formulas and some related notations have been changed. Also, a control block diagram is provided to illustrate the design structure of the optimal fault-tolerant control clearly, and some descriptions are further explained to enhance the contributions and differences in comparison to the existing results. To address these concerns of the honorable referee, the detailed corrections to the above-mentioned comments are listed as below.

a). For the notations and symbols in the formulas, we have utilized a consistent nomenclature to represent the subsystem states $\mathbf{x}_{i,1}$, $\mathbf{x}_{i,\hbar}$, $\mathbf{x}_{i,\mathrm{n}_i}$, the interconnection terms $\Delta_{i,1}(\bar{\mathbf{y}})$, $\Delta_{i,\hbar}(\bar{\mathbf{y}})$, $\Delta_{i,\mathrm{n}_i}(\bar{\mathbf{y}})$, the virtual optimal control input $\hat{\mathbf{a}}^*_{i,1}$, $\hat{\mathbf{a}}^*_{i,\hbar-1}$, $\hbar=2,3,\ldots,\mathrm{n}_i-1$, and so on. In Eq.(1), the large-scale interconnected system with N high-dimensional subsystems is considered, and the ith subsystem has n_i dimensions with n_i being a positive integer, $i=1,2,\ldots,\mathrm{N}$. That is to say, there are different dimensions in each subsystem for the large-scale interconnected system. Accordingly, the subscript 1, $\hbar$ and n_i in the subsystem states and the interconnections imply the 1-dimensional, $\hbar$-dimensional and n_i-dimensional in the ith subsystem. Also, the terms $\Delta_{i,1}(\bar{\mathbf{y}})$, $\Delta_{i,\hbar}(\bar{\mathbf{y}})$ and $\Delta_{i,\mathrm{n}_i}(\bar{\mathbf{y}})$ play a part in the interactions between ith subsystem and other subsystems, that is because the variable $\bar{\mathbf{y}}=[\mathbf{y}_1,\mathbf{y}_2,\ldots,\mathbf{y}_{\mathrm{N}}]^{\mathrm{T}}$ includes the output variables of all subsystems. In addition, the notations $\hat{\mathbf{a}}^*_{i,1}$, $\hat{\mathbf{a}}^*_{i,\hbar-1}$ in Eqs.(8) and (16) also mean the virtual optimal control input of the 1-dimensional and $\hbar-1$-dimensional formulas in the ith subsystem.

During the existing results, there are several representations of the large-scale interconnected systems. For example, the state-space form of large-scale interconnected system was proposed as $\dot{\mathbf{x}}_i=\mathrm{A}_i\mathbf{x}_i+\mathbf{B}_i\mathrm{u}_i+\sum^{\mathrm{N}}_{j=1,j\neq i}\mathrm{F}_{ij}\mathbf{x}_j$ and $\mathbf{y}_i=\mathrm{C}_i\mathbf{x}_i$, where A_i, B_i, C_i and F_{ij} are known parameter matrices with appropriate dimensions. Subsequently, the decentralized or distributed control method was utilized to stabilize the whole system. Furthermore, some results used the system model as $\dot{\mathbf{x}}_i=\mathrm{f}_i(\mathbf{x}_i)+\mathrm{g}_i(\mathbf{x}_i)(\mathrm{u}_i+\Delta_i(\bar{\mathbf{y}}))$ with $\mathbf{x}_i=[\mathbf{x}_{i,1},\mathbf{x}_{i,\hbar},\mathbf{x}_{i,\mathrm{n}_i}]^{\mathrm{T}}$ being the state vector, and a decentralized controller was designed to achieve control objectives. Hence, the state and control coefficients can be extended to state-dependent functions

rather than constants as before. Nevertheless, this model still has a limitation that the form of function $g_i(\mathbf{x}_i)$ may cause the interconnection term only appears in the n_i-dimensional formula. For instance, the power network system with two interconnected synchronous generators [37] cannot be represented by this model. That is why we use a general model as Eq.(1) to describe the characteristics of large-scale interconnected system. Afterwards, a learning-based optimal fault-tolerant control strategy is present to improve the tracking performance and security.

b). For the parameters in the formulas, clearer definitions and explanations are provided to illustrate the physical meanings. All these parts are marked in blue in the revised manuscript. As described before, the large-scale interconnected system with N subsystems is considered as Eq.(1), where n_i represents the total dimension of the ith subsystem. During the simulations, $n_i = 2$ for $i = 1, 2$ in the first example and $n_i = 3$ for $i = 1, 2, 3$ in the second example.

Assumption 2.2 is a bounded restriction for the interconnected term $\Delta_{i,\iota}(\bar{\mathbf{y}})$, $\iota = 1, 2, \ldots, n_i$, which is utilized in stability analysis of the inequalities (31), (36) and (41), with the help of the Young's inequality, i.e., the Lemma 2.2. From which, p is a known integer $p = \max\{p_{i,1}\}$ that can amplify the interconnections. More specifically, from the condition $|\Delta_{i,\iota}| \leq \sum_{s=1}^{p_{i,\iota}} \sum_{l=1}^{N} q_{i,\iota,l}^{s} |\mathbf{y}_l|^s$, one can derives that $\phi_{i,\iota}\Delta_{i,\iota} \leq \frac{1}{4}\phi_{i,\iota}^2 + (\sum_{s=1}^{p_{i,\iota}} q_{i,\iota,l}^{s} |\mathbf{y}_l|^s)^2$. By using the Cauchy-Schwartz inequality $(\sum_{s=1}^{p_{i,\iota}} a_s b_s)^2 \leq (\sum_{s=1}^{p_{i,\iota}} a_s^2)(\sum_{s=1}^{p_{i,\iota}} b_s^2)$, we can obtain $(\sum_{s=1}^{p_{i,\iota}} \sum_{l=1}^{N} q_{i,\iota,l}^{s} |\mathbf{y}_l|^s)^2 \leq N p_{i,\iota} \sum_{s=1}^{p_{i,\iota}} \sum_{l=1}^{N} (q_{l,\iota,i}^{s} |\mathbf{y}_i|^s)^2$. By substituting $\mathbf{y}_i = \mathbf{x}_{i,1}$ and $\mathbf{x}_{i,1} = \mathbf{z}_{i,1} + \mathbf{y}_{i,d}$ into it, and utilising Cauchy-Schwartz inequality $(\sum_{i=1}^{2} a_i)^{2k} \leq 2^{2k}(\sum_{i=1}^{2} a_i^{2k})$, one has $N p_{i,\iota} \sum_{s=1}^{p_{i,\iota}} \sum_{l=1}^{N} (q_{l,\iota,i}^{s} |\mathbf{y}_i|^s)^2 \leq \sum_{s=1}^{p} 2^{2s} \mathbf{q}_{l,\iota,i} (|\mathbf{z}_{i,1}|^{2s} + |\mathbf{y}_{i,d}|^{2s})$ where $\mathbf{q}_{l,\iota,i} = N p \sum_{l=1}^{N} q_{l,\iota,i}^{2s}$.

As for the $\mathbf{a}_{i-1}$ in Eq.(3) and $\mathbf{a}_{i,j}^*$ in Eq.(7) in the last round manuscript, the former one is a generalized symbol $\mathbf{a}_{i-1}$ in Eq.(3) to represent the reference trajectory $\mathbf{y}_{i,d}$ and the estimated optimal virtual control input $\hat{\mathbf{a}}_{i,1}^*$, $\hat{\mathbf{a}}_{i,\hbar}^*$, while the latter one means the optimal virtual control input that will be estimated by a critic-actor-identifier framework. To further promote the readability of the manuscript, the lemma about the asymmetric IBLF has been integrated into the **STABILITY ANALYSIS** section, and the explicitly notations and definitions are added in the revision.

c). For the presentations of the optimal fault-tolerant control design, another section is added to illustrate the procedure clearly. That is, the optimized virtual controller, the optimized actual controller and the learning laws of network weights for the backstepping steps are presented in the Section III, while the stability analysis for these three backstepping steps is shown in the Section IV. Also, the numbers of the equations in these two sections are reduced correspondingly. Owing to the Step i,1 and Step $i, \hbar$ have some similarities in the control design and stability analysis, several formulas are omitted in the Step $i, \hbar$. Moreover, a brief block diagram of the proposed optimal fault-tolerant control scheme is added to exhibit the design procedures and the methodology clearer, see the Fig.1 in the revised article (i.e., the figure 13 in the response).

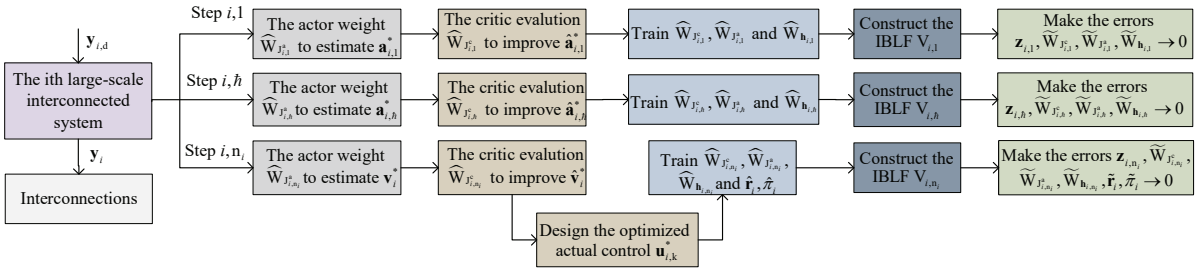

Figure 13: The block diagram of the proposed learning-based optimal FTC design.

d). For the brief explanation of 'Barrier Lyapunov Function (BLF)' and 'Integral BLF (IBLF)', some related sentences are added in the fourth paragraph of the **INTRODUCTION** section, e.g., 'BLF is a special Lyapunov functions, whose value approaches infinity when it nears the boundary of permissible set', 'Among them, the processing of constraint using IBLF has been greatly simplified and relaxed the feasibility conditions, i.e., it has a well calculate capability of not requiring to convert state-constraints into transformed error-constraints, but help to restrict a system state directly. Consequently, the conservatism of BLFs-based control can be reduced'. These parts are indicated in blue in the revised manuscript.

e). Due to the structure and formula changes made in the revision, the structure of some sections, and as a result, numbering of the literature have been changed. The references [40] and [41] design the training laws of critic and actor weights via using the gradient descent algorithm and the

PE condition. That is, by defining a function $\Phi_i = \frac{1}{2}\mathrm{B}_{ei,\iota}^2$ with the Bellman residual error as $\mathrm{B}_{ei,\iota} = \mathrm{H}_{i,\iota}(\mathbf{z}_{i,\iota}, \mathbf{a}_{i,\iota}, \mathrm{J}_{\mathbf{z}_{i,\iota}}) - \mathrm{H}_{i,\iota}(\mathbf{z}_{i,\iota}, \mathbf{a}_{i,\iota}^*, \mathrm{J}_{\mathbf{z}_{i,\iota}}^*) = \mathrm{H}_{i,\iota}(\mathbf{z}_{i,\iota}, \mathbf{a}_{i,\iota}, \mathrm{J}_{\mathbf{z}_{i,\iota}})$, $\iota = 1, 2, \ldots, \mathrm{n}_i$, the critic updating law can be yielded based on the gradient descent algorithm for minimizing the Bellman residual error:

$$\begin{aligned}\dot{\hat{\mathrm{W}}}_{\mathrm{J}_{i,\iota}^{\mathrm{c}}} &= -\frac{\lambda_{i,\iota}^{\mathrm{c}}}{1+\|\xi_{i,\iota}\|^2}\frac{\partial \Phi_i}{\partial \hat{\mathrm{W}}_{\mathrm{J}_{i,\iota}^{\mathrm{c}}}} \\ &= -\frac{\lambda_{i,\iota}^{\mathrm{c}}}{1+\|\xi_{i,\iota}\|^2}\xi_{i,\iota}\big(\xi_{i,\iota}^{\mathrm{T}}\hat{\mathrm{W}}_{\mathrm{J}_{i,\iota}^{\mathrm{c}}} - (\mathrm{K}_{i,\iota}^2 - 1)\mathrm{z}_{i,\iota}^2 \\ &\quad + 2\mathrm{K}_{i,\iota}\mathrm{z}_{i,\iota}(\hat{\mathrm{W}}_{\mathbf{h}_{i,\iota}}\mathrm{S}_{\mathbf{h}_{i,\iota}} - \dot{\hat{\mathrm{a}}}_{i,\iota-1}^*) + \frac{1}{4}\hat{\mathrm{W}}_{\mathrm{J}_{i,\iota}^{\mathrm{a}}}^{\mathrm{T}}\bar{\mathrm{S}}_{\mathrm{J}_{i,\iota}}\hat{\mathrm{W}}_{\mathrm{J}_{i,\iota}^{\mathrm{a}}}\big)\end{aligned} \tag{9}$$

where $\dot{\hat{\mathrm{a}}}_{i,0}^* = \dot{\mathbf{y}}_{i,\mathrm{d}}$ and $\xi_{i,\iota} = \mathrm{S}_{\mathrm{J}_{i,1}}(\hat{\mathrm{W}}_{\mathbf{h}_{i,\iota}}\mathrm{S}_{\mathbf{h}_{i,\iota}} - \dot{\hat{\mathrm{a}}}_{i,\iota-1}^* - \mathrm{K}_{i,\iota}\mathrm{z}_{i,\iota} - \frac{1}{2}\hat{\mathrm{W}}_{\mathrm{J}_{i,\iota}^{\mathrm{a}}}^{\mathrm{T}}\mathrm{S}_{\mathrm{J}_{i,1}})$. Also, the actor network weight is designed based on the stability analysis: $\dot{\hat{\mathrm{W}}}_{\mathrm{J}_{i,\iota}^{\mathrm{a}}} = \frac{1}{2}\mathrm{S}_{\mathrm{J}_{i,1}}\mathrm{z}_{i,\iota} - \lambda_{i,\iota}^{\mathrm{a}}\bar{\mathrm{S}}_{\mathrm{J}_{i,\iota}}\hat{\mathrm{W}}_{\mathrm{J}_{i,\iota}^{\mathrm{a}}} + \frac{\lambda_{i,\iota}^{\mathrm{c}}}{4(1+\|\xi_{i,\iota}\|^2)}\bar{\mathrm{S}}_{\mathrm{J}_{i,\iota}}\hat{\mathrm{W}}_{\mathrm{J}_{i,\iota}^{\mathrm{a}}}^{\mathrm{T}}\xi_{i,\iota}\hat{\mathrm{W}}_{\mathrm{J}_{i,\iota}^{\mathrm{c}}}$. For obtaining the desired control performance, the term $\xi_{i,\iota}\xi_{i,\iota}^{\mathrm{T}}$ should satisfy the PE condition. In order to simplify this design procedure, the updating laws of critic and actor weights are derived as Eqs. (12), (20) and (26) without using the PE condition. By denoting a function as $\mathrm{E}_i = \mathrm{Tr}\{(\hat{\mathrm{W}}_{\mathrm{J}_{i,\iota}^{\mathrm{a}}} - \hat{\mathrm{W}}_{\mathrm{J}_{i,\iota}^{\mathrm{c}}})^{\mathrm{T}}(\hat{\mathrm{W}}_{\mathrm{J}_{i,\iota}^{\mathrm{a}}} - \hat{\mathrm{W}}_{\mathrm{J}_{i,\iota}^{\mathrm{c}}})\}$, it is easy to verify that $\partial \mathrm{H}_{i,\iota}(\mathbf{z}_{i,\iota}, \mathbf{a}_{i,\iota}, \mathrm{J}_{\mathbf{z}_{i,\iota}})/\partial \hat{\mathrm{W}}_{\mathrm{J}_{i,\iota}^{\mathrm{a}}} = 0$ and $\mathrm{E}_i = 0$ are equivalent. Since $\partial \mathrm{E}_i/\partial \hat{\mathrm{W}}_{\mathrm{J}_{i,\iota}^{\mathrm{a}}} = -\partial \mathrm{E}_i/\partial \hat{\mathrm{W}}_{\mathrm{J}_{i,\iota}^{\mathrm{c}}} = 2(\hat{\mathrm{W}}_{\mathrm{J}_{i,\iota}^{\mathrm{a}}} - \hat{\mathrm{W}}_{\mathrm{J}_{i,\iota}^{\mathrm{c}}})$, the time-derivative of E_i can be calculated as:

$$\begin{aligned}\dot{\mathrm{E}}_i &= \mathrm{Tr}\{\frac{\partial \mathrm{E}_i}{\partial \hat{\mathrm{W}}_{\mathrm{J}_{i,\iota}^{\mathrm{a}}}}\dot{\hat{\mathrm{W}}}_{\mathrm{J}_{i,\iota}^{\mathrm{a}}} + \frac{\partial \mathrm{E}_i}{\partial \hat{\mathrm{W}}_{\mathrm{J}_{i,\iota}^{\mathrm{c}}}}\dot{\hat{\mathrm{W}}}_{\mathrm{J}_{i,\iota}^{\mathrm{c}}}\} \\ &= \mathrm{Tr}\{\frac{\partial \mathrm{E}_i}{\partial \hat{\mathrm{W}}_{\mathrm{J}_{i,\iota}^{\mathrm{a}}}}(-\lambda_{i,1}^{\mathrm{a}}\bar{\mathrm{S}}_{\mathrm{J}_{i,1}}\hat{\mathrm{W}}_{\mathrm{J}_{i,1}^{\mathrm{a}}} + \bar{\lambda}_{i,1}\bar{\mathrm{S}}_{\mathrm{J}_{i,1}}\hat{\mathrm{W}}_{\mathrm{J}_{i,1}^{\mathrm{c}}}) - \frac{\partial \mathrm{E}_i}{\partial \hat{\mathrm{W}}_{\mathrm{J}_{i,\iota}^{\mathrm{c}}}}\lambda_{i,1}^{\mathrm{c}}\bar{\mathrm{S}}_{\mathrm{J}_{i,1}}\hat{\mathrm{W}}_{\mathrm{J}_{i,1}^{\mathrm{c}}}\} \\ &= -\frac{\lambda_{i,1}^{\mathrm{a}}}{2}\mathrm{Tr}\{\frac{\partial \mathrm{E}_i}{\partial \hat{\mathrm{W}}_{\mathrm{J}_{i,\iota}^{\mathrm{a}}}^{\mathrm{T}}}\bar{\mathrm{S}}_{\mathrm{J}_{i,1}}\frac{\partial \mathrm{E}_i}{\partial \hat{\mathrm{W}}_{\mathrm{J}_{i,\iota}^{\mathrm{a}}}}\} \le 0\end{aligned} \tag{10}$$

which indicates that the updating laws (13), (19) and (25) can ensure the satisfaction of above inequality, and the Bellman residual error can be near to zero without the PE condition. However, these two types of the learning laws of network weights have similar convergence performance in the simulations. Furthermore, we give some explanations for this design procedure, see the **Remark 3.3** and **3.4** on page 4.

Remark 3.3. The existing results in [41], [42] need the persistent excitation (PE) condition to stabilize the control system. In contrast, we show that the Bellman residual error converges to zero without the PE condition. This can also be verified by defining a function $\mathrm{E}_i = \mathrm{Tr}\{(\hat{\mathrm{W}}_{\mathrm{J}_{i,1}^{\mathrm{a}}} - \hat{\mathrm{W}}_{\mathrm{J}_{i,1}^{\mathrm{c}}})^{\mathrm{T}}(\hat{\mathrm{W}}_{\mathrm{J}_{i,1}^{\mathrm{a}}} - \hat{\mathrm{W}}_{\mathrm{J}_{i,1}^{\mathrm{c}}})\}$. It can be verified that $\mathrm{E}_i = 0$ and $\frac{\partial \mathrm{H}_{i,1}(\mathbf{z}_{i,1}, \mathbf{a}_{i,1}, \mathrm{J}_{\mathbf{z}_{i,1}})}{\partial \hat{\mathrm{W}}_{\mathrm{J}_{i,1}^{\mathrm{a}}}} = 0$ are equivalent. Since $\frac{\partial \mathrm{E}_i}{\partial \hat{\mathrm{W}}_{\mathrm{J}_{i,1}^{\mathrm{a}}}} = -\frac{\partial \mathrm{E}_i}{\partial \hat{\mathrm{W}}_{\mathrm{J}_{i,1}^{\mathrm{c}}}} = 2(\hat{\mathrm{W}}_{\mathrm{J}_{i,1}^{\mathrm{a}}} - \hat{\mathrm{W}}_{\mathrm{J}_{i,1}^{\mathrm{c}}})$, the time-derivative of E_i can be calculated as:

$$\dot{\mathrm{E}}_i = \mathrm{Tr}\{\frac{\partial \mathrm{E}_i}{\partial \hat{\mathrm{W}}_{\mathrm{J}_{i,1}^{\mathrm{a}}}}\dot{\hat{\mathrm{W}}}_{\mathrm{J}_{i,1}^{\mathrm{a}}} + \frac{\partial \mathrm{E}_i}{\partial \hat{\mathrm{W}}_{\mathrm{J}_{i,1}^{\mathrm{c}}}}\dot{\hat{\mathrm{W}}}_{\mathrm{J}_{i,1}^{\mathrm{c}}}\} = -\frac{\lambda_{i,1}^{\mathrm{a}}}{2}\mathrm{Tr}\{\frac{\partial \mathrm{E}_i}{\partial \hat{\mathrm{W}}_{\mathrm{J}_{i,1}^{\mathrm{a}}}^{\mathrm{T}}}\bar{\mathrm{S}}_{\mathrm{J}_{i,1}}\frac{\partial \mathrm{E}_i}{\partial \hat{\mathrm{W}}_{\mathrm{J}_{i,1}^{\mathrm{a}}}}\} \le 0 \tag{11}$$

which implies that the learning laws (13a) and (13b) can ensure the satisfaction of (14), and the Bellman residual error can converge to zero without the PE condition.

Remark 3.4. The main advantages for the designed critic and actor training laws are: 1) it simplifies the design procedure in comparison to the existing optimal methods in [41], [42]; 2) it can reduce the computational complexity due to the unknown functions $\mathbf{f}_{i,1}(\bar{\mathbf{x}}_{i,1})$ and $\Delta_{i,1}(\bar{\mathbf{y}})$; 3) it enables to remove the PE condition commonly required in the optimal control.

Comment 3: The 'Simulation' section needs revision:
a. What is the difference between the two examples? What does Example 2 show that Example 1 does not? Better to stick to one example, but clearly demonstrate the paper contribution.
b. Results should be compared with a relevant paper to show the contribution.
c. Figures, and texts on them, are too small.
Re:
Thank you for your useful advice. Note that the selected practical example in the previous manuscript is

not reasonable to reflect the validity and the superiority of the proposed method due to the mismatching of the system model. In the simulations, two practical examples are presented to illustrate the effectiveness of the learning-based optimized fault-tolerant control scheme, i.e., the electrical power system with two-machine subsystems and the walking robot with three subsystems. Additionally, the difference between the two examples and the comparative results are explained and added clearer, and the sizes of the figures and texts on them are adjusted accordingly.

a). For the difference between the two examples, we concentrate on the different numbers of subsystems in the whole large-scale interconnected system or the different dimensions in each subsystem, that can verify the proposed control algorithm will stabilize the overall system and achieve the control objective. That is why we use two examples rather than only one example for simulations. More specifically, the Example 5.1 has two subsystems with two-dimensional in each subsystem, while the Example 5.2 owns three subsystems with two-dimensional in each subsystem. With the help of the appropriate parameters, the tracking trajectories of $\mathbf{y}_i$ and $\mathbf{y}_{i,\mathrm{d}}$, the boundedness of the network weights $\|\hat{\mathrm{W}}_{\mathrm{J}^{\mathrm{c}}_{i,\mathrm{t}}}\|$, $\|\hat{\mathrm{W}}_{\mathrm{J}^{\mathrm{a}}_{i,\mathrm{t}}}\|$, $\|\hat{\mathrm{W}}_{\mathbf{h}_{i,\mathrm{t}}}\|$ and control input $\mathbf{u}_{i,\mathrm{k}}$, $\mathbf{u}^{\mathrm{F}}_{i,\mathrm{k}}$, the tracking trajectories without fault-tolerant control, and other comparative results are both presented to make a further explanation of these two examples.

b). On the basis of the critic-actor-identifier architecture, the optimal fault-tolerant control problem is investigated for the large-scale interconnected systems with intermittent actuator faults. Among which, the actor is utilized to implement control actions, the critic is utilized to evaluate these actions from the environment and to return the evaluations to the actor so that the subsequent actions can be well, and the identifier is utilized to approximate the unknown dynamic. To illustrate the superiority of the proposed optimal fault-tolerant control scheme, the simulation results are compared with some relevant researches from the aspects of BLF and optimization. The control performance of the asymmetric IBLF, the tangent BLF in [27] and the logarithmic BLF in [29] are displayed in **Fig.6** and **Fig.12** (see the figure 10 in our response), i.e., (a1)-(a2) and (a1)-(a3) are tracking trajectories, and (b1)-(b2) and (b1)-(b3) are tracking errors. These three types BLFs have seen similar performance in tracking control, however, the output-variable with the proposed asymmetric IBLF is closer to the actual trajectories than the others due to its smaller tracking error. Through the selected mean square error performance criteria $\mathrm{MSE} = (1/\mathrm{T})\sum_{\mathrm{t}=0}^{\mathrm{T}}(\mathbf{y}_i(\mathrm{t}) - \mathbf{y}_{i,\mathrm{d}}(\mathrm{t}))^2$, it is possible to verify the well tracking performance and less conservative features of the proposed algorithm. Additionally, **Fig.7** and **Fig.13** (see the figure 11 in our response) show the comparisons of the tracking performance between the proposed algorithm and the algorithm without optimization, also, the MSE results of the proposed algorithm illustrate its efficiency than the one without optimization.

c). For the simulation figures and the texts on figures, we have adjusted the sizes and the arrangements of them into an appropriate presentation to fit the overall page. Then, the figures and the texts are clearer than before.

Comment 4: There are also typos and grammatical issues in the paper, some of them are:
a. Page 1, line 35: '... play a significant part in ...' -> '... play a significant role in ...'
b. Page 1, line 45: '..., due to it can ...' -> '..., because it can ...'
c. Page 1, line 46: '... only use ...' -> '... only using ...'
d. Page 2, first column, lines 10-13: The sentence is vague.
e. Page 2, the line above Eq.(2): It refers to 'stuck faults'; however, Eq.(2) does not cover the stuck fault considering the condition on $\psi_{i,\mathrm{k}}$.
f. Page 2, last line: What does the superscript (ℓ) in $\mathbf{y}^{(\ell)}$ mean?
g. Page 3, line 12: definition of $\mathrm{a}_{\mathrm{i}-1}$ is not complete. How a_1, a_2, ... will be calculated.

Re:
Thanks for the beneficial suggestion of the respectable reviewer. In order to address these deficiencies in the article, the authors have thoroughly rewritten the language and tried to resolve the variable definitions and demonstrations as many as possible, which are indicated in blue in the revised version. Now, we are confident to say that this paper is much more readable than before.

a)-c). On the basis of your suggestion, we have checked the language of this paper carefully, and we have corrected some grammatical, editorial and even conceptual errors as much as possible. Here, the sentences '... play a significant part in...' is revised by '... play a significant role in...', '... due to it can...' is changed into '... because it can...', and '... only use ...' is corrected as '... only using ...', etc. More sentences with grammatical errors are also corrected in the revised manuscript accordingly.

d). On page 2, the sentence in the lines 10-13 expresses the importance of accommodating the system

constraints during the control process. To avoid ambiguity, the sentence is written as 'It is known that most practical applications normally operate under various constraints, e.g., the performance requirements, physical limitations and security considerations. Neglecting to accommodate these constraints may cause inaccurate performance, system instability, or even unexpected accidents', which is indicated in blue in the revised article.

e). For the intermittent actuator fault model (2), the coefficient of the loss of effectiveness $\psi_{i,\mathrm{k}}^{\mathrm{h}}$ satisfying $0 \leq \underline{\psi}_{i,\mathrm{k}} \leq \psi_{i,\mathrm{k}}^{\mathrm{h}} \leq 1$ with $\underline{\psi}_{i,\mathrm{k}}$ being an unknown constant, $\zeta_{i,\mathrm{k}}^{\mathrm{h}}$ is the stuck fault value with $|\zeta_{i,\mathrm{k}}^{\mathrm{h}}| \leq \bar{\zeta}_{i,\mathrm{k}}^{\mathrm{h}}$. $\mathrm{t} \in [\mathrm{t}_{i,\mathrm{h}}, \mathrm{t}_{i,\mathrm{h}+1})$ for $\mathrm{h} \in \mathrm{Z}^{+}$, and $\mathrm{t}_{i,\mathrm{h}}$ represents the unknown failure time constant, which indicates the actuator faults are completely unpredictable in time, pattern, and value. From the Eq.(2), four types of states of the kth actuator are described as follows: i) $\psi_{i,\mathrm{k}}^{\mathrm{h}} \in (0,1)$ and $\zeta_{i,\mathrm{k}}^{\mathrm{h}} \neq 0$ indicate that the kth actuator has the loss of control effectiveness and stuck faults at the same time; ii) $\psi_{i,\mathrm{k}}^{\mathrm{h}} \in (0,1)$ and $\zeta_{i,\mathrm{k}}^{\mathrm{h}} = 0$ imply that it can only output a fraction of the control input; iii) $\psi_{i,\mathrm{k}}^{\mathrm{h}} = 1$ and $\zeta_{i,\mathrm{k}}^{\mathrm{h}} \neq 0$ signify stuck faults only; iv) $\psi_{i,\mathrm{k}}^{\mathrm{h}} = 1$ and $\zeta_{i,\mathrm{k}}^{\mathrm{h}} = 0$ means the fault-free case. Concise descriptions of the intermittent actuator faults are further explained in the revised article as a response to this comment (see the **Remark 2.1** and **2.2** on page 2).

Remark 2.1. The ith actuator mainly can experiment with the following four cases: i) $\psi_{i,\mathrm{k}}^{\mathrm{h}} \in (0,1)$ and $\zeta_{i,\mathrm{k}}^{\mathrm{h}} \neq 0$ indicate that the ith subsystem has the loss of control effectiveness and stuck faults at the same time; ii) $\psi_{i,\mathrm{k}}^{\mathrm{h}} \in (0,1)$ and $\zeta_{i,\mathrm{k}}^{\mathrm{h}} = 0$ imply that it can only output a fraction of the control input; iii) $\psi_{i,\mathrm{k}}^{\mathrm{h}} = 1$ and $\zeta_{i,\mathrm{k}}^{\mathrm{h}} \neq 0$ signify stuck faults only; iv) $\psi_{i,\mathrm{k}}^{\mathrm{h}} = 1$ and $\zeta_{i,\mathrm{k}}^{\mathrm{h}} = 0$ means the fault-free case.

Remark 2.2. The fault number h in [14], [28] is limited to finite under a single occurrence time. In contrast to this, the more general case is considered as Eq.(2), which indicates that the actuator can be intermittently revert to normal operation, or alternate intermittently between different fault modes. It is applicable not only to the actuator faults with uniform interval periods but to those with non-uniform interval periods.

f). Due to the change of notations and symbols in the formulas, $\mathbf{y}^{(\ell)}$ is represented by $\mathbf{y}_{i,\mathrm{d}}^{(\iota)}$, $\iota = 1, 2, \ldots, \mathrm{n}_i$. And the superscript (ι) in $\mathbf{y}_{i,\mathrm{d}}^{(\iota)}$ means the ιth-order derivatives of $\mathbf{y}_{i,\mathrm{d}}$, i.e., $\dot{\mathbf{y}}_{i,\mathrm{d}}, \ddot{\mathbf{y}}_{i,\mathrm{d}}, \mathbf{y}_{i,\mathrm{d}}^{(3)}, \ldots, \mathbf{y}_{i,\mathrm{d}}^{(\mathrm{n}_i)}$. This condition guarantees the optimized virtual control inputs $\hat{\mathbf{a}}_{i,1}^{*}$, $\hat{\mathbf{a}}_{i,\hbar}^{*}$ and the optimized actual control input $\hat{\mathbf{a}}_{i,\mathrm{n}_i}^{*}$ are both bounded.

g). For the Lemma 2.1 in the previous manuscript, the parameter $\mathrm{a}_{\mathrm{i}-1}$ denotes the optimized virtual controllers $\hat{\mathbf{a}}_{i,1}^{*}$, $\hat{\mathbf{a}}_{i,\hbar}^{*}$, which will be calculated in (12b) and (19b), respectively. This inequality is utilized in the stability analysis of each backstepping step. To avoid inconsistent notations and symbols, this lemma is omitted and represented directly in the **STABILITY ANALYSIS** section.

Once again, the authors would like to express their appreciation and sincere thanks for the respectable reviewer's encouraging, approving, constructive, fruitful and inspiring remarks and comments.

==========END OF DOCUMENT==========